CHAPTER 4

ANALYSIS OF THE INTERFACE BEHAVIOR IN BEAMS SUBJECTED TO TRANSVERSE LOADS

4.1. Introduction

In this section, the formulation previously found for a pure shear loaded element applying Non-Linear Fracture Mechanics (NLFM) will be extended to a general case of a beam under shear forces and bending moments.

First, in §4.2, the governing equations of interfacial shear stresses and laminate tensile stresses are derived by assuming a bilinear bond-slip relationship between the support and the external reinforcement, and taking into account the strain distribution in the concrete support.

Then, two cases are studied. Section 4.3 deals with the distribution of stresses in an element between two cracks subjected to pure flexure or flexure and shear. Section 4.4 studies the laminate end case, that is, an element between the end of the external reinforcement and the nearest crack in proximity (a case very similar to a pure shear loaded specimen due to its contour conditions).

Finally, this formulation is applied to a general case of a beam under transverse loads to find the stress and strain distribution along the laminate and the interface.

The conclusions drawn from these analyses are the basis for the design proposal that will be presented in Chapter 5.

4.2. Governing equations

Applying equilibrium and compatibility relations to a differential element (Figure 4.1), *dx*, it is possible to derive the differential equations for the interfacial shear stresses in a joint where a laminate has been glued to the soffit of a beam under a certain load configuration.

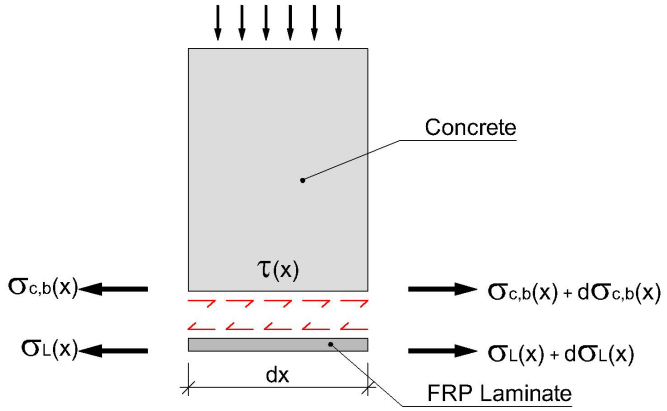

Figure 4.1. Forces acting on a differential section of a strengthened beam, dx.

The following assumptions are considered to derive the governing equations:

1) The thickness and width of the adherents are assumed to be constant along the bonded length.
2) No shear deformation is considered. Therefore, the shear stress and normal peeling stress problems are uncoupled, simplifying the mathematical resolution to a great extent.
3) The laminate bending stiffness is neglected since the following equations are derived for FRP externally bonded laminates which are of low thickness.
4) The relationship between the shear stress and the relative displacement of both adherents can be approached by a bilinear function (see Chapter 3).

As mentioned in Chapter 3, when the interface is governed by a bilinear bond-slip relationship, two states can be distinguished depending on the value of the slip in each point.

In the first state (Zone I), being in the upward branch of τ - s curve, the behavior of the interface is linear elastic. By following the same procedure of Chapter 3 which consisted of imposing both horizontal equilibrium and the bond-slip relationship of Zone I, the governing differential equation is derived as equation (4.1). Note that equation (4.1) is expressed in terms of laminate tensile stress to facilitate the application of contour conditions.

$$\frac{d^2\sigma_L^I}{dx^2}(x) - \Omega_1^2 \sigma_L^I(x) = -\Omega_1^2 \frac{E_L}{E_c}\sigma_{c,b}(x) \tag{4.1}$$

where:

$\sigma_{c,b}(x)$: concrete tensile stress in the bottom fiber of the section
Ω_1: constant given by equation (4.2) which is equal to equation (3.15) for a pure shear specimen and is equivalent to equation (2.13) from Chapter 2

$$\Omega_1^2 = \frac{1}{E_L t_L}\frac{\tau_{LM}}{s_{LM}} = \frac{1}{E_L t_L}\frac{2G_F^{\ I}}{s_{LM}^2} = \frac{1}{E_L t_L}\frac{\tau_{LM}^2}{2G_F^{\ I}} \tag{4.2}$$

The solution of the differential equation (4.1) gives a general expression of the laminate tensile stress in Zone I.

Once the maximum shear stress τ_{LM} is reached, a second state starts out. The formation of a crack is initiated with the appearance of microcracks, and the interface is behaving according to the descending branch of the bond-slip relationship (Zone II).

By following the same procedure as in Zone I, the differential equation governing the laminate stresses can be stated as (4.3).

$$\frac{d^2\sigma_L^{II}}{dx^2}(x) + \Omega_2^2\sigma_L^{II}(x) = \Omega_2^2\frac{E_L}{E_c}\sigma_{c,b}(x) \tag{4.3}$$

where:

Ω_2: constant given by equation (4.4) which is equal to equation (3.18) for a pure shear specimen

$$\Omega_2^2 = \frac{1}{E_L t_L}\frac{\tau_{LM}}{s_{L0} - s_{LM}} = \frac{1}{E_L t_L}\frac{2G_F^{\ II}}{(s_{L0} - s_{LM})^2} = \frac{1}{E_L t_L}\frac{\tau_{LM}^2}{2G_F^{\ II}} \tag{4.4}$$

The solution of the differential equation (4.3) gives the laminate tensile stress along Zone II of the bond-slip relationship.

A set of comments to equations (4.1) to (4.4) is presented below:

1) In equations (4.1) and (4.3), the term on the right hand side depends on the stress on the bottom concrete fiber of the unstrengthened section. The meaning of this term is related to the slip reduction resulting from the strains on the support.

2) If the bending stiffness of the beam is very high (or the concrete stress is very low), both equations (4.1) and (4.3) yield to equation (3.14) and (3.17) respectively, which were derived for a pure shear case.

3) The solution for equation (4.1) associated to Zone I will be similar to the solution of the governing equation describing the behavior of the laminate in a linear elastic case as presented in Chapter 2.

To find the general expressions for the tensile stresses in the laminate, the stress distribution in the bottom concrete fiber must be defined.

Assuming Bernouilli's law, the cross-section, originally plane, will remain plane and perpendicular to the deformed longitudinal axis of the beam, and the concrete stress distribution will be found by applying the strength of materials theory, as shown in Figure 4.2. Equation (4.7) gives the expression of concrete tensile stress in the bottom fiber of the cross-section as a function of the laminate tensile stress and the applied bending moment.

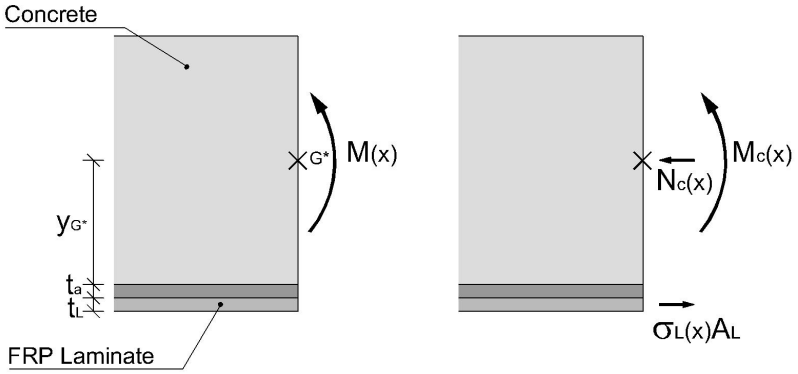

Figure 4.2. Forces acting in a section of an element between two existing cracks.

$$N_c(x) = A_L \sigma_L(x) \tag{4.5}$$

$$M_c(x) = M(x) - A_L \sigma_L(x)\left(y_{G*} + t_a + \frac{t_L}{2} \right) \tag{4.6}$$

$$\sigma_{c,b}(x) = \frac{M(x)}{I_{tr,c}^{*}} y_{G*} - \sigma_L(x)\left[\frac{A_L}{A_{tr,c}^{*}} + \frac{A_L}{I_{tr,c}^{*}} y_{G*}\left(y_{G*} + t_a + \frac{t_L}{2} \right) \right] \tag{4.7}$$

where:

N_c: axial force acting on the concrete section
M_c: bending moment acting on the concrete section
y_{G*}: distance from the bottom concrete fiber to the gravity center of the strengthened section
$A_{tr,c}^{*}$: area of the strengthened section transformed into concrete
$I_{tr,c}^{*}$: moment of inertia of the strengthened section transformed into concrete

In general, the thicknesses of the laminate and the adhesive are much lower compared to the distance between the gravity center of the strengthened section transformed to concrete and the bottom fiber, y_{G*}. Therefore, a simplification of equation (4.7) can be done.

$$\sigma_{c,b}(x)=\frac{M(x)}{I_{tr,c}^{*}}y_{G*}-\sigma_L(x)A_L\left[\frac{1}{A_{tr,c}^{*}}+\frac{y_{G*}^2}{I_{tr,c}^{*}}\right] \tag{4.8}$$

Incorporating expression (4.8) into (4.1), the governing differential equation of Zone I can be transformed into equation (4.9). By solving it, the tensile stress distribution in the laminate in Zone I is found as equation (4.11) except for the integration constants C_1 and C_2, which are both obtained by applying the appropriate boundary conditions.

$$\frac{d^2\sigma_L^I}{dx^2}(x)-\xi_1^2\sigma_L^I(x)=-\Omega_1^2\frac{E_L}{E_c I_{tr,c}^{*}}y_{G*}M(x) \tag{4.9}$$

where:

$$\xi_1^2=\Omega_1^2\left(1+\frac{E_L A_L}{E_c A_{tr,c}^{*}}+\frac{E_L A_L}{E_c I_{tr,c}^{*}}y_{G*}^2\right) \tag{4.10}$$

$$\sigma_L^I(x)=C_1\cosh(\xi_1 x)+C_2\sinh(\xi_1 x)+\psi\left(M(x)+\frac{1}{\xi_1^2}\frac{dV}{dx}(x)\right) \tag{4.11}$$

where:

$$\psi=\frac{E_L}{E_c I_{tr,c}^{*}}y_{G*}\frac{\Omega_1^2}{\xi_1^2}=\frac{E_L}{E_c I_{tr,c}^{*}}y_{G*}\left(1+\frac{E_L A_L}{E_c A_{tr,c}^{*}}+\frac{E_L A_L}{E_c I_{tr,c}^{*}}y_{G*}^2\right) \tag{4.12}$$

By repeating the same procedure in Zone II, the differential equation (4.3) becomes (4.13). Again, by solving this equation, the general expression for the tensile stresses is found as (4.15) where C_3 and C_4 are integration constants and ψ coincides with the constant defined by equation (4.12).

$$\frac{d^2\sigma_L^{II}}{dx^2}(x)+\xi_2^2\sigma_L^{II}(x)=\Omega_2^2\frac{E_L}{E_c I_{tr,c}^{*}}y_{G*}M(x) \tag{4.13}$$

where:

$$\xi_2^2=\Omega_2^2\left(1+\frac{E_L A_L}{E_c A_{tr,c}^{*}}+\frac{E_L A_L}{E_c I_{tr,c}^{*}}y_{G*}^2\right) \tag{4.14}$$

$$\sigma_L^{II}(x)=C_3\cos(\xi_2 x)+C_4\sin(\xi_2 x)+\psi\left(M(x)-\frac{1}{\xi_2^2}\frac{dV}{dx}(x)\right) \tag{4.15}$$

Since the axial stiffness of the laminate is usually much lower than the axial stiffness of the concrete section, a good approximation of equations (4.10) and (4.14) will be equations (4.16) and (4.17) respectively. According to this simplification, the

differential equations (4.9) and (4.13) can be approximated by (4.18) and (4.19) respectively.

$$\xi_1^2 \approx \Omega_1^2 \tag{4.16}$$

$$\xi_2^2 \approx \Omega_2^2 \tag{4.17}$$

$$\frac{d^2\sigma_L^I}{dx^2}(x) - \Omega_1^2 \sigma_L^I(x) = -\Omega_1^2 \frac{E_L}{E_c I_{tr,c}^*} y_{G^*} M(x) \tag{4.18}$$

$$\frac{d^2\sigma_L^{II}}{dx^2}(x) + \Omega_2^2 \sigma_L^{II}(x) = \Omega_2^2 \frac{E_L}{E_c I_{tr,c}^*} y_{G^*} M(x) \tag{4.19}$$

The shear stress along the bonded length can be obtained by differentiating the laminate tensile stress expressions (4.11) and (4.15) and afterwards multiplying the result by the thickness of the external reinforcement (see equation (3.9) of Chapter 3). In addition, the relative displacement between the laminate and the support is obtained from the shear stress distribution by applying the bilinear bond-slip relationship given by equation (3.12) of Chapter 3.

To obtain the integration constants C_1, C_2, C_3 and C_4, some contour conditions which depend on each particular case must be applied.

Equations from (4.9) to (4.19) will only be valid if the concrete's tensile stress is calculated according to the linear elastic strength of materials. Since in a normal reinforced concrete beam, the concrete will be cracked at some sections, the direct application of equations (4.11) and (4.15) is of little interest. In the following section, equations (4.1) and (4.3) will be modified to take into account the situation between two cracks.

4.3. Stress and strain distribution in an element between two cracks

4.3.1. Conceptual analysis

In the previous section, the governing equation of laminate stresses in the upward and downward branch of the bond-slip relationship has been determined. In distinguishing a specific case of an element between two cracks (crack I and crack J) (Figure 4.3), the stress and strain distribution of each element cannot be found by applying contour conditions to the general solution (4.11) and (4.15) because, obviously, in a cracked section, equations (4.11) and (4.15) are no longer valid. As a consequence, the concrete tensile stress in the bottom fiber should be defined in a different way, and equations (4.1) and (4.3) should be solved after assuming a concrete tensile stress distribution between the two cracks. The definition of this distribution will be dealt in §4.3.2. Prior

to this definition, a conceptual description of the crack propagation process as the applied load increases will be given in this section to understand the behavior of the interface between two cracks. Equations associated to this description will be presented in §4.3.2.

In the following discussion, the bending moment will be higher in crack J than in crack I. As a consequence, crack J will always be the crack with the highest tensile stress.

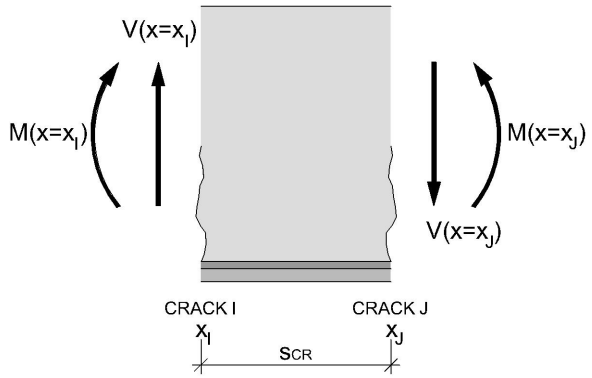

Figure 4.3. Forces acting in an element between two existing cracks.

As shown in Figure 4.3, there is an increase of laminate tensile stresses due to the bending moment increment between two existing cracks that is caused by the shear force. To achieve equilibrium in the laminate, some shear stresses appear and balance the increment on the laminate tensile force. In addition, the concrete between the two cracks contributes to the transfer of tensile stresses between the external reinforcement and the concrete itself. This concrete stress contribution, known as tension stiffening, is only possible if shear stresses are induced between concrete and laminate. In short, the shear stresses that appear between two cracks are on one hand required for equilibrium and are on the other hand induced by a tension stiffening effect. When no shear force is acting between both cracks, the shear stresses only appear due to the tension stiffening effect.

In this case, similar to the pure shear specimens studied in Chapter 3, different stages can be distinguished depending on the tensile force of the external reinforcement in each crack.

Stage 1

In Stage 1, the complete interface between both cracks is under a linear elastic state. To reach equilibrium, the shear stresses should be opposite to the tensile stress surrounding each crack. The shear stresses follow an exponential distribution which has a maximum value for both cracks I and J. The interfacial shear stress in each crack is always lower than the maximum shear value, τ_{LM}. During this Stage 1, there is always a zero shear stress location (x_K) which corresponds to a minimum value on the tensile stress distribution. As Stage 1 develops, the zero shear stress location moves towards crack I.

According to equation (3.9) of Chapter 3, the laminate tensile stresses are obtained by integrating the shear stresses. By knowing the shape of the shear stress distribution, it can be inferred that the tensile stresses diminish from each crack location to the point of zero shear stress which is always located much closer to crack I, whenever the tensile stress in crack J is higher than in crack I.

In addition, as the applied load increases, the laminate slides in relation to the concrete support, from the zero shear stress point towards each crack location. The relative displacement between concrete and laminate is always lower than s_{LM}.

A schematic profile of the interfacial shear and laminate tensile stresses in Stage 1 is shown in Figure 4.4.

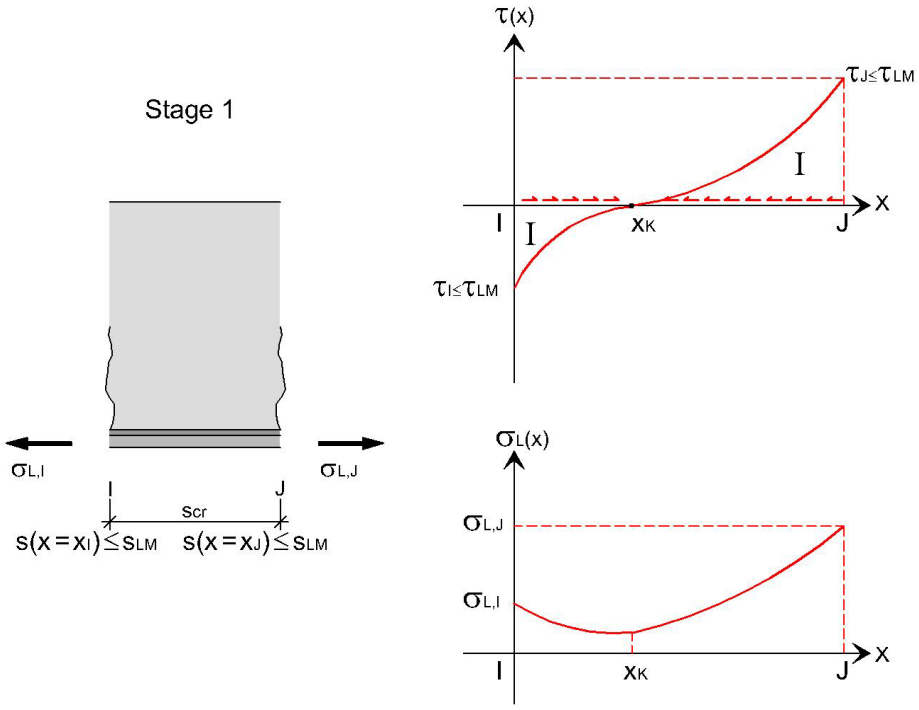

Figure 4.4. Interfacial shear and laminate tensile stress distribution between two cracks in Stage 1.

Stage 2

Stage 2 is characterized by having part of the bonded connection in Zone II of the bilinear bond-slip relationship. At the end of Stage 1, Stage 2a.1 initiates. The development of Stage 2a.1 leads to Stage 2a.2. Depending on the distance between cracks I and J, Stage 2a.1 or Stage 2a.2 may result in Stage 2b. The descriptions of Stages 2a.1, 2a.2 and 2b are given below.

Stage 2a.1

Stage 2a.1 is initiated after reaching the maximum shear stress τ_{LM} in crack J. Here, a part of the connection between this crack and a certain point associated to the maximum shear stress (x_{LM}) is situated in the descending branch of the τ - s curve (Zone II).

Microcracks appear along the bonded length between crack J and the coordinate x_{LM}. In this area, the interface is still able to transfer forces by aggregate interlock and there is still no real macrocrack. In addition, the behavior of the interface between x_{LM} and crack I which passes through the point of zero shear stress (x_K), remains linear elastic (Zone I). As Stage 2a.1 evolves, the maximum shear stress location approaches the zero shear stress location which simultaneously moves towards the less loaded crack.

As in the previous stage, the tensile stress distribution in the laminate reaches its maximum value under each crack and has a minimum value under the zero shear stress location. The slope of the tensile stress distribution is steeper in Zone II than in Zone I.

In addition, the relative sliding between laminate and concrete is zero at the zero shear stress point and increases towards both crack tips. In crack J, the relative sliding is always higher than s_{LM}. However, the s_{LM} value has still not been reached in the other crack tip. The slope of the slip distribution is steeper in Zone II than in Zone I.

A graphic illustration of the interfacial shear and laminate tensile stress distribution in Stage 2a.1 is shown in Figure 4.5.

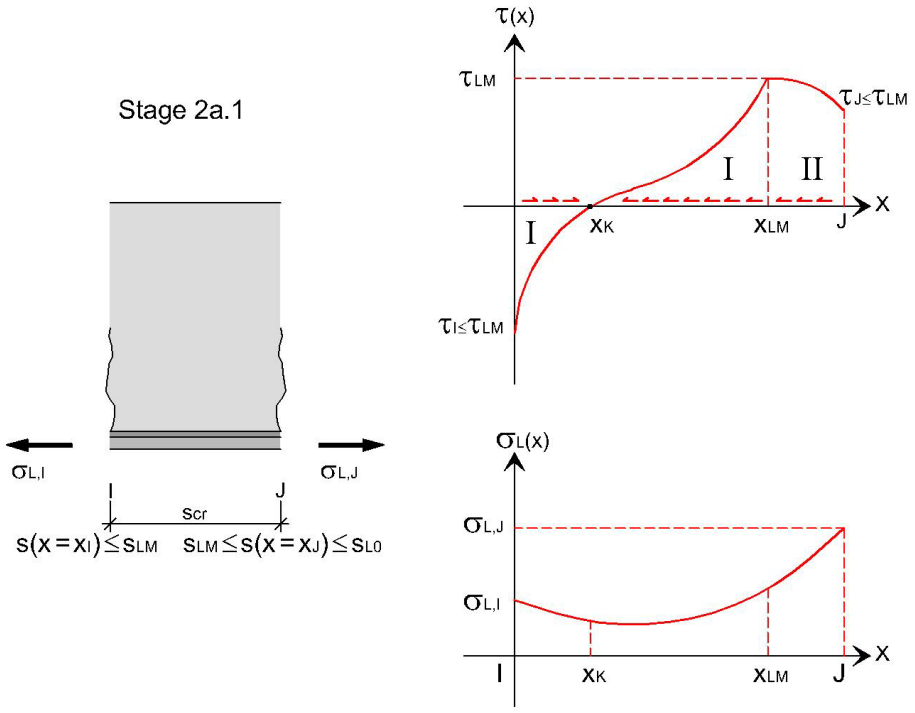

Figure 4.5. Interfacial shear and laminate tensile stresses between two cracks in Stage 2a.1.

Stage 2a.2

Stage 2a.2 starts once the maximum shear stress is reached not only in crack J but in crack I as well. Then, between cracks I and J, the laminate can be divided into four parts as shown in Figure 4.6. This division depends on the location of each point in the bond-slip curve.

The regions between each crack tip and the points where the maximum shear stress is reached, $x_{LM,left}$ and $x_{LM,right}$, are located in the descending branch of the bond-slip relationship (Zone II). Consequently, along these regions, microcracks initiate in the concrete but it is still possible to transfer the tensile force from the laminate to the support. Between the maximum shear stress locations, $x_{LM,left}$ and $x_{LM,right}$, the interface behaves like a linear elastic material, in the ascending branch of the bond-slip relationship (Zone I).

At increasing deformations, the points of maximum shear stress move towards the zero shear stress point, x_K. Therefore, the length of the two areas of Zone II increases as long as the length of Zone I decreases. At the same time, in a general case, when the load increases, the position of the zero shear stress point, x_K, situated between $x_{LM,left}$ and $x_{LM,right}$, moves towards crack I. In addition, $x_{LM,left}$ and $x_{LM,right}$ move together with the zero shear stress point x_K as it moves towards the less-loaded crack (crack I). It should be mentioned that in a pure flexure case, as the applied load increases, the zero shear stress point x_K is fixed at the midpoint of the crack distance.

The tensile stress profile is very similar to that of Stages 1 and 2a.1, with a minimum value at the zero shear stress location. The higher the applied load, the greater the laminate tensile stress and strain under each crack tip and in between them.

In addition, the slip distribution is similar to the previous stages. The slip has a zero value at x_K, and increases in both directions towards crack I and J. The slope in Zone II is steeper than in Zone I.

Figure 4.6 shows a scheme of the interfacial shear and laminate tensile stress distribution between both cracks I and J.

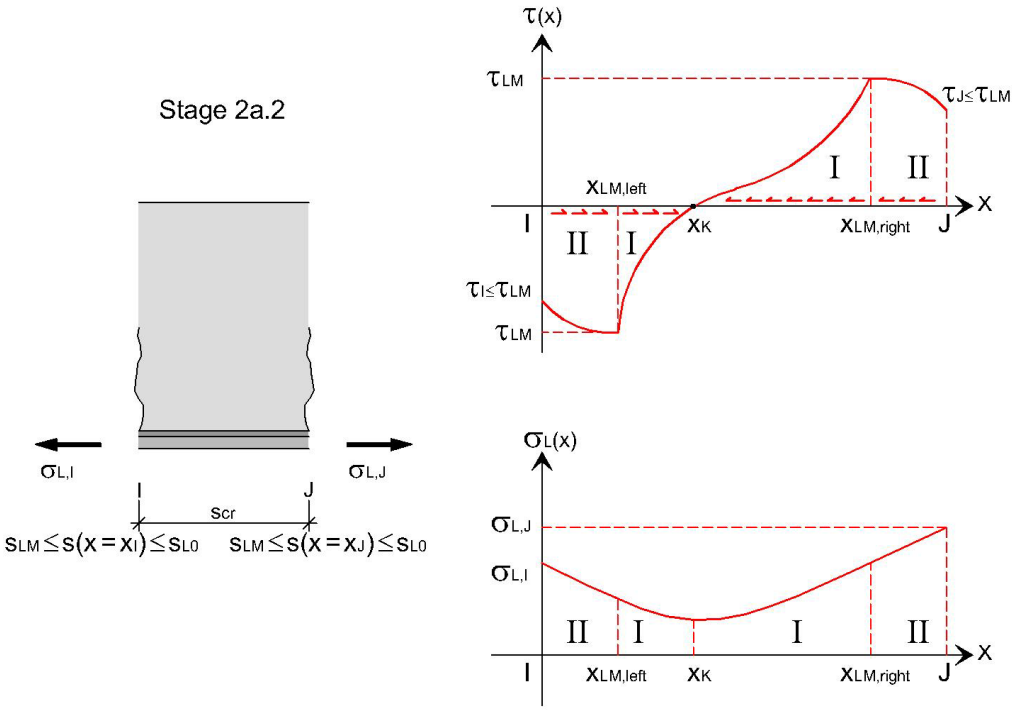

Figure 4.6. Interfacial shear and laminate tensile stress distribution between two cracks in Stage 2a.2.

Stage 2b

In a typical range of crack distances and at high load levels (during Stage 2a.1 or 2a.2), the maximum shear stress which is moving away from crack J ($x_{LM,right}$) may reach the less-loaded crack (Figure 4.7). When the maximum shear stress τ_{LM} arrives at crack I, the following observations can be drawn:

1) The transferred force between crack I and J reaches its maximum value.
2) The complete bonded length is in Zone II of the bond-slip relationship. Therefore, microcracks have initiated along the entire crack distance.
3) There is no zero shear stress point and the shear stresses have the same algebraic sign.
4) The laminate tensile stress is at maximum in crack J and is at minimum in crack I.
5) The complete bonded length is sliding in relation to the support from crack I towards crack J.

From this point on, Stage 2a.1 or 2a.2 turn into what will be called Stage 2b. The behavior of the interface during Stage 2b is described as follows:

1) The shear stresses in betweeen both cracks I and J are progressively reduced as Stage 2b evolves, because of the slip increase.
2) As a consequence, the transferred force between both crack tips, which is given by the area under the shear stress distribution, decreases progressively as well.
3) The decreasing trend on the transferred force indicates that in a usual load control situation, the laminate suddenly debonds in the limit between Stage 2a.1 or 2a.2 and Stage 2b.
4) Therefore, from this point on, the description of the phenomena is only of academic interest.
5) If the internal steel remains unyielded in both cracks, Stage 2b will finish after reaching the maximum sliding along the complete bonded length. At this point, the laminate will be completely detached. In case the internal steel has yielded in crack J during the current or the previous stages, the end of Stage 2b will occur when the maximum sliding is reached in crack J. Under these circumstances, the laminate will still be bonded along the crack distance, and Stage 3b (and not Stage 3a) will initiate.

Stage 2b occurs as a result of the existence of a shear force acting on the flexural crack tips. It will never occur if the segment between two subsequent cracks is loaded in pure flexure.

In addition, if the bonded length between two cracks is long enough, Stage 3a will be initiated before the maximum shear stress location $x_{LM,right}$ arrives at crack I.

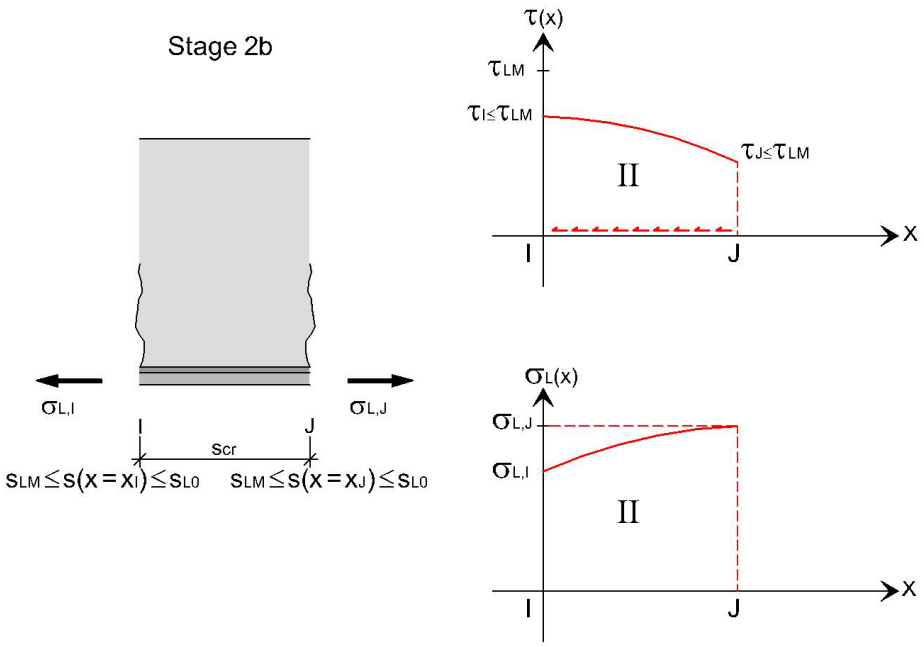

Figure 4.7. Shear stress distribution once the maximum shear stress is reached in crack I.

Stage 3

In every form of Stage 3, a horizontal macrocrack opens in crack J and propagates towards crack I. Part of the laminate is detached from the concrete surface and the remaining bonded length is in Zone I or II of the bond-slip relationship. Stage 3a starts at the end of Stage 2a.2, if Stage 2b has not appeared. Stage 3b can appear at the end of Stage 3a or alternatively, in some particular cases after Stage 2b. The evolution of the debonding process during both Stages 3a and 3b is described below.

Stage 3a

Looking back to Figure 4.6, an increase in the applied load causes an increase in the slip in crack J (and a decrease on the shear stress). Alternatively to Stage 2b, if the distance between the cracks is long enough, the slip in crack J can eventually reach the maximum value s_{L0}. At this point Stage 3a initiates. A real macrocrack between the concrete and the laminate opens. As the applied load on the beam increases, the extension of the macrocrack between the maximum slip location x_{L0} and crack J propagates from crack J to crack I. Therefore, the bonded length between the maximum slip location and crack I decreases.

In Figure 4.8, a scheme of the shear stress distribution during Stage 3a is shown. It can be noticed that along the interfacial macrocrack the shear stresses are zero because the laminate is detached. Thus no transfer of force is possible in this area. In relation to the laminate tensile stresses, it should be pointed out that they remain constant along the macrocrack length.

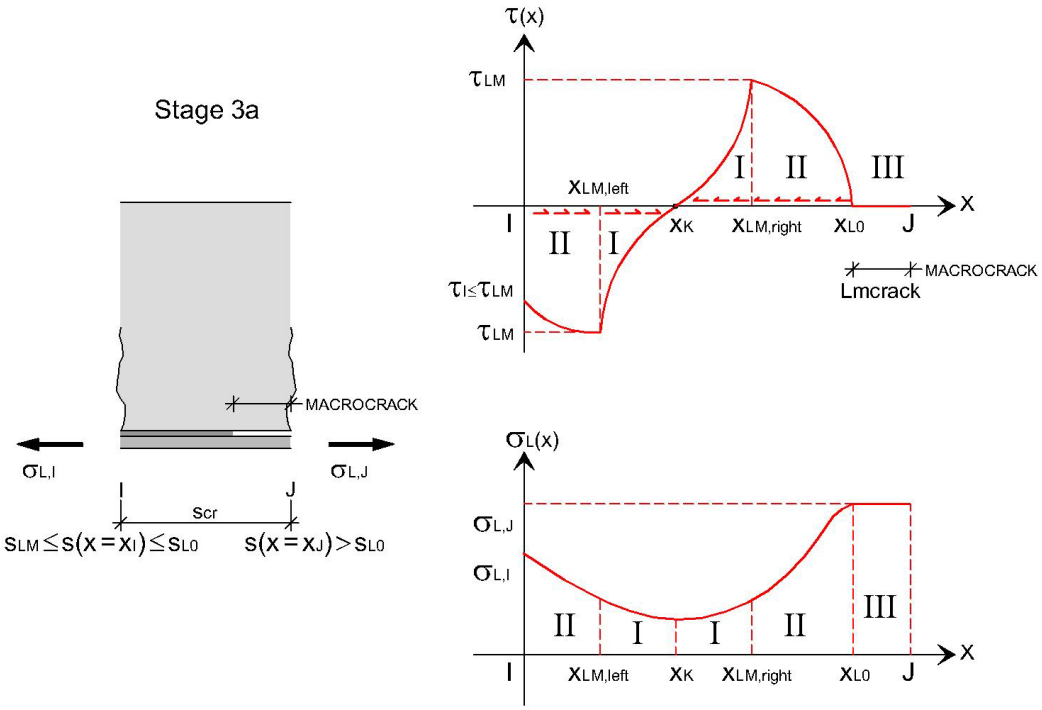

Figure 4.8. Interfacial shear and laminate tensile stress distribution between two cracks in Stage 3a.

As in the previous stages, the sliding is calculated from the shear stresses through the bond-slip relationship. However, along the debonded length, it is calculated as the maximum sliding s_{L0} plus the elastic elongation of the laminate over the real macrocrack.

Stage 3b

Stage 3b appears in two different situations that are described below. The main difference between them is the shear stress in crack I at the beginning of the stage. In the first situation, the shear stress will be at maximum, while in the second situation, it will be lower than the maximum value τ_{LM}.

1) In case the laminate is long enough for the non-appearance of Stage 2b, during Stage 3a (in a similar manner than for a short bonded length during Stages 2a.1 or 2a.2), the maximum shear stress location, $x_{LM,right}$, may reach crack I. Then, the transferred force between both cracks will attain its maximum value. From this point on, Stage 3b starts and the same observations described in Stage 2b for the complete bonded length can be applied here for the remaining bonded interface.
2) It should be mentioned that a particular case of Stage 3b will initiate at the end of Stage 2b in case the internal steel has yielded only in crack J. The macrocrack just opens and starts propagating at the beginning of Stage 3b. At this point, the complete interface is in Zone II of the bond-slip relationship, and the shear stresses in crack I are lower than the maximum shear stress τ_{LM}, because $x_{LM,right}$ has reached crack I in the previous Stage 2b.

Stage 3b is described in Figure 4.9. The entire laminate is in Zone II or III of the bond-slip curve. The same observations of Stage 2b in terms of laminate tensile stress and transferred force can be applied here for the remaining bonded length.

In case the crack distance is long enough that Stage 2b does not develop, a macrocrack opens when the maximum sliding is reached in crack J. During the macrocrack growth, the maximum shear stress can reach crack I. From this point on, in a normal load control situation, an attempt to increase the applied load will lead into a sudden laminate debonding. In the event that displacement control is possible, the macrocrack propagation process will be observed. Therefore, Stage 3b will develop. In a similar manner, and as previously mentioned, for short crack distances, Stage 2b and Stage 3b will only appear under displacement control.

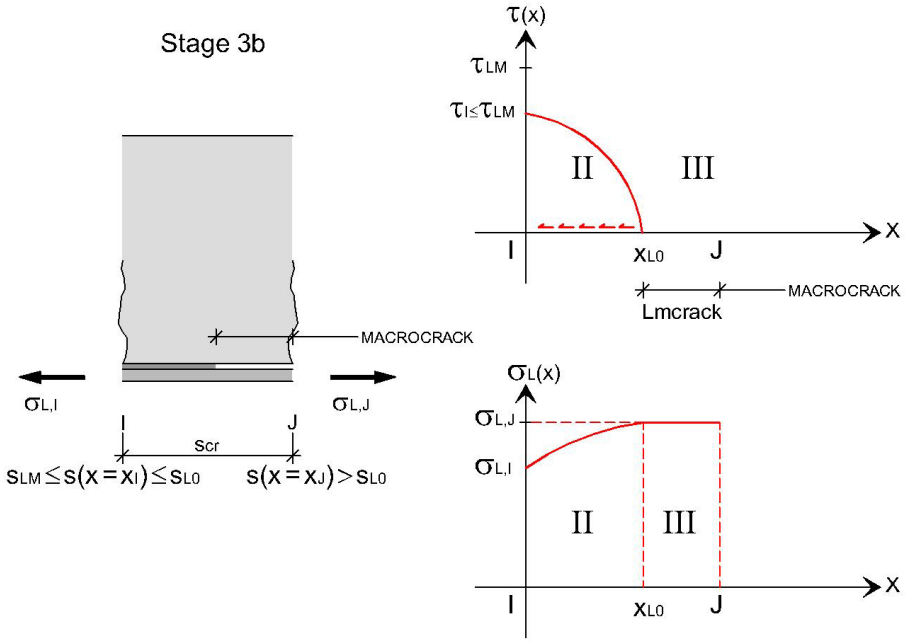

Figure 4.9. Shear stress and laminate tensile stress distribution in Stage 3b once the maximum shear stress reaches crack I.

Stage 3c

If the laminate is long enough, the macrocrack may initiate under both cracks tips: first in crack J at the beginning of Stage 3a, and later on in crack I, after the maximum slip s_{L0} is attained at this location (Figure 4.10). No force transfer will be possible along both macrocracks. In the remaining bonded length, the same general behavior as Stage 2a.2 will be observed. As the applied load increases, both macrocracks grow and the remaining bonded length decreases. At the same time, the zero shear stress location moves towards crack I and, both maximum shear stress locations move closer to the zero shear stress location, x_K. This situation will be infrequent, as the typical range of crack distances is classified as a short enough for the non-development of this stage.

In addition, in a pure flexure case, Stage 3a will never exist, and a macrocrack will be initiated simultaneously under both cracks I and J. For a typical crack distance, Stage 3c

will be initiated when both maximum shear stresses have almost reached the zero shear stress location.

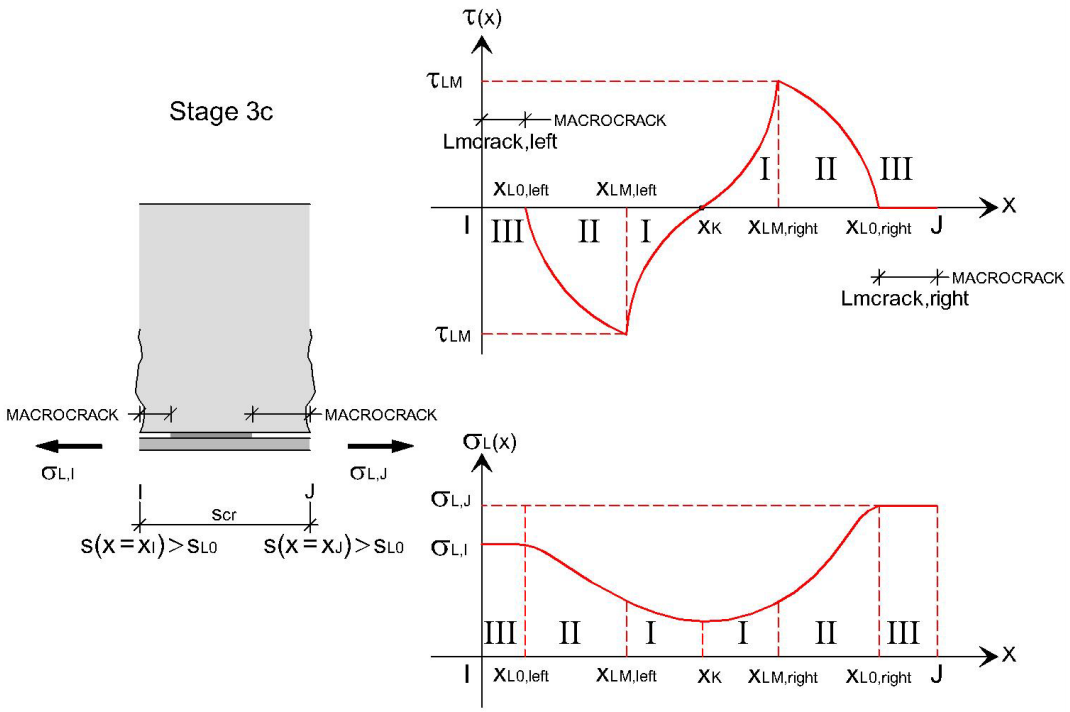

Figure 4.10. Shear stress and laminate tensile stress distribution between two cracks in Stage 3c.

Influence of steel yielding

In a beam under transverse loads, the yielding of the internal steel constitutes an important factor of the debonding process. By choosing those well-known tests without external anchorages that failed due to the peeling effect from the bending test database, the laminate debonded after internal steel yielding in 85.8 percent of the total number of assembled tests.

As shown in Figure 4.11, once the steel yields, the internal reinforcement is not able to increase its tensile stress. The subsequent load increments will be assumed alone by the external reinforcement. As a consequence, the tensile force of the laminate will increase more rapidly, and the debonding process will accelerate.

Depending on the steel yielding, three cases can be distinguished between two cracks. Figure 4.12 summarizes them. In the first case, the steel rebars behave in a linear elastic manner. In the second case, the steel has only yielded in the crack with the highest tensile stress. Finally, in the last case, the steel has yielded in both cracks. The transfer of the tensile force from the concrete to both the internal steel and the laminate is different in each case. Special attention should be drawn in the case where the internal steel has yielded in both cracks because the total tensile force increment between the two cracks is transferred through shear stresses from the concrete support to the laminate.

The yielding of the internal steel usually occurs during the Stages 2, or 3 of the debonding process where part of the interface is behaving in Zone II of the bond-slip relationship and the debonding process is in an advanced situation.

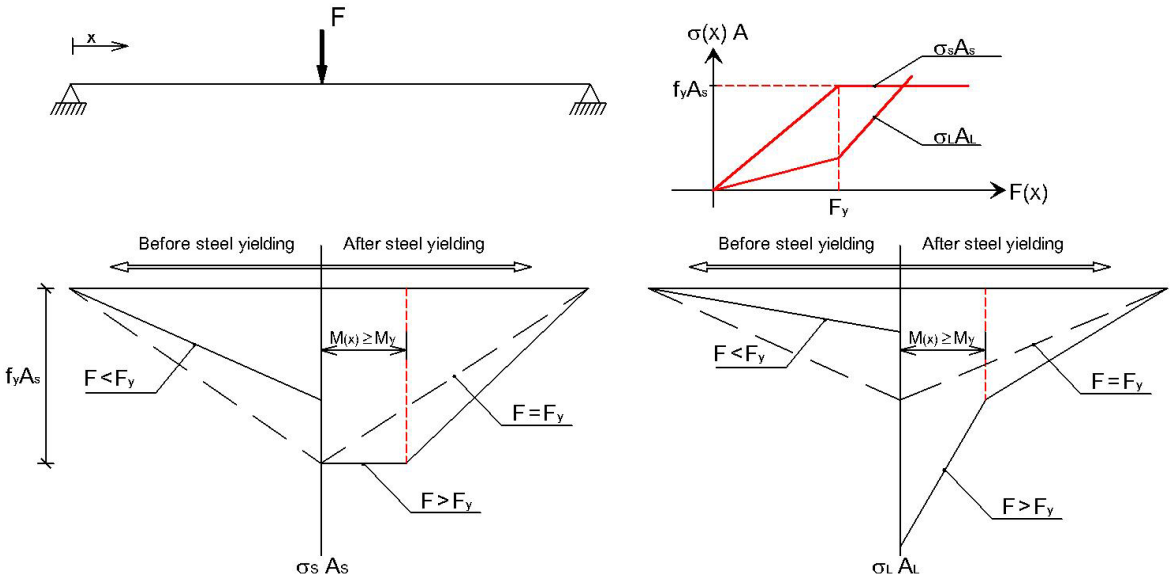

Figure 4.11. Comparison of the tensile stresses in the internal reinforcement and the laminate before and after steel yielding.

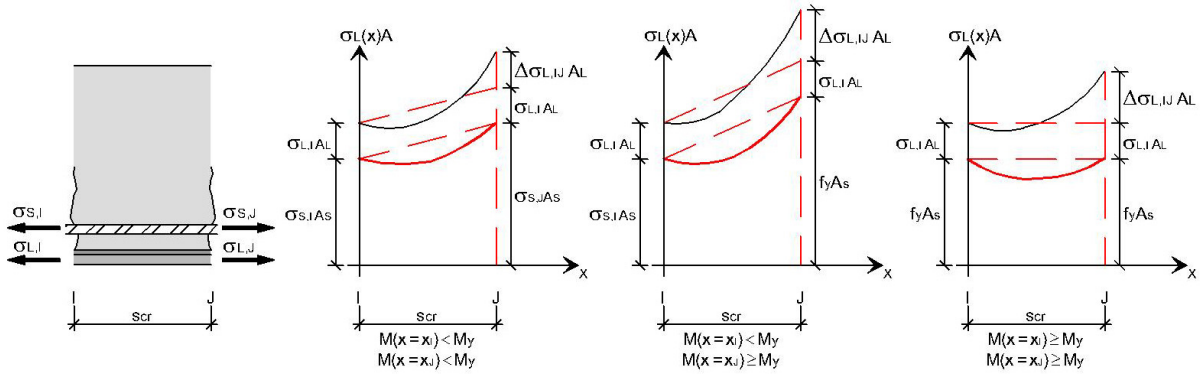

Figure 4.12. Cases between two cracks depending on the steel tensile stress.

4.3.2. General equations for the stress distribution between two cracks

Once the propagation process is known, the governing equations (4.1) and (4.3) must be solved to find the stresses on the interface and on the laminate in the different stages described in the previous paragraphs.

Firstly, to solve the differential equations (4.1) and (4.3) it is necessary to define the concrete stress in the fiber in contact with the laminate along the bonded length. In a cracked section, the tensile stress is entirely absorbed by the internal and the external reinforcement. However, in the vicinity of the cracks there is a tensile stress transfer between the reinforcement and the concrete due to the existence of shear stresses. This

concrete contribution between cracks (usually known as tension stiffening) reduces the value of tensile stresses in the laminate.

It is difficult to deal with the definition of the concrete's stress distribution because of the complexity of the concrete cracking problem. As a first approximation, knowing that the concrete stress in the crack tips is equal to zero, and assuming a value for the concrete stress in half of the crack distance, a parabolic concrete stress distribution can be assumed between two cracks.

As a maximum, the concrete stress in half of the crack distance can be assumed as the concrete tensile strength f_{ctm}. If the stress in the concrete exceeds this value, another crack will form in between the two existing cracks. Therefore, the concrete stress in half of the crack distance can be defined as a fraction β of the concrete tensile strength.

$$\sigma_{c,b}\left(x=\frac{s_{cr}}{2}\right)=\beta f_{ctm} \tag{4.20}$$

It is very difficult to give a value for the β fraction, which is affected moreover by the presence of steel reinforcement. However, as will be shown later on in this chapter, the results do not dependent heavily on this β parameter.

Assuming a parabolic tensile stress distribution in the concrete, as a function of the concrete tensile strength (equation (4.21)), the differential equations (4.1) and (4.3) will turn into (4.22) and (4.24) respectively.

$$\sigma_{c,b}(x)=-\frac{4}{s_{cr}^2}\beta f_{ctm}\left((x-x_I)^2-s_{cr}(x-x_I)\right) \tag{4.21}$$

$$\frac{d^2\sigma_L^I}{dx^2}(x)-\Omega_1^2\sigma_L^I(x)=-\Omega_1^2\mu\left((x-x_I)^2-s_{cr}(x-x_I)\right) \tag{4.22}$$

where:

Ω_1: constant given by equation (4.2)
μ: constant given by equation (4.23)

$$\mu=-\frac{4}{s_{cr}^2}\beta f_{ctm}\frac{E_L}{E_c} \tag{4.23}$$

$$\frac{d^2\sigma_L^{II}}{dx^2}(x)+\Omega_2^2\sigma_L^{II}(x)=\Omega_2^2\mu\left((x-x_I)^2-s_{cr}(x-x_I)\right) \tag{4.24}$$

where:

Ω_2: constant given by equation (4.4)

The general solution to the governing equations (4.22) and (4.24) is given by equations (4.25) and (4.26) respectively, as a function of the integration constants C_1, C_2, C_3 and

C_4 which will be derived by applying the appropriate boundary conditions detailed in Appendix D.

$$\sigma_L^I(x) = C_1 \cosh(\Omega_1 x) + C_2 \sinh(\Omega_1 x) + \frac{2\mu}{\Omega_1^2} + \mu\left((x - x_I)^2 - s_{cr}(x - x_I)\right) \tag{4.25}$$

$$\sigma_L^{II}(x) = C_3 \cos(\Omega_2 x) + C_4 \sin(\Omega_2 x) - \frac{2\mu}{\Omega_2^2} + \mu\left((x - x_I)^2 - s_{cr}(x - x_I)\right) \tag{4.26}$$

Theoretically, in defining the concrete tensile stress contribution, it should be assumed that there is a slip, not only between the concrete and the external reinforcement, but also between the concrete and the internal rebars. In this case, a more accurate way to describe the interfacial crack propagation process can be found. After establishing a bond-slip relationship for the steel rebars, two problems should be solved, one for each interface. However, this accurate solution for both interface problems is rejected due to its complexity. The approach developed in this section will be applied from this point onwards.

4.3.3. Stress distribution between two cracks prior to the initiation of the debonding process

In the following, the tensile stresses in the laminate are given for the different stages studied. To obtain the interfacial shear stresses, this expression must be differentiated by x and multiplied by the thickness of the laminate, as shown in equation (3.9) of Chapter 3. Once the shear stress is known, the relative displacement between concrete and the laminate is easily found using the bond-slip relationship (equation (3.12) of Chapter 3).

Stage 1: $s(x = x_J) \leq s_{LM}$

For $x_I \leq x \leq x_J$ (Zone I)

$$\sigma_L^I(x) = \frac{1}{\sinh(\Omega_1 s_{cr})}\left\{\left(\sigma_{L,I} - \frac{2\mu}{\Omega_1^2}\right)\sinh(\Omega_1(x_J - x)) + \left(\sigma_{L,J} - \frac{2\mu}{\Omega_1^2}\right)\sinh(\Omega_1(x - x_I))\right\} + \frac{2\mu}{\Omega_1^2} + \mu\left((x - x_I)^2 - s_{cr}(x - x_I)\right) \tag{4.27}$$

Stage 2a.1: $s(x = x_J) > s_{LM}$ and $s(x = x_I) \le s_{LM}$

For $x_I \le x \le x_K$ (Zone I)

$$\sigma_{L}^{I}(x) = \frac{1}{\cosh(\Omega_1(x_K - x_I))}\left\{\left(\sigma_{L,I} - \frac{2\mu}{\Omega_1^2}\right)\cosh(\Omega_1(x_K - x)) - \frac{\mu}{\Omega_1}(2(x_K - x_I) - s_{cr})\right. \\ \left.\sinh(\Omega_1(x - x_I))\right\} + \frac{2\mu}{\Omega_1^2} + \mu\left((x - x_I)^2 - s_{cr}(x - x_I)\right) \tag{4.28}$$

For $x_K \le x \le x_{LM}$ (Zone I)

$$\sigma_{L}^{I}(x) = \frac{1}{\sinh(\Omega_1(x_{LM} - x_K))}\left\{\left(\frac{\tau_{LM}}{t_L\Omega_1} - \frac{\mu}{\Omega_1}(2(x_{LM} - x_I) - s_{cr})\right)\cosh(\Omega_1(x - x_K)) + \right. \\ \left. + \frac{\mu}{\Omega_1}(2(x_K - x_I) - s_{cr})\cosh(\Omega_1(x_{LM} - x))\right\} + \frac{2\mu}{\Omega_1^2} + \mu\left((x - x_I)^2 - s_{cr}(x - x_I)\right) \tag{4.29}$$

For $x_{LM} \le x \le x_J$ (Zone II)

$$\sigma_{L}^{II}(x) = \frac{1}{\cos(\Omega_2(x_J - x_{LM}))}\left\{\left(\sigma_{L,J} + \frac{2\mu}{\Omega_2^2}\right)\cos(\Omega_2(x - x_{LM})) - \left(\frac{\tau_{LM}}{t_L\Omega_2} - \right.\right. \\ \left.\left. - \frac{\mu}{\Omega_2}(2(x_{LM} - x_I) - s_{cr})\right)\sin(\Omega_2(x_J - x))\right\} - \frac{2\mu}{\Omega_2^2} + \mu\left((x - x_I)^2 - s_{cr}(x - x_I)\right) \tag{4.30}$$

The location of the points of zero and of maximum stress, x_K and x_{LM} respectively, can be found by solving a system of equations formed by (4.31) and (4.32).

$$\frac{1}{\cosh(\Omega_1(x_K - x_I))}\left\{\left(\sigma_{L,I} - \frac{2\mu}{\Omega_1^2}\right) - \frac{\mu}{\Omega_1}(2(x_K - x_I) - s_{cr})\sinh(\Omega_1(x_K - x_I))\right\} = \\ \frac{1}{\sinh(\Omega_1(x_{LM} - x_K))}\left\{\frac{\tau_{LM}}{t_L\Omega_1} - \frac{\mu}{\Omega_1}(2(x_{LM} - x_I) - s_{cr}) + \frac{\mu}{\Omega_1}(2(x_K - x_I) - s_{cr})\right. \\ \left.\cosh(\Omega_1(x_{LM} - x_K))\right\} \tag{4.31}$$

$$\frac{1}{\sinh(\Omega_1(x_{LM} - x_K))}\left\{\left(\frac{\tau_{LM}}{t_L\Omega_1} - \frac{\mu}{\Omega_1}(2(x_{LM} - x_I) - s_{cr})\right)\cosh(\Omega_1(x_{LM} - x_K))\right. \\ \left. + \frac{\mu}{\Omega_1}(2(x_K - x_I) - s_{cr})\right\} + \frac{2\mu}{\Omega_1^2} = \frac{1}{\cos(\Omega_2(x_J - x_{LM}))}\left\{\left(\sigma_{L,J} + \frac{2\mu}{\Omega_2^2}\right) - \right. \\ \left. - \left(\frac{\tau_{LM}}{t_L\Omega_2} - \frac{\mu}{\Omega_2}(2(x_{LM} - x_I) - s_{cr})\right)\sin(\Omega_2(x_J - x_{LM}))\right\} - \frac{2\mu}{\Omega_2^2} \tag{4.32}$$

Stage 2a.2: $s(x = x_J) > s_{LM}$ and $s(x = x_I) > s_{LM}$

For $x_I \le x \le x_{LM,left}$ (Zone II)

$$\sigma_L^{II}(x) = \frac{1}{\cos\left(\Omega_2\left(x_{LM,left} - x_I\right)\right)}\left\{\left(\sigma_{L,I} + \frac{2\mu}{\Omega_2^2}\right)\cos\left(\Omega_2\left(x_{LM,left} - x\right)\right) - \left[\frac{\tau_{LM}}{t_L\Omega_2} + \right.\right.$$
$$\left.\left. + \frac{\mu}{\Omega_2}\left(2\left(x_{LM,left} - x_I\right) - s_{cr}\right)\right]\sin\left(\Omega_2\left(x - x_I\right)\right)\right\} - \frac{2\mu}{\Omega_2^2} + \mu\left(\left(x - x_I\right)^2 - s_{cr}\left(x - x_I\right)\right) \tag{4.33}$$

For $x_{LM,left} \le x \le x_K$ (Zone I)

$$\sigma_L^{I}(x) = \frac{1}{\sinh\left(\Omega_1\left(x_K - x_{LM,left}\right)\right)}\left\{\left[\frac{\tau_{LM}}{t_L\Omega_1} + \frac{\mu}{\Omega_1}\left(2\left(x_{LM,left} - x_I\right) - s_{cr}\right)\right]\cosh\left(\Omega_1\left(x_K - x\right)\right) - \right.$$
$$\left. - \frac{\mu}{\Omega_1}\left(2\left(x_K - x_I\right) - s_{cr}\right)\cosh\left(\Omega_1\left(x - x_{LM,left}\right)\right)\right\} + \frac{2\mu}{\Omega_1^2} + \mu\left(\left(x - x_I\right)^2 - s_{cr}\left(x - x_I\right)\right) \tag{4.34}$$

For $x_K \le x \le x_{LM,right}$ (Zone I)

$$\sigma_L^{I}(x) = \frac{1}{\sinh\left(\Omega_1\left(x_{LM,right} - x_K\right)\right)}\left\{\left[\frac{\tau_{LM}}{t_L\Omega_1} - \frac{\mu}{\Omega_1}\left(2\left(x_{LM,right} - x_I\right) - s_{cr}\right)\right]\cosh\left(\Omega_1\left(x - x_K\right)\right) + \right.$$
$$\left. + \frac{\mu}{\Omega_1}\left(2\left(x_K - x_I\right) - s_{cr}\right)\cosh\left(\Omega_1\left(x_{LM,right} - x\right)\right)\right\} + \frac{2\mu}{\Omega_1^2} + \mu\left(\left(x - x_I\right)^2 - s_{cr}\left(x - x_I\right)\right) \tag{4.35}$$

For $x_{LM,right} \le x \le x_J$ (Zone II)

$$\sigma_L^{II}(x) = \frac{1}{\cos\left(\Omega_2\left(x_J - x_{LM,right}\right)\right)}\left\{\left(\sigma_{L,J} + \frac{2\mu}{\Omega_2^2}\right)\cos\left(\Omega_2\left(x - x_{LM,right}\right)\right) - \left[\frac{\tau_{LM}}{t_L\Omega_2} - \right.\right.$$
$$\left.\left. - \frac{\mu}{\Omega_2}\left(2\left(x_{LM,right} - x_I\right) - s_{cr}\right)\right]\sin\left(\Omega_2\left(x_J - x\right)\right)\right\} - \frac{2\mu}{\Omega_2^2} + \mu\left(\left(x - x_I\right)^2 - s_{cr}\left(x - x_I\right)\right) \tag{4.36}$$

All these formulae depend on the location of three points: two of them, $x_{LM,left}$ and $x_{LM,right}$, are the ones where the shear stress between cracks I and J is at maximum (τ_{LM}) and the third one is the point between $x_{LM,left}$ and $x_{LM,right}$ where the shear stress is zero (x_K). All of them are obtained by solving a set of three equations given by (4.37), (4.38) and (4.39).

$$\frac{1}{\cos\left(\Omega_2\left(x_{LM,left}-x_I\right)\right)}\left\{\left(\sigma_{L,I}+\frac{2\mu}{\Omega_2^2}\right)-\left[\frac{\tau_{LM}}{t_L\Omega_2}+\frac{\mu}{\Omega_2}\left(2\left(x_{LM,left}-x_I\right)-s_{cr}\right)\right]\right.$$
$$\left.\sin\left(\Omega_2\left(x_{LM,left}-x_I\right)\right)\right\}-\frac{2\mu}{\Omega_2^2}=\frac{1}{\sinh\left(\Omega_1\left(x_K-x_{LM,left}\right)\right)}\left\{\left[\frac{\tau_{LM}}{t_L\Omega_1}+\right.\right. \quad (4.37)$$
$$\left.\left.+\frac{\mu}{\Omega_1}\left(2\left(x_{LM,left}-x_I\right)-s_{cr}\right)\right]\cosh\left(\Omega_1\left(x_K-x_{LM,left}\right)\right)-\frac{\mu}{\Omega_1}\left(2\left(x_K-x_I\right)-s_{cr}\right)\right\}+\frac{2\mu}{\Omega_1^2}$$

$$\frac{1}{\cos\left(\Omega_2\left(x_J-x_{LM,right}\right)\right)}\left\{\left(\sigma_{L,J}+\frac{2\mu}{\Omega_2^2}\right)-\left[\frac{\tau_{LM}}{t_L\Omega_2}-\frac{\mu}{\Omega_2}\left(2\left(x_{LM,right}-x_I\right)-s_{cr}\right)\right]\right.$$
$$\left.\sin\left(\Omega_2\left(x_J-x_{LM,right}\right)\right)\right\}-\frac{2\mu}{\Omega_2^2}=\frac{1}{\sinh\left(\Omega_1\left(x_{LM,right}-x_K\right)\right)}\left\{\left[\frac{\tau_{LM}}{t_L\Omega_1}-\right.\right. \quad (4.38)$$
$$\left.\left.-\frac{\mu}{\Omega_1}\left(2\left(x_{LM,right}-x_I\right)-s_{cr}\right)\right]\cosh\left(\Omega_1\left(x_{LM,right}-x_K\right)\right)+\frac{\mu}{\Omega_1}\left(2\left(x_K-x_I\right)-s_{cr}\right)\right\}+\frac{2\mu}{\Omega_1^2}$$

$$\frac{1}{\sinh\left(\Omega_1\left(x_K-x_{LM,left}\right)\right)}\left\{\frac{\tau_{LM}}{t_L\Omega_1}+\frac{\mu}{\Omega_1}\left(2\left(x_{LM,left}-x_I\right)-s_{cr}\right)-\frac{\mu}{\Omega_1}\left(2\left(x_K-x_I\right)-s_{cr}\right)\right.$$
$$\left.\cosh\left(\Omega_1\left(x_K-x_{LM,left}\right)\right)\right\}=\frac{1}{\sinh\left(\Omega_1\left(x_{LM,right}-x_K\right)\right)}\left\{\frac{\tau_{LM}}{t_L\Omega_1}+\frac{\mu}{\Omega_1}\left(2\left(x_{LM,right}-x_I\right)-s_{cr}\right)+\right. \quad (4.39)$$
$$\left.+\frac{\mu}{\Omega_1}\left(2\left(x_K-x_I\right)-s_{cr}\right)\cosh\left(\Omega_1\left(x_{LM,right}-x_K\right)\right)\right\}$$

If the concrete's contribution is not taken into account in Stage 2a.2 (μ = 0), both lengths of Zone I, which are defined as the distance between the maximum shear stress locations and the zero shear stress point, (x_K - $x_{LM,left}$) and ($x_{LM,right}$ - x_K), will be identical. Therefore, as the debonding process develops, the length of Zone II near crack J increases at the same amount as the length of Zone II near crack I. Under these circumstances, only the location of the zero shear stress point and one of the maximum shear stress points will be required. Both will be obtained by solving only equations (4.37) and (4.38).

Stage 2b: $s(x = x_J) > s_{LM}$ and $s(x = x_I) > s_{LM}$

As explained in §4.3.1, during Stage 2a.1 or 2a.2, the maximum shear stress location, $x_{LM,right}$ which is moving from crack J, may reach crack I. This is only possible if the crack distance is shorter than a certain limit which will be obtained at the end of this section.

From this point on, the solution from equations (4.37) to (4.39) for the maximum and zero shear stress location will give negative values, indicating that the derived equations are no longer valid. During Stage 2b, the laminate tensile stresses are derived from equation (4.40).

For $x_I \le x \le x_J$ (Zone II)

$$\sigma_{L}^{II}(x) = \frac{1}{\sin(\Omega_2 s_{cr})}\left\{\left(\sigma_{L,J} + \frac{2\mu}{\Omega_2^2}\right)\sin(\Omega_2(x - x_I)) + \left(\sigma_{L,I} + \frac{2\mu}{\Omega_2^2}\right)\sin(\Omega_2(x_J - x))\right\} - \frac{2\mu}{\Omega_2^2} + \mu\left((x - x_I)^2 - s_{cr}(x - x_I)\right) \quad (4.40)$$

Since the complete interface is in Zone II of the bond-slip relationship, the shear stress distribution will decrease during Stage 2b (see Figure 4.7). Consequently, for the development of Stage 2b, the shear stress in crack I should be lower than the maximum value τ_{LM}, as shown in equation (4.41).

$$\frac{\Omega_2 t_L}{\sin(\Omega_2 s_{cr})}\left\{\left(\sigma_{L,J} + \frac{2\mu}{\Omega_2^2}\right) - \left(\sigma_{L,I} + \frac{2\mu}{\Omega_2^2}\right)\cos(\Omega_2 s_{cr})\right\} - \mu t_L s_{cr} \le \tau_{LM} \quad (4.41)$$

The tensile stresses $\sigma_{L,J}$ and $\sigma_{L,I}$ can be related through a function υ that depends on the bending moment acting on each crack, which is equivalent to saying that υ depends on the bending moment and shear force acting on crack J.

$$\sigma_{L,I} = \upsilon \sigma_{L,J} \quad (4.42)$$

where:

$$\upsilon = \begin{cases} \dfrac{M(x = x_I)}{M(x = x_J)} & \text{if } M(x = x_J) \le M_y \text{ and } M(x = x_I) \le M_y \\ \dfrac{M(x = x_I)\left(1 - \dfrac{f_y A_s z_s}{M_y}\right)}{M(x = x_J) - f_y A_s z_s} & \text{if } M(x = x_J) > M_y \text{ and } M(x = x_I) \le M_y \\ \dfrac{M(x = x_I) - f_y A_s z_s}{M(x = x_J) - f_y A_s z_s} & \text{if } M(x = x_J) > M_y \text{ and } M(x = x_I) > M_y \end{cases} \quad (4.43)$$

This relationship is plotted in Figure 4.13 for a general example in a three or four-point bending configuration. Under this load configuration, the shear force is constant along the shear span. As observed, the tensile stress in crack I is proportional to the tensile stress in crack J (υ is constant) while the steel is still linear elastic. Once the internal steel yields in crack J, the laminate should by itself absorb the tensile increments at this location. Since the internal steel is still linear elastic in crack I, the tensile stress in crack J increases by an amount much higher than in crack I, resulting in a decreasing υ value. However, after the internal steel yields along the crack distance, the laminate in crack I should increase its tensile stress substantially, leading into an increasing value of υ.

After incorporating equation (4.42) into (4.41), a limit value for the laminate tensile stress in crack J during Stage 2b can be obtained as a function of the relationship between the tensile force on crack I and crack J.

$$\sigma_{L,J} \le \frac{1}{1-\upsilon\cos(\Omega_2 s_{cr})}\left[\frac{\tau_{LM}\sin(\Omega_2 s_{cr})}{\Omega_2 t_L} - \frac{2\mu}{\Omega_2^2}\left[1-\cos(\Omega_2 s_{cr})\right] + \frac{\mu s_{cr}}{\Omega_2}\sin(\Omega_2 s_{cr})\right] \quad (4.44)$$

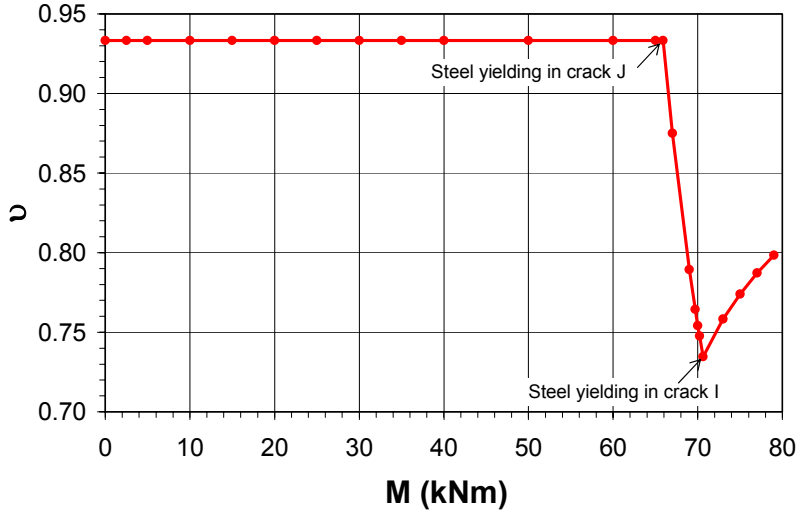

Figure 4.13. Relationship between the laminate tensile stress in crack I and in crack J in a three or four-point bending load configuration.

Equation (4.45) gives the maximum transferred force derived for a pure specimen in Chapter 3 (equation 3.76), but particularised for a laminate length equal to the distance between cracks I and J. Note that the crack distance is assumed to be shorter than or equal to the limit between a short and a long laminate given in Chapter 3 as $\pi/2\Omega_2$.

$$P_{\max,\, L=scr} = b_L \frac{\tau_{LM}}{\Omega_2}\sin(\Omega_2 s_{cr}) \quad (4.45)$$

After incorporating equation (4.45) into equation (4.44), the condition for the development of Stage 2b in terms of laminate tensile stress in crack J is expressed as (4.46).

$$\sigma_{L,J} \le \frac{1}{(1-\upsilon\cos(\Omega_2 s_{cr}))}\left\{\frac{P_{\max,\, L=scr}}{A_L} - \frac{2\mu}{\Omega_2^2}(1-\cos(\Omega_2 s_{cr})) + \frac{\mu s_{cr}}{\Omega_2}\sin(\Omega_2 s_{cr})\right\} \quad (4.46)$$

If the concrete's contribution in tension is not considered, equation (4.46) is simplified as (4.47).

$$\sigma_{L,J} \le \frac{P_{\max,\, L=scr}}{A_L(1-\upsilon\cos(\Omega_2 s_{cr}))} \quad (4.47)$$

The development of Stage 2b depends mainly on the yielding of internal steel, which influences the laminate tensile stress. In the following paragraphs, the limit condition of

Stage 2b is described according to the steel yielding and the bending moments derived from the applied force in a three or four-point bending configuration:

1) In case the internal steel has not yielded once Stage 2b is initiated, ($M(x = x_I) \leq M_y$, $M(x = x_J) \leq M_y$), υ (equation (4.43)) will be a constant value that depends only on the location of both cracks I and J (see Figure 4.13). Hence, the limit value for the development of Stage 2b, given as equation (4.46) or the more simplified equation (4.47), is constant while the applied force increases and the internal steel remains unyielded in crack J.
2) If the internal steel has yielded in crack J but not in crack I, ($M(x = x_I) \leq M_y$, $M(x = x_J) > M_y$), the value of υ (equation (4.43)) will decrease as the applied force increases (see Figure 4.13). The tensile stress limit given by equation (4.46) will decrease with increasing values of the applied force whenever the internal steel does not yield in crack I.
3) In case the internal steel has yielded in both crack tips, ($M(x = x_I) > M_y$, $M(x = x_J) > M_y$), υ (equation (4.43)) will increase as the applied force increases (see Figure 4.13). As a consequence, the limit given by equation (4.46) will increase as well.

Figure 4.14 shows the trends of the limit condition (4.46) in terms of tensile stress in crack J as the debonding process develops. As mentioned above, the limit condition for the development of Stage 2b is characterized by a horizontal branch (internal steel has not yielded in both cracks); a descending branch (steel has yielded in crack J but not in crack I); and an ascending branch (steel has yielded in both cracks).

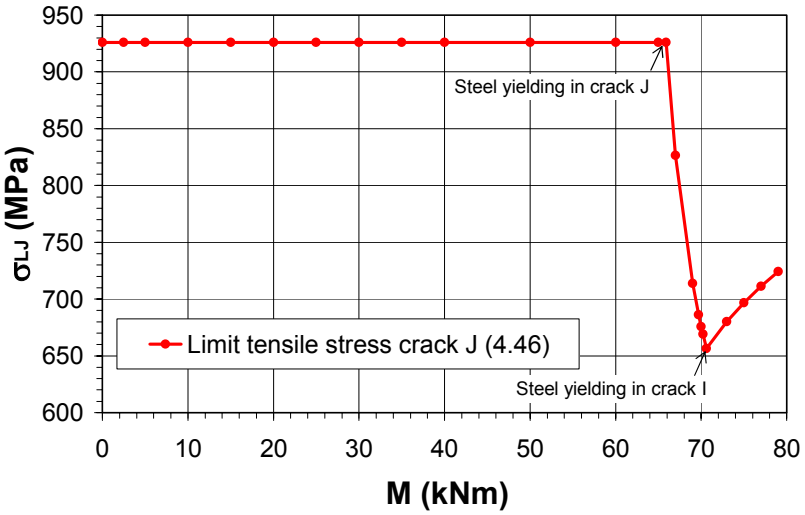

Figure 4.14. Limit condition for the development of Stage 2b.

Depending on the load configuration and the steel state, the laminate tensile stress in crack J, having a bilinear shape with a smooth slope that increases once the steel yields, will intersect with one of the branches of the limit line at the beginning of Stage 2b. Afterwards, if the tensile stress exceeds this limit, equation (4.46) will not be valid anymore and the laminate will debond. (see Figure 4.15)

Therefore, for the development of Stage 2b, it can be inferred that the tensile stress in crack J together with the applied moment on crack J, should decrease regardless of the internal steel state at first. An increase in the tensile stress in crack J can lead to a premature debonding of the laminate. Thus, the slip between concrete and laminate instead of the transferred force should be controlled for the development of Stage 2b. In a common load control situation, this stage will never occur.

In accordance with this and knowing that the complete interface is in Zone II of the bilinear relationship, the shear stress should diminish at every location along the evolution of Stage 2b. The transferred force, which is the sum of the shear stresses, will decrease as well. In addition, since the laminate tensile stress in crack I is related to crack J through equation (4.42), the limit condition of Figure 4.15 will also give a maximum value of the transferred force for those laminate lengths where Stage 2b develops (see §4.3.6).

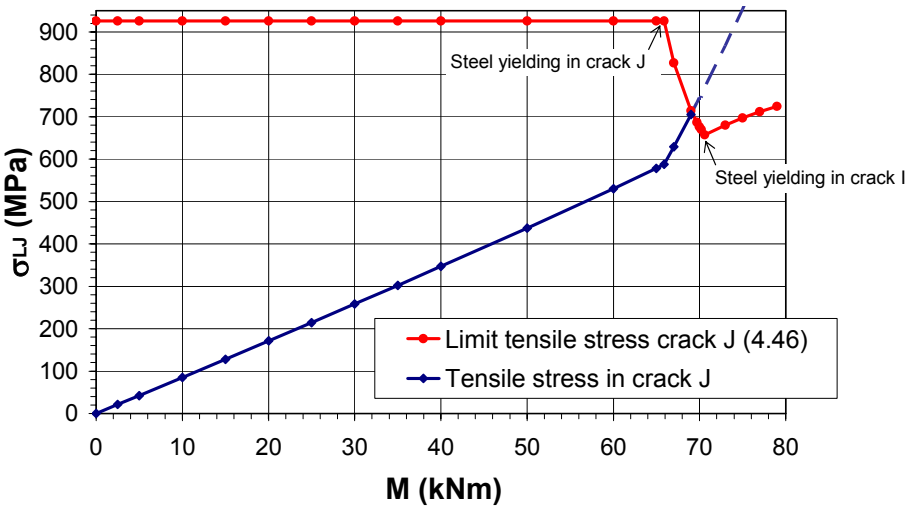

Figure 4.15. Limit condition for the development of Stage 2b together with the evolution of the tensile stress in crack J.

Short and long crack distances

As previously mentioned, during the development of Stage 2a.2, two possible situations may arise. In the first situation, the maximum sliding, s_{L0}, can be reached in crack J before the maximum shear stress location, $x_{LM,right}$ arrives at crack I. At this point, a macrocrack opens and Stage 3a is initiated (see Figure 4.8). Nevertheless this situation never occurs for short crack distances, where the maximum shear stress location $x_{LM,right}$ reaches crack I before the macrocrack opening (during Stages 2a.1 or 2a.2). In this case, Stage 2b starts (see Figure 4.7).

In the limit between both situations, the maximum shear stress location, $x_{LM,right}$, reaches crack I while the shear stress decreases to a zero value in crack J (see Figure 4.14).

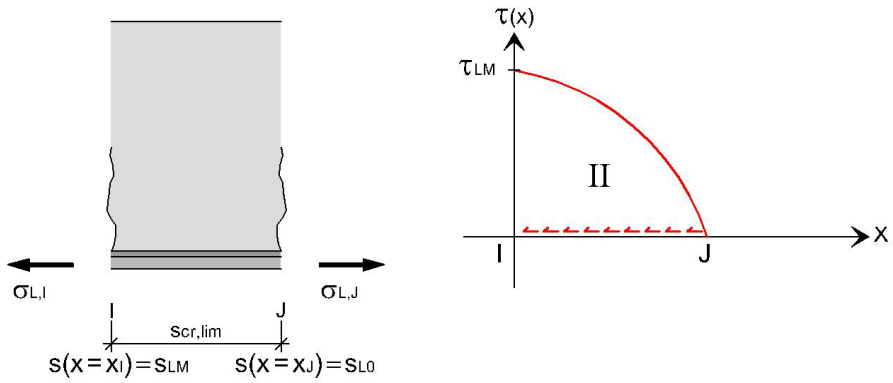

Figure 4.16. Shear stress distribution for the crack distance limit.

Both conditions can be introduced in the shear stress distribution obtained from the laminate tensile stress of Stage 2b (4.40). If so, equations (4.48) and (4.50) are obtained. Equation (4.48) gives the transferred force between crack I and J as a function of the maximum transferred force in a pure shear specimen whose length is $s_{cr,\lim}$ (see equation (3.76) of Chapter 3). The solution for equation (4.50) gives the crack distance limit, $s_{cr,\lim}$, under which Stage 2b develops.

$$\Delta\sigma_{L,IJ} A_L = \frac{P_{\max,\, L=scr,\lim}}{1+\cos\left(\Omega_2 s_{cr,\lim}\right)} \tag{4.48}$$

where:

$$P_{\max,\, L=scr,\lim} = b_L \frac{\tau_{LM}}{\Omega_2}\sin\left(\Omega_2 s_{cr,\lim}\right) \tag{4.49}$$

$$\sigma_{L,J}\cos\left(\Omega_2 s_{cr,\lim}\right) - \sigma_{L,I} = \frac{2\mu}{\Omega_2^2}\left(1-\cos\left(\Omega_2 s_{cr.\lim}\right)\right) - \frac{\mu}{\Omega_2} s_{cr,\lim}\sin\left(\Omega_2 s_{cr.\lim}\right) \tag{4.50}$$

As shown in equation (4.50), the limit length $s_{cr,\lim}$ depends on the laminate tensile stress acting in both cracks. By incorporating equation (4.42) into (4.50), the limit length $s_{cr,\lim}$ can be obtained as a function of υ. When neglecting the concrete's contribution in tension, an explicit expression for the crack distance $s_{cr,\lim}$ can be obtained as follows:

$$s_{cr,\lim} = \frac{1}{\Omega_2}\arccos(\upsilon) \tag{4.51}$$

Note that when the laminate tensile stress in crack I is zero, $\upsilon = 0$, equation (4.51) turns into the limit length between a short and long bonded length in a pure shear specimen as given in §3.3.3 of Chapter 3.

$$s_{cr,\lim} = \frac{\pi}{2\Omega_2} \tag{4.52}$$

In case the concrete's contribution in tension is neglected, Figure 4.17 shows the crack distance limit $s_{cr,\lim}$ for the development of Stage 2b as a function of the bending moment acting on crack J in a general case of a three or four-point bending configuration. The length $s_{cr,\lim}$ is a constant value in relation to the applied bending moment, but only if the steel has not yielded either in crack I or J. $s_{cr,\lim}$ starts to increase once the steel yields in crack J. The limit length decreases after the internal steel has yielded in both cracks. As an upper limit, if the crack distance is longer than the limit obtained when the internal steel has yielded in both cracks, Stage 2b will never appear.

For the crack distance limit, the transferred force between both cracks I and J, ΔP_{scr}, which is associated to the crack distance limit, $s_{cr,\lim}$, can be rewritten as equation (4.53).

$$\Delta P_{scr,\lim} = \Delta\sigma_{L,IJ} A_L = \frac{P_{\max,\, L=scr,\lim}}{1+\upsilon} \tag{4.53}$$

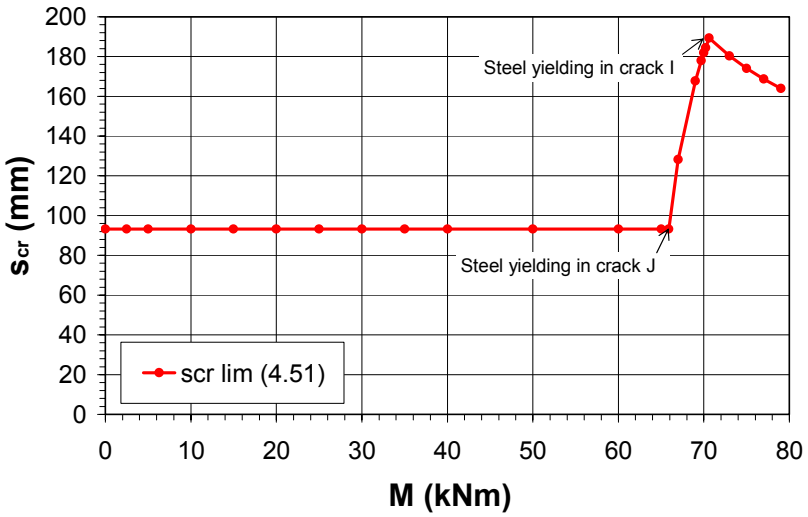

Figure 4.17. Crack distance limit for the development of Stage 2b for a certain three point bending load configuration.

The main difference regarding the crack distance limit when considering the concrete contribution in tension is that the horizontal branch associated to the non-steel-yielding in both cracks has a slight slope in this case.

From now on, the definition of a short crack distance will comprise those crack distances whose lengths are shorter than the limit $s_{cr,\lim}$, while long crack distances are longer than $s_{cr,\lim}$.

$$s_{cr} \le s_{cr,\lim} \qquad \text{Short crack distance} \tag{4.54}$$

$$s_{cr} \ge s_{cr,\lim} \qquad \text{Long crack distance} \tag{4.55}$$

4.3.4. Stress distribution between two cracks during the debonding process

The debonding process initiates when the maximum sliding s_{L0} is reached in crack J. At this point a macrocrack opens and starts its propagation process. As the macrocrack grows, an increasing part of the laminate debonds from the support.

In the following paragraphs, the laminate tensile stress equations are given for Stage 3 of the debonding process regarding the crack distance.

Long crack distances

Stage 3a: $s(x = x_J) > s_{L0}$ and $s(x = x_I) > s_{LM}$

By defining the location of the interfacial macrocrack tip as x_{L0} (where the sliding is the maximum value for Zone II, s_{L0}), the laminate bonded length between two cracks, s_{cr}, is reduced during Stage 3a by the macrocrack length L_{mcrack} (see Figure 4.8) to s_{cr} - L_{mcrack} (or x_{L0} - x_I).

Stage 3a initiates when the tensile stress in crack J reaches the value given by equation (4.56), a value associated to a sliding equal to s_{L0} in crack J:

$$\sigma_{L,J} = \frac{1}{\sin\left(\Omega_2\left(x_J - x_{LM,right}\right)\right)}\left[\frac{\tau_{LM}}{t_L\Omega_2} - \frac{\mu}{\Omega_2}\left(2\left(x_{LM,right} - x_I\right) - s_{cr}\right)\right] + \\ + \frac{\mu s_{cr}}{\Omega_2 \tan\left(\Omega_2\left(x_J - x_{LM,right}\right)\right)} - \frac{2\mu}{\Omega_2^2} \tag{4.56}$$

If the concrete's contribution in tension is not taken into account, equation (4.56) will turn into (4.57).

$$\sigma_{L,J} = \frac{\tau_{LM}}{t_L\Omega_2}\frac{1}{\sin\left(\Omega_2\left(x_J - x_{LM,right}\right)\right)} = \frac{P_{\max,L=x_J-x_K}}{A_L} \tag{4.57}$$

Since x_J - $x_{LM,right}$ is the length of Zone II, the laminate tensile force in crack J (equation (4.57) multiplied by the laminate area) is similar to the transferred force for a pure shear specimen where the shear stress is zero at the loaded laminate end (see equation (3.28) of Chapter 3 for $\tau_B = 0$).

The formulae for Stage 3a which provide the laminate tensile stresses are similar to Stage 2a.2 when substituting the crack distance s_{cr} by the remaining bonded length s_{cr} - L_{mcrack}, and x_J by x_{L0}. Note that the macrocrack length L_{mcrack} is x_J - x_{L0}. These modifications affect the constant μ as well.

The location of the interfacial crack tip can be obtained by assuming a zero shear stress at this location, that is, by solving equation (4.58).

$$\frac{t_L\Omega_2}{\cos\left(\Omega_2\left(x_{L0}-x_{LM,right}\right)\right)}\left\{-\left(\sigma_{L,J}+\frac{2\mu}{\Omega_2^2}\right)\sin\left(\Omega_2\left(x_{L0}-x_{LM,right}\right)\right)+\frac{\tau_{LM}}{t_L\Omega_2}-\right.$$
$$\left.-\frac{\mu}{\Omega_2}\left(2\left(x_{LM,right}-x_I\right)-\left(s_{cr}-L_{mcrack}\right)\right)\right\}+\mu t_L\left(s_{cr}-L_{mcrack}\right)=0 \tag{4.58}$$

If the concrete's contribution in tension is neglected, the location of the macrocrack tip, x_{L0}, can be explicitly written as equation (4.59).

$$x_{L0}=x_{LM,right}+\frac{1}{\Omega_2}\arcsin\left(\frac{\tau_{LM}}{t_L\Omega_2\sigma_{L,J}}\right) \tag{4.59}$$

The macrocrack tip x_{L0} moves towards crack I during the development of Stage 3a, as shown by the decreasing trend of x_{L0} in equation (4.59) which is justified by the decreasing trend of its terms. As previously mentioned, with the debonding propagation process, the maximum shear stress location $x_{LM,right}$ moves towards crack I. In a coordinate system that increases from crack I to crack J, the movement of $x_{LM,right}$ is mathematically expressed by its decreasing value. In addition, the arc sinus of (4.59) decreases with increasing values of the laminate tensile stress in crack J.

As in Stage 2a.2, if the concrete's contribution is not taken into account in Stage 3a ($\mu = 0$), both Zone I will be identical in length.

Stage 3b: $s(x = x_J) > s_{L0}$ and $s(x = x_I) > s_{LM}$

As explained in §4.3.1, the maximum shear stress location $x_{LM,right}$ can reach crack I during Stage 3a before Stage 3c initiates, that is, before a macrocrack opens near crack I. This situation occurs when the remaining bonded length along the crack distance s_{cr} - L_{mcrack} is below a certain limit, which will be called $(s_{cr} - L_{mcrack})_{,\lim}$.

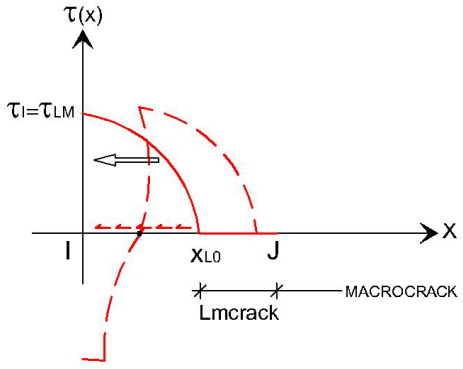

Figure 4.18. Maximum shear stress reaches crack I at the beginning of Stage 3b.

For this limit length, the maximum shear stress τ_{LM} is reached in crack I while the shear stresses are zero at the macrocrack tip. In a similar manner as in Stage 2b, the limit for the remaining bonded crack distance can be obtained as equation (4.60), where no contribution of concrete in tension has been considered. If the remaining bonded length

along the crack distance is longer than the limit given by (4.60), Stage 3b will never occur.

$$\left(s_{cr} - L_{mcrack}\right)_{\lim} = \frac{1}{\Omega_2}\arccos(\upsilon) \tag{4.60}$$

Equation (4.60) is similar to the limit between short and long crack distances, $s_{cr,\lim}$ (see equation (4.51)) and shows the same trends described for $s_{cr,\lim}$. The main difference is the considered length, which was the whole crack distance in Stage 2b and now refers to the remaining bonded length.

During Stage 3b, the solutions of equations (4.37) to (4.39) for the maximum and zero shear stress location, after substituting the crack distance s_{cr} by the remaining bonded length s_{cr} - L_{mcrack}, give negative values, indicating that the derived equations are no longer valid. So, as Stage 3b develops, the laminate tensile stresses will be derived from equation (4.61), which is similar to Stage 2b when substituting the crack distance, s_{cr}, by the remaining bonded length, s_{cr} - L_{mcrack}, and the crack J location, x_J, by the macrocrack tip location, x_{L0}.

For $x_I \le x \le x_{L0}$ (Zone II)

$$\begin{aligned}\sigma_{L}^{II}(x) = {} & \frac{1}{\sin\left(\Omega_2\left(s_{cr} - L_{mcrack}\right)\right)}\left\{\left(\sigma_{L,J} + \frac{2\mu}{\Omega_2^2}\right)\sin\left(\Omega_2\left(x - x_I\right)\right) + \right. \\ & \left. + \left(\sigma_{L,I} + \frac{2\mu}{\Omega_2^2}\right)\sin\left(\Omega_2\left(x_{L0} - x\right)\right)\right\} - \frac{2\mu}{\Omega_2^2} + \mu\left(\left(x - x_I\right)^2 - \left(s_{cr} - L_{mcrack}\right)\left(x - x_I\right)\right)\end{aligned} \tag{4.61}$$

The location of the interfacial crack tip, x_{L0}, or alternatively, the macrocrack length, L_{mcrack} (see Figure 4.9), can be obtained from equation (4.62).

$$\begin{aligned}& \frac{\Omega_2 t_L}{\sin\left(\Omega_2\left(s_{cr} - L_{mcrack}\right)\right)}\left\{\left(\sigma_{L,J} + \frac{2\mu}{\Omega_2^2}\right)\cos\left(\Omega_2\left(s_{cr} - L_{mcrack}\right)\right) - \left(\sigma_{L,I} + \frac{2\mu}{\Omega_2^2}\right)\right\} + \\ & + \mu t_L\left(s_{cr} - L_{mcrack}\right) = 0\end{aligned} \tag{4.62}$$

When the concrete's contribution is not taken into account, the remaining bonded length can be explicitly written as follows:

$$s_{cr} - L_{mcrack} = \frac{1}{\Omega_2}\arccos\left(1 - \frac{\Delta\sigma_{L,IJ}}{\sigma_{L,J}}\right) = \frac{1}{\Omega_2}\arccos(\upsilon) \tag{4.63}$$

Equation (4.63) coincides with the limit length given by equation (4.60). Therefore, as previously mentioned, the remaining bonded length follows the same trends as the limit $s_{cr,\lim}$ (see Figure 4.17). As shown in (4.63), the macrocrack length, L_{mcrack}, may or may not continue to grow along Stage 3b. It depends on the internal steel state, which also depends on the υ value. In a three or four-point bending configuration, the macrocrack length evolves as follows:

1) In case the internal steel has not yielded either in crack I or crack J at the beginning or during Stage 3b, the macrocrack length will remain constant as Stage 3b develops.
2) If the internal steel has yielded in crack J but not in crack I, the macrocrack length should decrease with increasing values of the bending moment. This fact is not physically possible, so the laminate will suddenly debond. On the contrary, the macrocrack length will increase if the bending moment decreases.
3) Finally, when the internal steel has yielded in both cracks at the beginning of Stage 3b, according to equation (4.63), the macrocrack will continue to grow with increasing values of the applied moment. Conversely, the laminate will debond in a brittle manner if the applied moment decreases.

For the development of Stage 3b, another condition for the macrocrack length should be verified in addition to equation (4.63): the shear stress in crack I should be lower than the maximum shear stress τ_{LM}. In other words, equation (4.64) should be fulfilled.

$$\frac{\Omega_2 t_L}{\sin\left(\Omega_2\left(s_{cr}-L_{mcrack}\right)\right)}\left\{\left(\sigma_{L,J}+\frac{2\mu}{\Omega_2^2}\right)-\left(\sigma_{L,I}+\frac{2\mu}{\Omega_2^2}\right)\cos\left(\Omega_2\left(s_{cr}-L_{mcrack}\right)\right)\right\} - \mu t_L\left(s_{cr}-L_{mcrack}\right)\le\tau_{LM} \tag{4.64}$$

By incorporating equation (4.42) into equation (4.64), the following condition (4.65) is obtained for the development of Stage 3b in terms of laminate tensile stress in crack J. Note that $P_{\max,L=scr-Lmcrack}$ is the maximum transferred force calculated from equation (3.76) of Chapter 3 for a bonded length equal to the remaining bonded crack distance.

$$\sigma_{L,J}\le\frac{1}{1-\upsilon\cos\left(\Omega_2\left(s_{cr}-L_{mcrack}\right)\right)}\left\{\frac{P_{\max,\,L=scr-Lmcrack}}{A_L}-\frac{2\mu}{\Omega_2^2}\left[1-\cos\left(\Omega_2\left(s_{cr}-L_{mcrack}\right)\right)\right]+ + \frac{\mu s_{cr}}{\Omega_2}\sin\left(\Omega_2\left(s_{cr}-L_{mcrack}\right)\right)\right\} \tag{4.65}$$

When the concrete's contribution is not considered, equation (4.65) is simplified as equation (4.66).

$$\sigma_{L,J}\le\frac{P_{\max,\,L=scr-Lmcrack}}{A_L\left(1-\upsilon\cos\left(\Omega_2\left(s_{cr}-L_{mcrack}\right)\right)\right)}=\frac{P_{\max,\,L=scr-Lmcrack}}{A_L\left(1-\upsilon^2\right)} \tag{4.66}$$

For a certain macrocrack length and in a three or four-point bending configuration, the limit condition given by equation (4.65) follows the same trends given by equation (4.46) in Stage 2b, with a horizontal branch before steel yields in both crack tips, a descending branch when steel has yielded in crack J, and an ascending branch when steel has yielded in both crack tips (see Figure 4.14).

This limit condition is only attained at the beginning of Stage 3b. If the limit is exceeded afterwards, the laminate will suddenly debond.
Since the remaining bonded length is in Zone II of the bond-slip relationship, the shear stresses decrease as the sliding between the support and laminate increases. By knowing that the transferred force diminishes as Stage 3b develops, and by applying equation (4.42), it can be concluded that the tensile stress in crack J should decrease with the

evolution of Stage 3b. Then, since the tensile stress in crack J is proportional to the bending moment at this point, the external load should decrease to accomplish condition (4.65). Similar to Stage 2b, Stage 3b will develop when the slip and not the applied load on the beam is controlled. An increase in the tensile stress in crack J can result in a premature laminate debonding.

In addition, since the macrocrack length, shown in equation (4.63), is a function of υ, the development of Stage 3b will only be possible when the bending moment is lower than a value that causes steel yielding in both cracks I and J. Before steel yields in crack J, the macrocrack length will remain constant and equal to the value obtained at the end of Stage 3a (see Figure 4.21). Once the steel yields in crack J, the macrocrack will start to grow with decreasing values of the tensile stress in crack J (see Figure 4.21). Finally, after the steel yields in both cracks, the macrocrack should decrease as the tensile stress in crack J decreases, which is not physically possible. As a consequence, the laminate debonds.

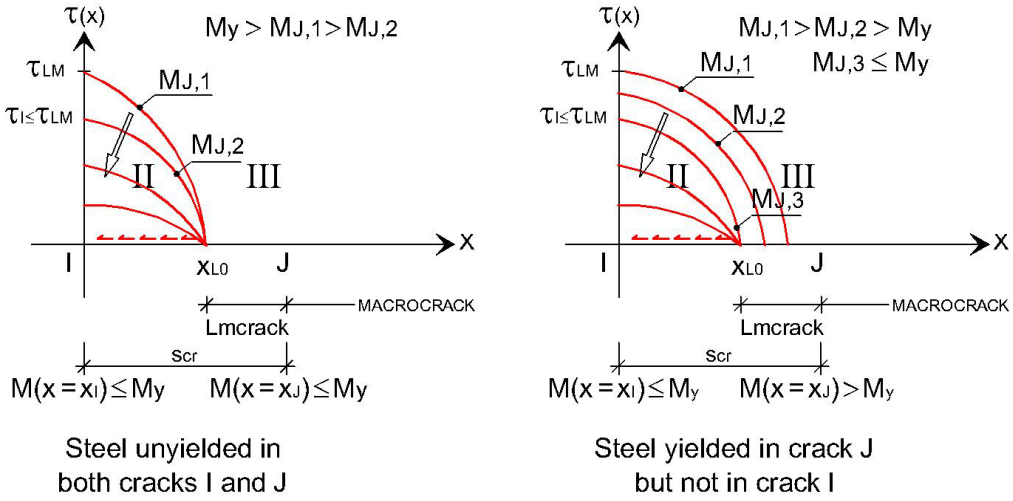

Figure 4.19. Evolution of shear stresses along Stage 3b depending on the internal steel yielding.

Stage 3c: $s(x = x_J) > s_{L0}$ and $s(x = x_I) > s_{L0}$

To find the laminate tensile stress and interfacial shear stress distribution of Stage 3c both interfacial macrocrack tips locations $x_{L0,right}$ (which appeared in Stage 3a), and $x_{L0,left}$ should be obtained (see Figure 4.10). Both coordinates can be calculated by solving equations (4.67) and (4.68) respectively. The macrocrack lengths near both cracks I and J can be derived from the crack tip locations as $L_{mcrack,right} = x_J - x_{L0,right}$ and $L_{mcrack,left} = x_{L0,left} - x_I$. Thus, as in Stage 3a, the formulae of Stage 3c will be similar to Stage 2a.2, when substituting: the crack distance s_{cr} by the remaining bonded length $s_{cr} - L_{mcrack,left} - L_{mcrack,right}$; x_J by $x_{L0,right}$; and x_I by $x_{L0,left}$.

$$\frac{t_L\Omega_2}{\cos\left(\Omega_2\left(x_{L0,right}-x_{LM,right}\right)\right)}\left\{-\left(\sigma_{L,J}+\frac{2\mu}{\Omega_2^2}\right)\sin\left(\Omega_2\left(x_{L0,right}-x_{LM,right}\right)\right)+\frac{\tau_{LM}}{t_L\Omega_2}-\right.$$
$$\left.-\frac{\mu}{\Omega_2}\left(2\left(x_{LM,right}-x_I\right)-\left(s_{cr}-L_{mcrack,left}-L_{mcrack,right}\right)\right)\right\}+ \tag{4.67}$$
$$+\mu t_L\left(s_{cr}-L_{mcrack,right}-L_{mcrack,left}\right)=0$$

$$\frac{t_L\Omega_2}{\cos\left(\Omega_2\left(x_{LM,left}-x_{L0,left}\right)\right)}\left\{\left(\sigma_{L,I}+\frac{2\mu}{\Omega_2^2}\right)\sin\left(\Omega_2\left(x_{LM,left}-x_{L0,left}\right)\right)-\left[\frac{\tau_{LM}}{t_L\Omega_2}+\right.\right.$$
$$\left.\left.+\frac{\mu}{\Omega_2}\left(2\left(x_{LM,left}-x_I\right)-\left(s_{cr}-L_{mcrack,left}-L_{mcrack,right}\right)\right)\right]\right\}+ \tag{4.68}$$
$$+\mu t_L\left(s_{cr}-L_{mcrack,left}-L_{mcrack,right}\right)=0$$

If the concrete's contribution in tension is not taken into account, both macrocrack tip locations can be rewritten as (4.69) and (4.70).

$$x_{L0,right}=x_{LM,right}+\frac{1}{\Omega_2}\arcsin\left(\frac{\tau_{LM}}{t_L\Omega_2\sigma_{L,J}}\right) \tag{4.69}$$

$$x_{L0,left}=x_{LM,left}-\frac{1}{\Omega_2}\arcsin\left(\frac{\tau_{LM}}{t_L\Omega_2\sigma_{L,I}}\right) \tag{4.70}$$

The minimum crack distance for the development of Stage 3c, $s_{cr,\min\ Stage\ 3c}$, if the contribution of concrete in tension is neglected is given by equation (4.71):

$$s_{cr,\min\ Stage3c}=\frac{1}{\Omega_2}\left[\arcsin\left(\frac{\tau_{LM}}{t_L\Omega_2\sigma_{L,J}}\right)+\arcsin\left(\frac{\tau_{LM}}{t_L\Omega_2\upsilon\sigma_{L,J}}\right)\right] \tag{4.71}$$

Short crack distances

Stage 3b: $s(x=x_J) > s_{L0}$ and $s(x=x_I) > s_{LM}$

At the end of Stage 2b, the maximum sliding reaches crack J while the shear stress on the other crack is lower than the maximum value τ_{LM}. From this point on, Stage 3b will develop only in some specific conditions that depend on the internal steel state. Under these conditions, the laminate tensile stresses expression coincides with (4.61), which is repeated here for the sake of completeness.

For $x_I \le x \le x_J$ (Zone II)

$$\sigma_{L}^{II}(x) = \frac{1}{\sin(\Omega_2(s_{cr} - L_{mcrack}))}\left\{\left(\sigma_{L,J} + \frac{2\mu}{\Omega_2^2}\right)\sin(\Omega_2(x - x_I)) + \right.$$
$$\left. + \left(\sigma_{L,I} + \frac{2\mu}{\Omega_2^2}\right)\sin(\Omega_2(x_J - x))\right\} - \frac{2\mu}{\Omega_2^2} + \mu\left((x - x_I)^2 - (s_{cr} - L_{mcrack})(x - x_I)\right) \quad (4.72)$$

Stage 3b will only develop for a short crack distance, if the internal steel has yielded in crack J and remains unyielded in crack I at the end of Stage 2b (when the maximum sliding s_{L0} reaches crack J). The same trends observed in the evolution of Stage 3b for long bonded lengths can be applied here for a short bonded length. The only difference is that the macrocrack length at the beginning of the stage is equal to zero.

Stage 3b will not develop if the internal steel has yielded in both cracks I and J at the end of Stage 2b. Under these circumstances, according to equation (4.63), the macrocrack should shrink with decreasing values of the applied moment. Since this fact is not physically possible, the laminate will debond in a brittle manner. As described for long bonded lengths, Stage 3b will only develop with decreasing values of the external load. Due to this reason and since the evolution of Stage 3b is only possible when the internal steel has yielded in crack J but not in crack I at the end of the previous stage, the internal steel will never yield in crack I during Stage 3b.

In case the internal steel remains unyielded along the crack distance when the maximum sliding reaches crack J, the laminate suddenly debonds because the maximum sliding will have been reached not only in crack J but along the whole crack distance. Therefore, Stage 3b will not develop in this case. However, during the evolution of Stage 3b, the bending moment in crack J can decreased below the value related to steel yielding. In this case, Stage 3b will continue evolving with an almost constant value of the macrocrack length.

4.3.5. Summary

After the description and development of the formulae related to each Stage, a brief summary of the evolution of the possible stages that can arise during the debonding process is presented in Table 4.1. A distinction between long and short laminates has been made. Each row represents the sequence of the different stages that can appear depending on the crack distance and the load configuration.

Table 4.1. Stages that arise between two cracks for long and short laminates.

Progressive stages between cracks					
LONG CRACK DISTANCES					
Flexure and shear	Stage 1	Stage 2a.1	Stage 2a.2	Stage 3a	Stage 3b(*)
					Stage 3c
Pure flexure	Stage 1	Stage 2a.2	Stage 3c		
SHORT CRACK DISTANCES					
Flexure and shear	Stage 1	Stage 2a.1	Stage 2a.2	Stage 2b(*)	
			Stage 2a.2	Stage 2b(*)	Stage 3b(*)(**)
			Stage 2b(*)		
			Stage 2b(*)	Stage 3b(*)(**)	
Pure flexure	Stage 1	Stage 2a.2	Stage 3c		

(*) This stage will arise if displacement control is performed
(**) This stage will arise if the internal steel has yielded in crack J but remains linear elastic in crack I

4.3.6. Transferred force

Some general comments regarding the transferred force along the complete debonding process described in the formulae developed in §4.3.3 and §4.3.4 are listed below:

1) The transferred force between two subsequent cracks can be obtained as the difference between the laminate tensile forces in each crack tip. Since the tensile stress in crack I can be expressed as a function of the tensile stress in crack J (equation (4.42)), the transferred force can be written as equation (4.73).

$$\Delta P_{scr} = \Delta\sigma_{L,IJ} A_L = \sigma_{L,J} A_L (1-\upsilon) \tag{4.73}$$

2) From equation (4.73) and as shown in Figure 4.20, the slope of the transferred force function with respect to the applied load on the beam depends mainly on the internal steel yielding.
3) The applied load will increase gradually with a constant slope if the steel has not yielded in both crack tips. Once the steel yields in crack J, the slope increases significantly because the laminate will carry the tensile force increment completely in those sections along the crack distance with the steel yielded. Finally, when the internal steel in both crack sections I and J has yielded, the slope of the transferred force will be significantly reduced to a value higher than the initial slope. In the last situation, the laminate alone assumes the increment in tensile stress within both crack sections due to the increasing values of applied force.

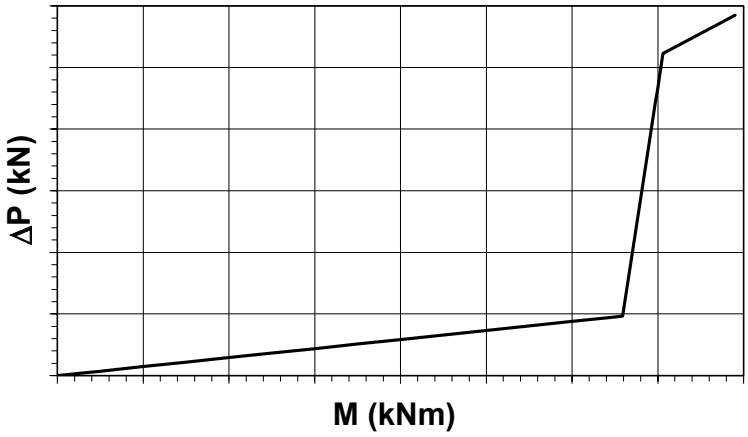

Figure 4.20. Transferred force between two cracks.

4) In addition, the transferred force can also be calculated by integrating the shear stresses along the crack distance. The transferred force can be obtained by subtracting the transferred force (in other words, the shear stress integral) between the zero shear stress location and crack I from the transferred force between crack J and the zero shear stress location.
5) For both short and long crack distances, the transferred force is an increasing function of the applied load until the maximum shear stress location $x_{LM,right}$ reaches crack I, that is up to the beginning of Stage 2b or 3b. From this point on, the development of these stages will only be possible when the transferred force starts to decrease. The increasing trend of the transferred force for long and short crack distances is stunted by the limit condition given by equations (4.46) and (4.65) of Stages 2b and 3b, which is a restraint on the maximum value of the shear stress within crack I.
6) For short crack distances, the maximum transferred force will take place when Stage 2b starts, that is, when the maximum shear stress location $x_{LM,right}$ reaches crack I. This maximum transferred force can be obtained after incorporating equation (4.46) into (4.73), and is written as equation (4.74).

$$\Delta P_{\max,\,scr} = \Delta\sigma_{L,IJ}\,A_L = \frac{(1-\upsilon)}{(1-\upsilon\cos(\Omega_2 s_{cr}))}\left\{ P_{\max,\,L=scr} - \frac{2\mu A_L}{\Omega_2^2}(1-\cos(\Omega_2 s_{cr})) + \right.$$
$$\left. + \frac{\mu s_{cr} A_L}{\Omega_2}\sin(\Omega_2 s_{cr}) \right\} \tag{4.74}$$

7) When the concrete's contribution in tension is not considered (μ = 0), the maximum transferred force can be expressed as (4.75).

$$\Delta P_{\max,\,s_{cr}} = \Delta\sigma_{L,IJ}\,A_L = \frac{(1-\upsilon)}{(1-\upsilon\cos(\Omega_2 s_{cr}))} P_{\max,\,L=scr} \tag{4.75}$$

8) In the particular case of a pure flexure case, where the bending moment is constant between cracks I and J ($M(x = x_J) = M(x = x_I)$), υ is equal to 1, and the transferred force is reduced to a zero value. In case the tensile stress in crack I is

zero (at the laminate end), υ is equal to 0 and the maximum transferred force is equal to the maximum transferred force of a pure shear specimen.

$$\upsilon = 1 \longrightarrow \Delta P_{\max,\, scr} = 0 \tag{4.76}$$

$$\upsilon = 0 \longrightarrow \Delta P_{\max,\, scr} = P_{\max,\, L=scr} \tag{4.77}$$

9) For crack distances higher than the limit given by equation (4.51) but not substantially long for the development of Stage 3c (equation (4.71)), the maximum transferred force is reached when Stage 3b initiates. At this point, the shear stress is at maximum in crack I and the maximum sliding is reached at the macrocrack tip. In other words, the remaining bonded length is equal to the crack distance limit between a short and long laminate. The maximum force can be obtained from equation (4.78) when substituting the crack distance by the limit given by equation (4.51).

$$\Delta P_{\max,\, scr} = \Delta\sigma_{L,IJ} A_L = \frac{(1-\upsilon)}{(1-\upsilon\cos(\Omega_2 s_{cr,\lim}))}\left\{ P_{\max,\, L=scr.\lim} - \frac{2\mu A_L}{\Omega_2^2}(1-\cos(\Omega_2 s_{cr,\lim}))+ \right.$$
$$\left. + \frac{\mu s_{cr,\lim} A_L}{\Omega_2}\sin(\Omega_2 s_{cr,\lim}) \right\} \tag{4.78}$$

10) Equation (4.78) can be simplified to (4.53), when the concrete's contribution in tension is neglected, that is, for $\mu = 0$, and when equation (4.51) is incorporated into (4.78). Equation (4.53) is repeated here for the sake of completeness.

$$\Delta P_{\max,\, scr} = \Delta\sigma_{L,IJ} A_L = \frac{P_{\max,\, L=scr,\lim}}{(1+\upsilon)} \tag{4.79}$$

11) Figure 4.21 shows the maximum transferred force in two different cases: for a short laminate which is attained at the beginning of Stage 2b, and for a long laminate which is reached when Stage 3b starts. Both profiles are similar once the steel has yielded in one of the cracks (crack J). Before steel yields, the maximum transferred force increases with the laminate length up to the maximum potential value that can be attained, and which corresponds to the limit length between short and long bonded lengths. For laminate lengths longer than the limit between short and long laminates, the transferred force does not increase above the value associated to this limit.

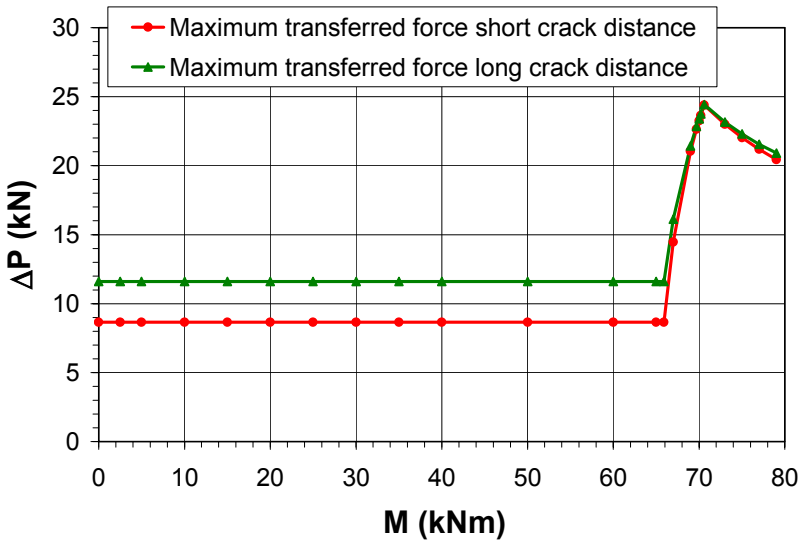

Figure 4.21. Maximum transferred force in a short and long crack distance.

12) The maximum value of the transferred force is attained when the internal steel yields in crack I. If this situation occurs just at the beginning of Stage 2b or 3b (depending on the crack distance), the transferred force will reach the maximum possible value.
13) The maximum transferred force shows a similar shape for short and long crack distances (see Figure 4.21). If the bending moment on crack J is lower than the yield bending moment and the concrete's contribution in tension is neglected, the maximum transferred force will be a constant value that does not depend on the applied force. When the steel has yielded only in crack J, the maximum transferred force will increase with increasing values of the applied moment. This increasing trend is because the laminate in crack J is assuming alone the tensile stress increments while the laminate in crack I is sharing the tensile stress increment with the internal steel. Finally, once the internal steel yields in both cracks I and J, the transferred force at the beginning of Stages 2b or 3b decreases with the applied moment on crack J. At this point, the steel has yielded along the crack distance, and the laminate tensile stress in crack I will start to increase significantly, so the difference in tensile stress between crack I and J will be reduced.
14) The transferred force which is obtained as the difference between the tensile forces acting in both cracks I and J is plotted in Figure 4.22 together with the maximum transferred force associated to different values of the bending moment. The maximum transferred force is attained at the beginning of Stage 2b for short crack distances and at the beginning of Stage 3b for long crack distances. The maximum transferred force will be obtained at the intersection of the maximum attainable transferred force with transferred force. From this point on, the transferred force cannot increase further. Then, the transferred force that is shown by the dashed line will not be possible.

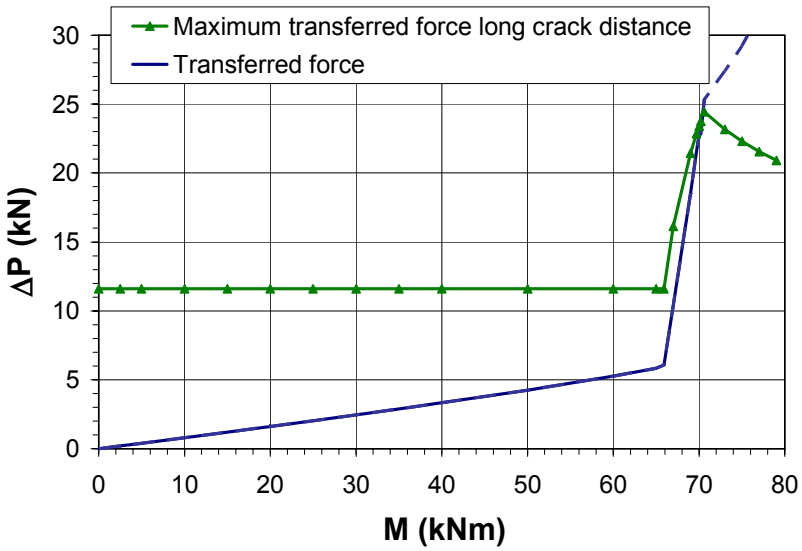

Figure 4.22. Maximum transferred force between two cracks in a three-point bending load configuration.

4.3.7. Analysis of a beam element between two cracks subjected to pure flexure

To clarify all the formulae shown in the previous section, an example of a beam segment between two cracks is studied. The crack distance is fixed at 200 *mm*. The geometry dimensions of the section and the material properties are the same as in Beam 2 (see Chapter 2). The model parameters in this example are: τ_{LM} = 2.46 *MPa*, s_{LM} = 0.008 *mm*, and s_{L0} = 0.764 *mm*.

Firstly, the beam segment is analyzed while being subjected only to bending moments (Figure 4.23). The bending moment applied on both cracks is increased by using different steps from 2.5 *kNm* to the bending moment associated to concrete crushing, 79.5 *kNm*. Note that the bending moment at failure is higher than the bending moment associated to steel yielding, 65.9 *kNm*.

One of the requirements to find the stress profiles on the laminate and the interface applying the formulae of the previous section is to know the value of the laminate tensile stress in each crack. This value was calculated by means of a moment-curvature analysis of the Beam 2 section, assuming a σ - ε relationship for the concrete in compression according to the Spanish Concrete Code EHE (1999) and neglecting the concrete's contribution in tension.

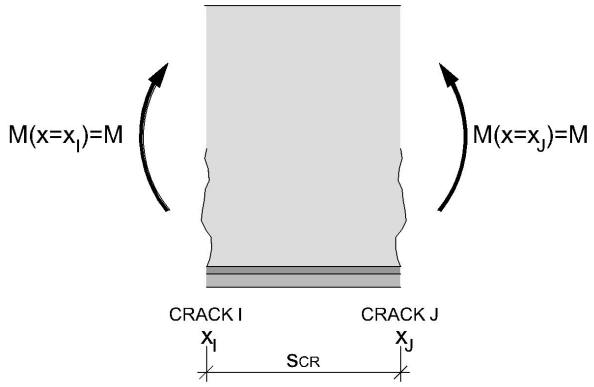

Figure 4.23. Beam segment in a zero shear force region.

As mentioned before, to solve the differential equations governing the interface, the concrete tensile stress distribution in the fiber next to the laminate was approached by a parabolic function depending on a β parameter.

First of all, a value of β = 1.0 is assumed: that is, the concrete tensile stress at the midpoint crack distance is assumed to be equal to the tensile strength f_{ctm} and an intermediate crack does not have appeared at this location yet. The different stress profiles for a pure flexure state are then derived with the following input data: geometry, material properties and applied load. When calculating the stresses, it is assumed that the interface behaves under different stages depending on the applied bending moment on each crack.

Some comments about the derived stresses profiles are presented in the following discussion.

Figure 4.24 shows the evolution of the shear stress distribution as the applied bending moment increases. In pure flexure, the shear stresses are not required for equilibrium; they are exclusively induced by tension-stiffening for strain compatibility. A list of observations from Figure 4.24 is given below.

1) If the beam segment is subjected to equal bending moments, the shear stress distribution will be skew-symmetric in relation to the middle of the crack spacing.
2) The symmetry implies that Stage 2a.1 will never appear. As a consequence, immediately after finishing Stage 1, when the maximum shear stress is reached in both crack tips, Stage 2a.2 initiates. In this case, this happens after the moment acting on both cracks reaches 5.0 *kNm*.
3) During Stage 2a.2, as the applied moment increases, the transition points between Zone I and II also known as the maximum shear stress points, $x_{LM,left}$ or $x_{LM,right}$, move towards the middle of the laminate.
4) Because the bending moments on the crack tips are of equal value, the zero shear stress point x_K is fixed at the midpoint of the crack distance.
5) The maximum transferred force between one crack and the zero shear stress location x_K is reached when the area under the shear stress profile is at maximum. From this point on, the movement of $x_{LM,left}$ and $x_{LM,right}$ towards x_K will be much slower.

6) According to the moment-curvature analysis of the strengthened section, the steel yields when the acting bending moment is 65.9 *kNm*. Once the steel yields in both crack tips, the debonding process speeds up and, consequently, the slope of the shear stress profile in Zone II increases more rapidly.
7) When the applied bending moment is equal to the value associated to concrete crushing, the shear stresses under each crack location are almost zero. If the applied bending moment increases over 79.5 *kNm*, Stage 2a.2 will finish and Stage 3c will initiate. An interfacial macrocrack will open under both crack locations. Therefore, in a similar manner as to Stage 2a.1, Stage 3a will never occur due to the symmetry.
8) During Stage 3c, the shear stress decreases from its maximum value attained near the zero shear stress point to the zero value at the macrocrack tip.
9) As previously mentioned, Stage 2b or 3b never appear in a pure flexure case due to symmetry.

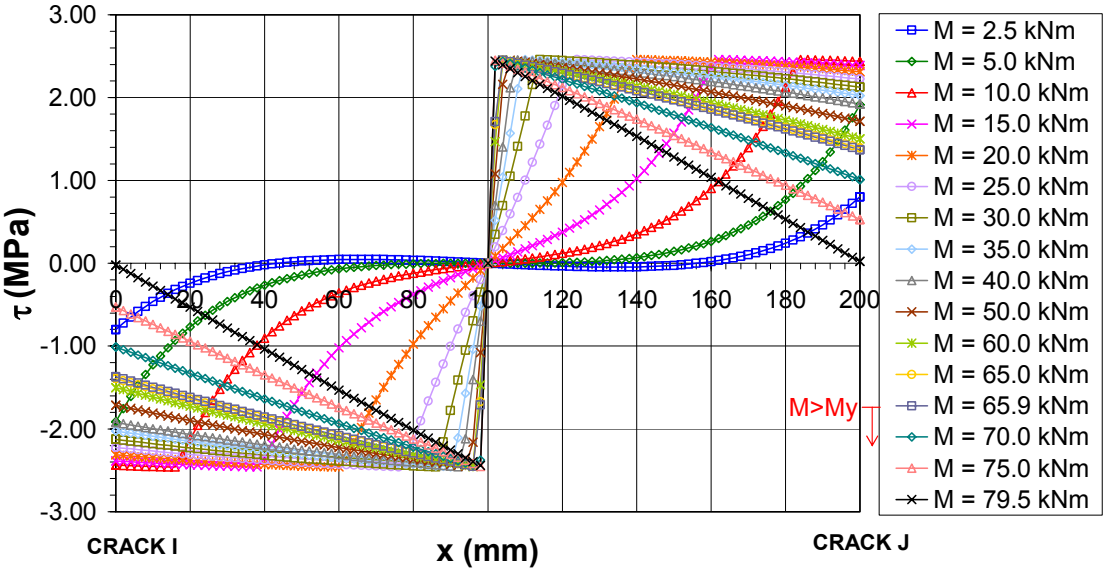

Figure 4.24. Shear stress distribution between two cracks under a pure flexure state.

In the following lines a set of comments regarding the laminate tensile stress distribution of Figure 4.25 is listed.

1) The tensile stress distribution is symmetrical at the zero shear stress location.
2) As shown in Figure 4.25, the laminate stress has a minimum extreme value at the zero shear stress point due to the tension stiffening effect.
3) A noticeable increase is observed on the tensile stress values from 60.0 *kNm* to 79.5 *kNm*. As previously mentioned, the internal steel yields when the applied moment is 65.9 *kNm*. Once the steel yields, the internal reinforcement cannot increase its stress and the laminate alone should absorb the increment of tensile stresses due to an increase of the applied moment. Therefore, after steel yielding, the increase in the laminate tensile stress is more acute. Between 50.0 *kNm* and 60.0 *kNm*, a range just before steel yields, the laminate tensile stress in the crack tip increases by a percentage of 17.5% in relation to the stress at the lowest moment. However, after steel yielding, when the same 10.0 *kNm* moment

increment is used, the laminate tensile stress increases by a percentage of 41.3%. Moreover, in the last load step to 79.5 *kNm*, the percentage of increase is 62.9%.

4) As observed in Figure 4.25, the tensile stress slope shows an increasing trend from the beginning up to an applied moment of 35.0 *kNm*. From this point on, it is hardly noticeable that the slope has a decreasing trend, which is more evident for higher applied moments, especially once the internal steel yields.

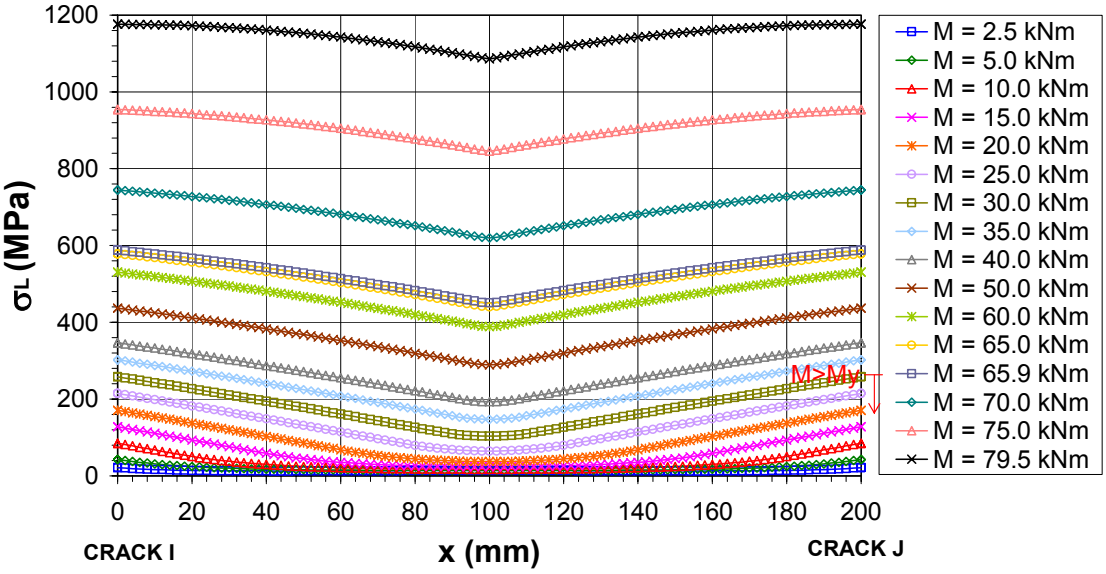

Figure 4.25. Tensile stress in the laminate along the crack spacing.

The force transferred between crack I and crack J is the increment of the tensile force between sections I and J. It can be obtained it by subtracting the force transferred between crack I and the zero shear stress point x_K from the increment of force transferred between crack J and the zero shear stress point x_K.

In this example, the transferred force is zero due to the symmetry on the shear stresses. This can be explained because there is no shear force acting on the beam element, so there is no tensile stress increment between both cracks. As a consequence, the shear stresses appear only due to the tension stiffening effect.

The force transferred along the bonded length between a flexural crack and the zero shear stress location x_K can be obtained as the area enclosed by the shear stress distribution. As the location of the zero shear stress point x_K is fixed on the middle of the laminate, the maximum force transferred will be the maximum area under the shear stress distribution in half of the crack distance.

The increment of force between one crack and the zero shear stress location x_K, $\Delta P_{scr/2}$, is plotted against the applied moment in Figure 4.26. A set of comments are presented below.

1) There is a maximum value reached whereby an increase of the moment at the crack location does not imply an increase of the force transferred between the laminate and the support. In this case, the maximum force, 21.7 *kN*, corresponds to a 35.0 *kNm* applied moment.

2) For higher applied moments, there is a decrease in the transferred force though with an initial smooth slope. Once the internal steel has yielded, the slope of the curve decreases significantly.
3) After reaching its maximum value, the transferred force decreases despite of the increase in the laminate tensile stress in crack J. This fact can be explained as the slope of the tensile stress between crack J and x_K slightly decreases from this point.
4) In addition, in Figure 4.26, the theoretical value of the maximum transferable force of a pure shear specimen is calculated and plotted according to equation (3.76) of Chapter 3 for a 100 *mm* length laminate, which corresponds to half of the crack distance. In this case, the theoretical maximum force is never reached in any of the load cases studied. The maximum force is similar to 90% of the maximum transferred force in a pure shear specimen which is 21.6 *kN*.
5) If the concrete's contribution is not taken into account ($\beta = 0$), the pure flexure case along half of the crack distance will be similar to a pure shear specimen with the boundary condition of zero shear stress at the laminate end. In this case the expression for the maximum transferred force will be given by equation (3.72) of Chapter 3. The only difference with the general case is the equation to find the maximum shear stress location, which is given by equation (4.80) instead of (3.30).

$$-\frac{\tau_B}{\tau_{LM}} = \frac{\Omega_2}{\Omega_1}\frac{\sin(\Omega_2 x_{LM})}{\tanh(\Omega_1(L - x_{LM}))} - \cos(\Omega_2 x_{LM}) \tag{4.80}$$

6) The transferred force gives an idea of the correct value for the β fraction that defines the concrete's contribution in tension. β can be obtained as shown in equation (4.81) by dividing the maximum transferred force by both the integral of the concrete stress on the bottom fiber along half of the crack distance, as given by equation (4.21), and the area of influence of the concrete tensile stresses. By applying equation (4.81) into this example, the β value is found to be equal to 0.032, which is almost zero.

$$\beta = \frac{3\Delta P_{\max,K-I}}{s_{cr} f_{ctm} r(b_L + 2r)} \tag{4.81}$$

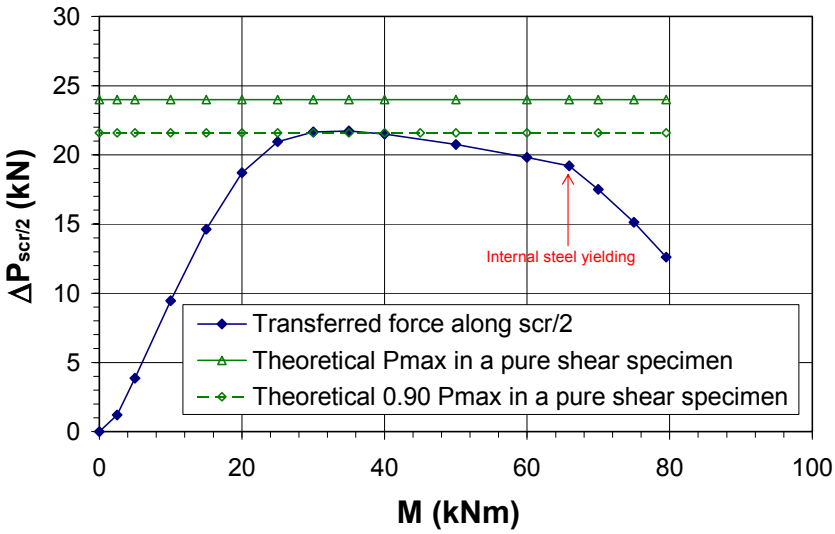

Figure 4.26. Force increment between one crack and the middle point of the crack spacing.

Finally, in Figure 4.27, the relative displacement between concrete and laminate is presented.

1) Because of pure flexure, the sliding is skew-symmetrical at the middle of the crack spacing.
2) The slope of the relative displacement profile increases with the applied bending moment.
3) If the maximum sliding s_{L0} is reached in both flexural cracks, Stage 3c will initiate. Thus, two symmetrical interfacial macrocracks will open in the vicinity of the flexural crack tips. From this point in time, the interfacial crack propagation process will be symmetric as well. The complete debonding of the laminate will take place when the relative displacement on the zero shear stress location x_K reaches the maximum value of Zone II, s_{L0}. Theoretically, this extreme situation is not possible due to symmetry, because x_K cannot move in opposite directions. However, the laminate debonds while the maximum sliding is reached in points infinitely close to the zero shear stress location. At this point, both macrocracks are connected one to each other.
4) In this example, as shown in Figure 4.27, the maximum sliding s_{L0} is not reached for the load cases studied. It should be mentioned that the section fails due to concrete crushing when the applied moment is 79.5 *kNm*. When this moment is acting, the maximum sliding will reach 0.758 *mm* which is slightly lower than the maximum value s_{L0} = 0.764 *mm*. The maximum sliding will be reached under both flexural crack tips for an applied moment of 79.9 *kNm*.
5) Therefore, such a connection, loaded in a pure flexure state, will probably fail due to concrete crushing just before an interfacial macrocrack appears and the peeling effect takes place.

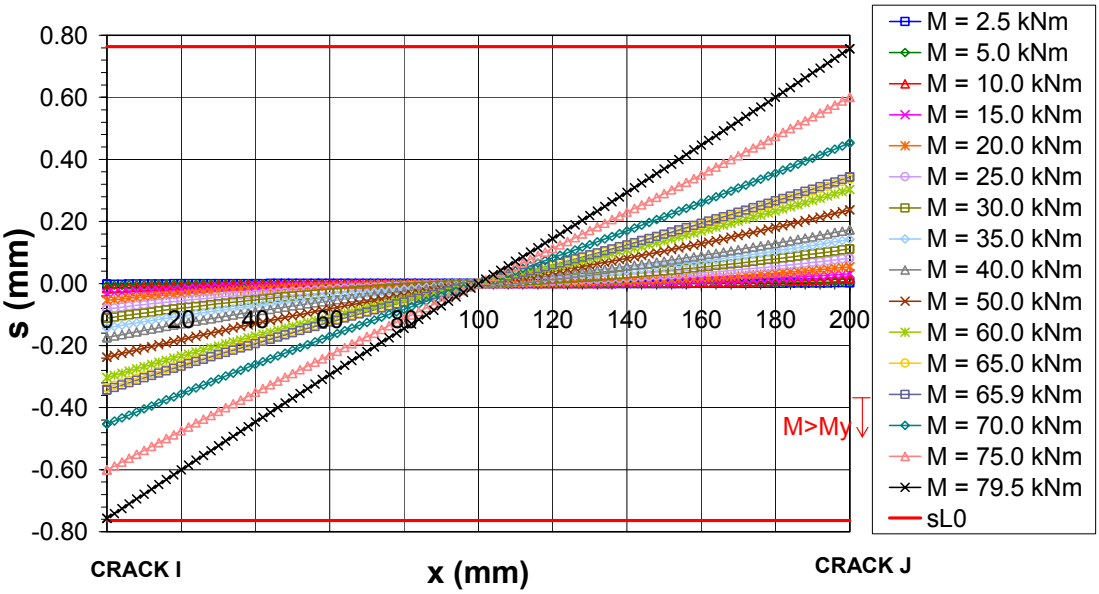

Figure 4.27. Relative displacement between concrete and laminate under a pure flexure state.

In this analysis, the laminate tensile stress under both cracks I and J has been obtained for the applied bending moments by a moment-curvature analysis. The moment-curvature analysis assumes that the section remains plane after deformation. This assumption implies that the laminate elongation at the crack location can be obtained as shown in equation (4.82). In the analysis performed, the laminate elongation is approximately equal to the slip (it is exactly the slip for $\beta = 0$).

$$u_L(x = x_J) = \varepsilon_L(x = x_J)\frac{s_{cr}}{2} = \frac{\sigma_L(x = x_J)}{E_L}\frac{s_{cr}}{2} = \frac{P(x = x_J)}{E_L A_L}\frac{s_{cr}}{2} \tag{4.82}$$

In Figure 4.28, the transferred force obtained in the analysis is plotted together with equation (4.82). By fixing a tensile force value on crack J (P), the slip is very similar in both cases, being slightly higher according to the moment-curvature analysis. Thus, using a moment-curvature analysis to obtain the laminate tensile stresses under each crack tip provides good results.

After the general description of the behavior in a pure flexure state, the influence of the β parameter on the laminate tensile stress distribution and on the interface shear stress distribution is studied by fixing different β values within a range between 0 and 1. The analyzed cases are: $\beta = 0.0$, $\beta = 0.5$, $\beta = 1.0$ and finally a β value derived assuming that the Navier-Bernouilli condition is accomplished in a section placed on half of the crack distance.

The first case with $\beta = 0.0$ implies that the concrete tensile stress is zero along the crack distance in the fiber next to the laminate, $\sigma_{c,b}(x) = 0$. When incorporating $\sigma_{c,b}(x) = 0$ into the differential equations (4.1) and (4.3), they will turn into homogenous equations. Therefore, the governing equations will be similar to a pure shear state in an element between two cracks but the solution will be obtained with different boundary conditions.

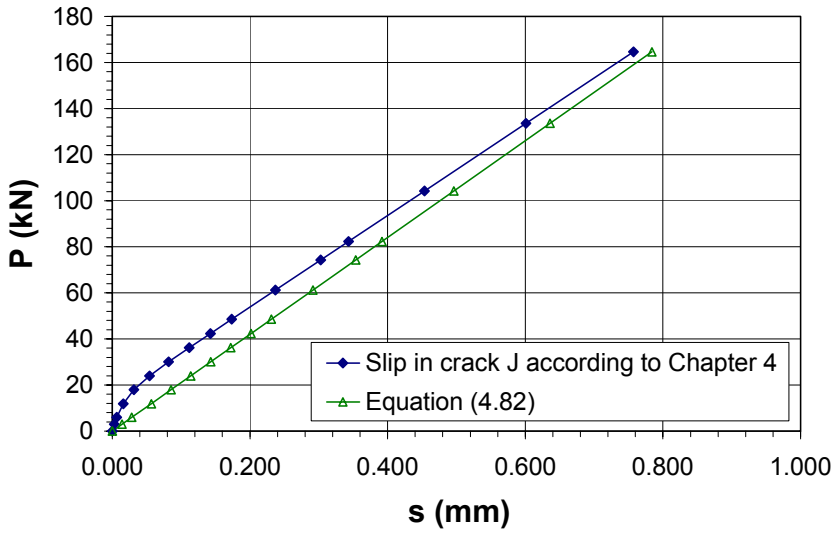

Figure 4.28. Force transferred vs. slip in the pure flexure case according to the analysis performed and equation (4.82).

The last case studied was with a β value derived by the Navier-Bernouilli assumption on half of the crack distance. This criteria is not very realistic for high load levels because β is higher than 1.0. If such a thing happens, the concrete will reach its ultimate tensile strength and a flexural crack will appear between the two existing cracks. In the case studied for an applied moment of 9.0 *kNm*, β was 1.00. From this point to 79.5 *kNm* which is the last moment value studied, the β factor is always higher than 1.0.

Using some of the load cases studied before, Figure 4.29 compares the shear stress distribution obtained with β = 0.0, β = 0.5, and β = 1.0. Some observations are listed below:

1) The main difference is on the location of the maximum shear stress points $x_{LM,left}$ or $x_{LM,right}$. As long as the β factor decreases, the location of the maximum shear stress will be much farther to the zero shear stress point. Therefore, the lower the β factor, the longer the extension of Zone II.
2) Although the stress distribution in Zone II is very similar for the different β values, the shear stress profile of Zone I differs a little for low load levels. For example, when the applied moment on each crack is 10.0 *kNm*, the shear stresses at x = 140 *mm*, which is in Zone I, are: 0.55 *MPa* for β = 0.0, 0.44 *MPa* for β = 0.5, and 0.35 *MPa* with β = 1.0.
3) It can be observed that once the maximum shear stress points are close to the zero shear stress point, the shear stress profile of Zone I is almost vertical and the influence of the β parameter is imperceptible.

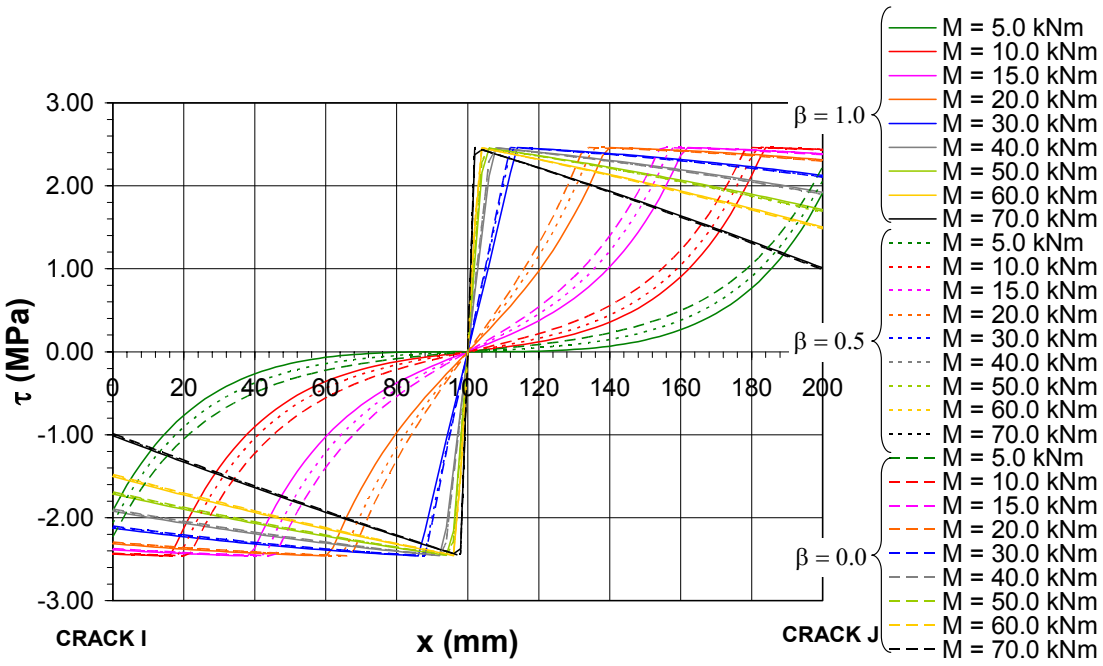

Figure 4.29. Shear stress distribution between two cracks in a bending state for different β values.

As shown in Figure 4.30, the influence of the β factor on the tensile stresses of the laminate is negligible when the applied moment is higher than 20.0 *kNm*. As in the shear stress profiles, for lower applied moments, there is a noticeable difference in the tensile stress values within the maximum shear stress locations and the zero shear stress point (Zone I). This point can be better appreciated in Figure 4.31.

Although the β factor helps to reduce the laminate tensile stress due to the tension stiffening effect, this parameter has no significant influence in both interfacial shear and laminate tensile stress distributions at failure load levels, as observed in both Figure 4.29 and Figure 4.30. Therefore, in a general design situation, the influence of the β value chosen is irrelevant.

In general, the most conservative solution is $\beta = 0.0$. By using this value, the debonding process is more accelerated than in any other case. This is shown by a longer length for Zone II, and higher shear stress values for Zone I. In addition, the governing equations are highly simplified because of their homogeneity.

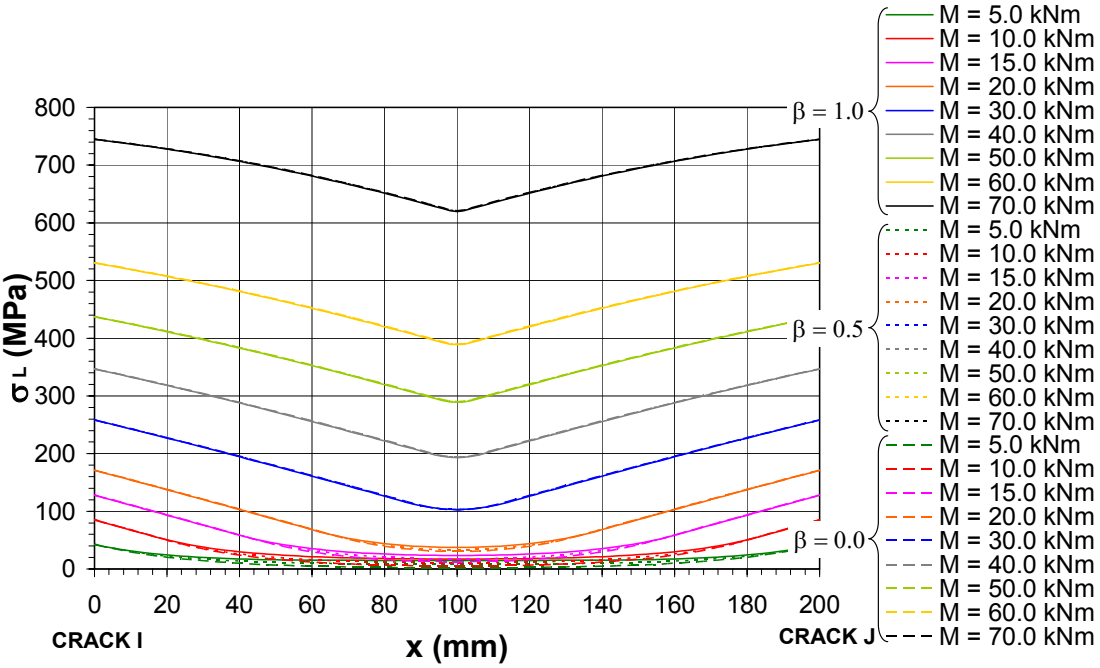

Figure 4.30. Tensile stress distribution between two cracks for different β values.

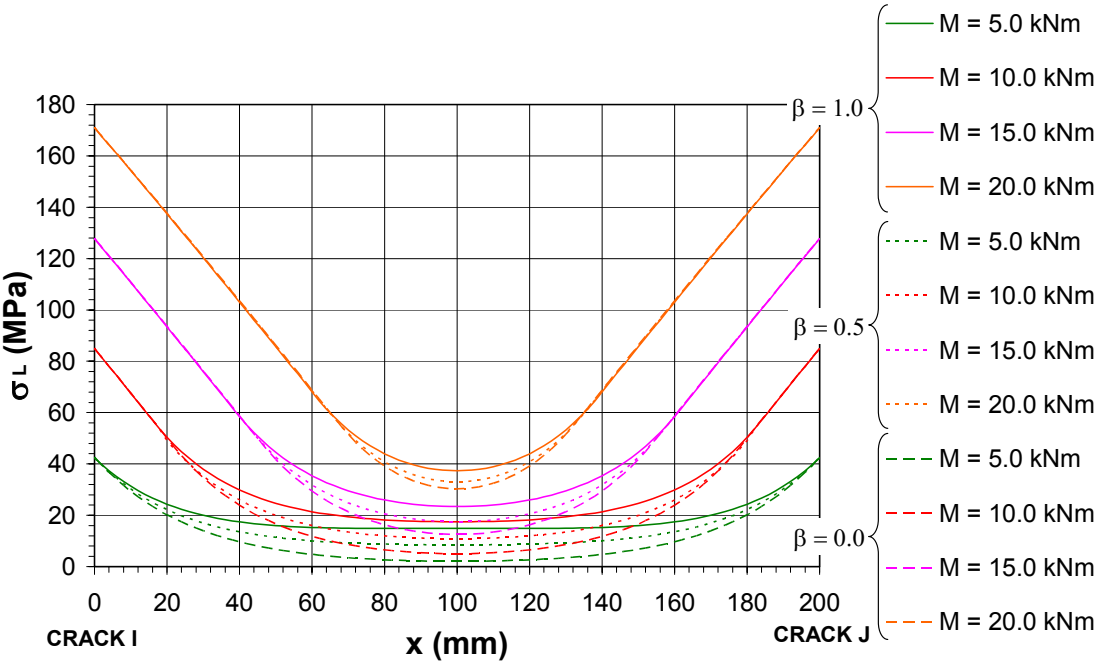

Figure 4.31. Tensile stress distribution between two cracks for low load levels.

4.3.8. Analysis of a beam element between two cracks subjected to bending and shear

A similar case is studied but subjected to bending moments and shear forces (Figure 4.32). Some different bending moment values are applied on one of the cracks (crack J) located at $x = 200\ mm$. The applied moment on the other crack is calculated by using the shear force-bending moment relationship. In this example, the studied element is placed near the midspan of a 6.0 m length beam loaded in a three-point bending configuration. To apply the formulae developed in §4.3.3 and 4.3.4 for the interfacial shear and laminate tensile stresses, the tensile stress value in the laminate in each crack should be known. Both values are determined by a moment-curvature analysis.

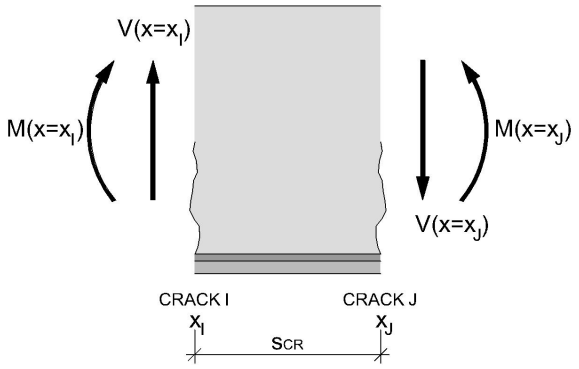

Figure 4.32. Beam segment subjected to bending moments and shear forces.

Similar to the previous example, equations (4.22) and (4.24) are first solved by assuming $\beta = 1.0$, the limit value of this parameter. In the following, there is a description of the interface general behavior when bending moments and shear forces are acting between two cracks by using $\beta = 1.0$.

First, the shear stress distribution is obtained as shown in Figure 4.33 for increasing moment values at crack J, $x = 200\ mm$. It should be pointed out that: the bending moment increases with the x location. Crack I is located at $x = 0\ mm$ and crack J at $x = 200\ mm$. In addition, the legend indicates the bending moment applied on crack J. The same shear stress distribution of Figure 4.33 is shown in Figure 4.34, Figure 4.35, and Figure 4.36. However, in these cases, the stage associated to each applied moment is distinguishable from each other. Some general observations are summarized below:

1) The influence of the shear force implies a loss of symmetry in the shear stress distribution.
2) The shape of the shear stresses is similar to those schemes given in Figure 4.4 to Figure 4.10.
3) When a shear force is acting in addition to the bending moments, the shear stresses are induced by the tension stiffening effect, such as in a zero shear region, and are also needed for equilibrium.
4) The complete interface behaves in a linear elastic way up to an applied moment of 5.0 *kNm* (see Figure 4.34). By slightly increasing the bending moment of crack J, Stage 2a.1 will initiate. When this happens, Zone II will appear near the location of crack J ($x = 200\ mm$). This stage is not apparent in Figure 4.33 due to

the sequence of the applied moment values chosen for the plot. Before the bending moment arrives at 10.0 *kNm* on crack J, Zone II has already appeared near crack I (x = 0 *mm*). Therefore, in this case, for this applied moment, Stage 2a.2 has already been initiated.

5) As the bending moment increases, the zero shear stress point, x_K, moves towards the less loaded crack.
6) The movement of the maximum shear stress point $x_{LM,right}$, previously defined in §4.3.2, is always towards crack I. The higher the bending moment acting on crack J, the shorter the distance between $x_{LM,right}$ and the zero shear stress point x_K.
7) As observed in Figure 4.35, the maximum shear stress point on the left $x_{LM,left}$ moves towards the zero shear stress location: first towards crack J, and later on when it is very close to x_K, $x_{LM,left}$ accompanies the zero shear stress point in its movement towards crack I.
8) When the applied moment on crack J reaches 65.9 *kNm*, the internal steel begins to yield at this location. In addition, the applied moment on crack J is 70.6 *kNm* when the internal steel yields in crack I. Note that once the steel yields in crack J, the crack propagation process is more accelerated. The movement of the zero shear stress location, x_K, towards crack I is much faster. The same occurs with the movement of both maximum shear stress locations which, at present, are close to the zero shear stress point.
9) The limit length for a short crack distance before steel yields in crack J is 93.2 *mm*. Since the crack distance 200 *mm* is longer than this limit, Stage 2b will never occur before the steel yields. Once the steel yields in crack J but not in crack I, this limit increases with the applied moment, from 93.2 *mm* to 189.2 *mm*. The last value is obtained when steel has yielded in both cracks I and J. Since the crack distance is not included in the range from 93.2 *mm* to 189.2 *mm*, Stage 2b will not appear whether the steel has yielded or not in one of the cracks.
10) At an applied moment on crack J of 69.0 *kNm*, the shear stress in crack J will have decreased to a zero value and Stage 3a will have initiated. Then, according to the bilinear bond-slip relationship, the maximum sliding of Zone II s_{L0} will be attained and the debonding of the external reinforcement will have started due to the formation of a macrocrack.
11) As shown in Figure 4.36, the macrocrack propagates as the applied moment on crack J increases beyond 69.0 *kNm*. The macrocrack length can be obtained as the extension of the zero shear stress points.
12) The maximum shear stress location $x_{LM,right}$ reaches crack I for an applied moment of 69.7 *kNm*. At this point, the macrocrack length is 32 *mm* and the remaining bonded length is lower than the limit given by solving equation (4.50). Then, Stage 3b initiates. As observed in Figure 4.36, the shear stresses along the remaining bonded length all run counter to the laminate tensile force on crack J.
13) An instant after Stage 3b initiates, the laminate completely debonds if the applied moment on crack J is increased. In this case, the condition for the development of Stage 3b given by equation (4.65) in terms of laminate tensile stress in crack J is not fulfilled.
14) To satisfy equation (4.65), the applied moment on crack J must decrease. Hence, the shear stress profile decreases with the evolution of Stage 3b up to the point when the remaining bonded length reaches the maximum sliding.

15) Since the internal steel has yielded only in crack J at the beginning of Stage 3b, the macrocrack (given by solving equation (4.62)) should increase in length as the applied moment decreases (see Figure 4.36). If so, the macrocrack enlarges from 32 *mm* at the beginning of Stage 3b to 103 *mm* for an applied moment of 65.9 *kNm*. Once the applied moment diminishes to the point that causes steel yielding in crack J (65.9 *kNm*), the macrocrack length will almost be constant. The evolution of the macrocrack length as Stage 3a and 3b develops is plotted in Figure 4.37.
16) From this point on, the shear stresses continue its decreasing trend to zero along the remaining bonded length without observing a significant macrocrack growth.
17) To conclude, if the external load was applied to this long crack distance by the use of load control, the laminate debonding would have occurred once the applied moment on crack J had reached 69.7 *kNm*; in other words at the end of Stage 3a. However, in the current example, after this bending moment has been attained, the debonding process will continue because slip control instead of load control will have been performed. Therefore, the laminate will debond at the end of Stage 3b, when the maximum sliding has been reached throughout the crack distance.

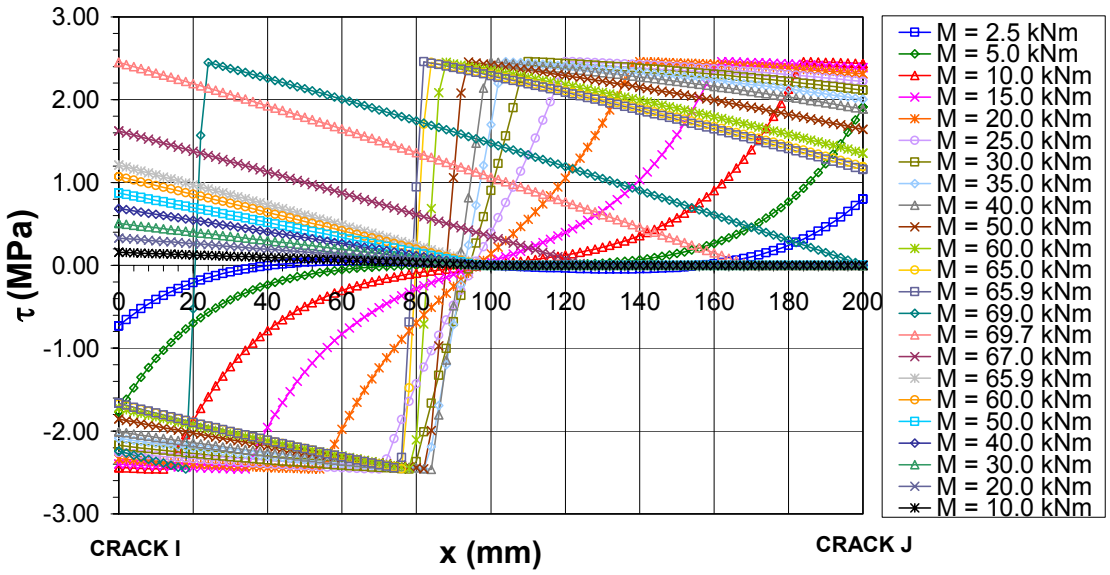

Figure 4.33. Shear stress distribution at the interface between two cracks subjected to shear forces and bending moments.

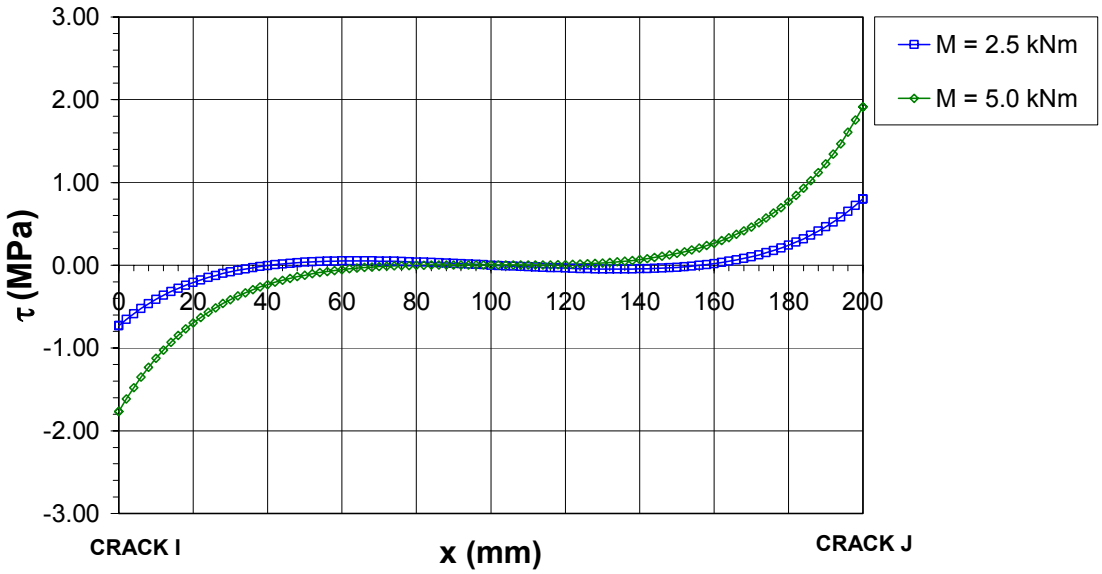

Figure 4.34. Shear stress distribution at the interface between two cracks subjected to shear and bending during Stage 1.

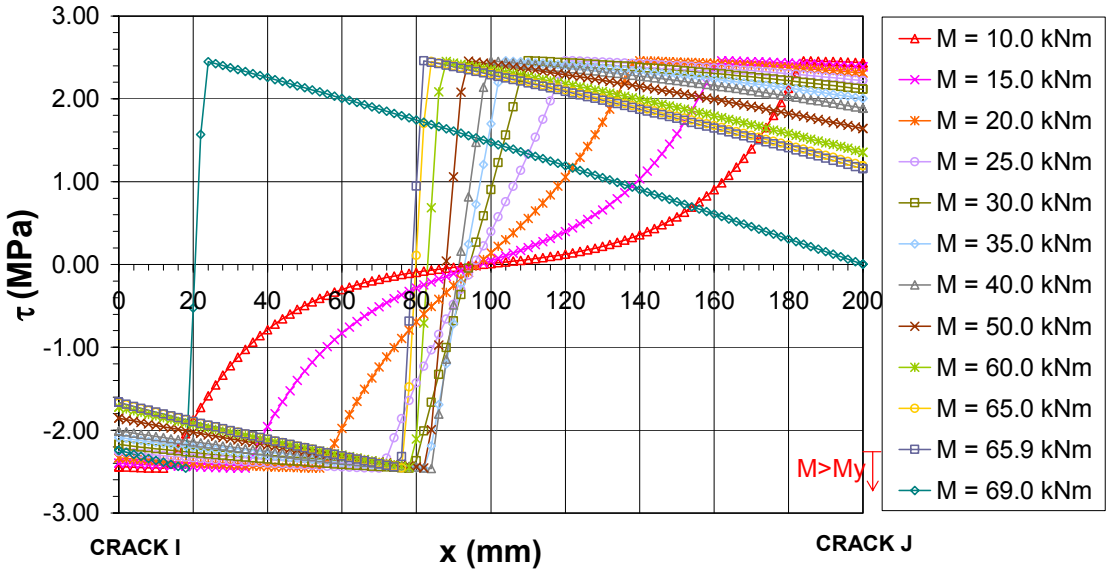

Figure 4.35. Shear stress distribution at the interface between two cracks subjected to shear and bending during Stage 2a.2.

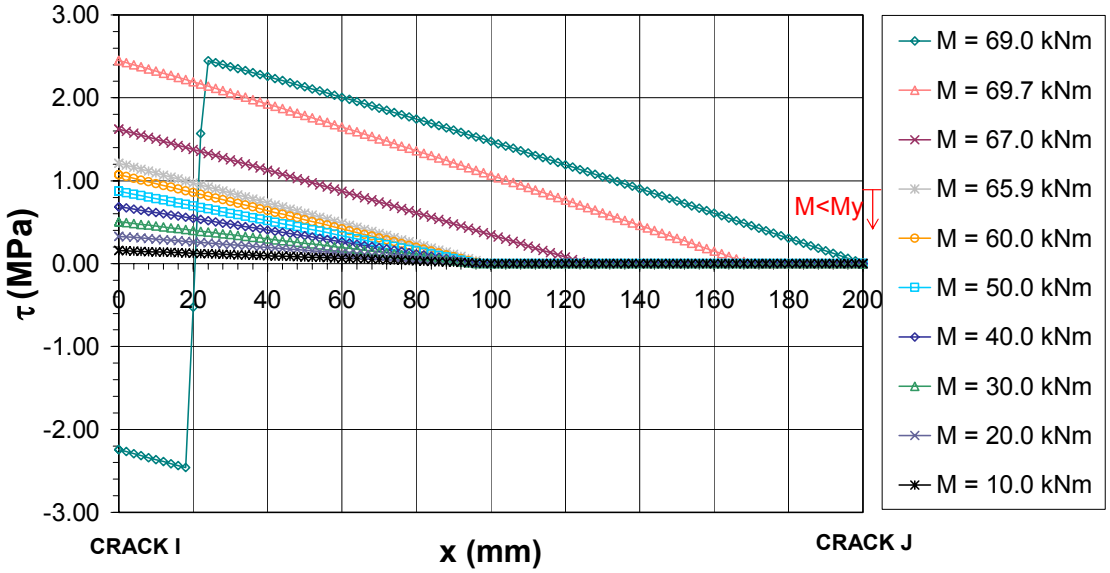

Figure 4.36. Shear stress distribution at the interface between two cracks subjected to shear and bending during Stage 3a and 3b.

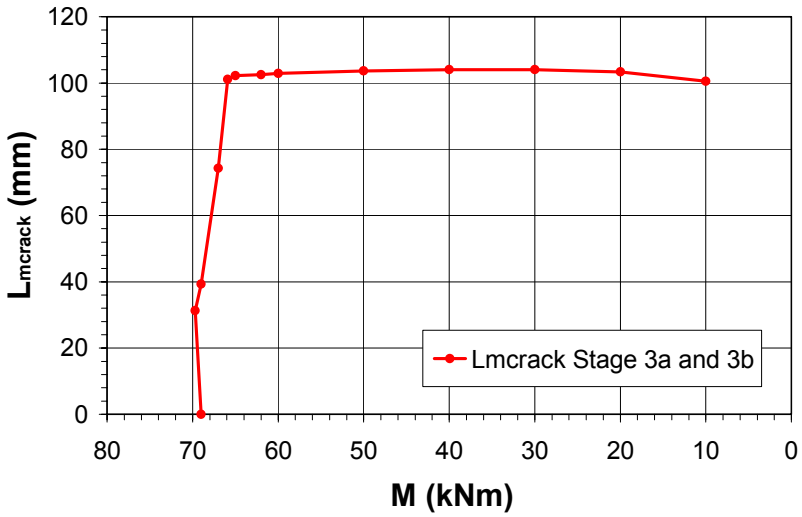

Figure 4.37. Evolution of the macrocrack length along Stages 3a and 3b.

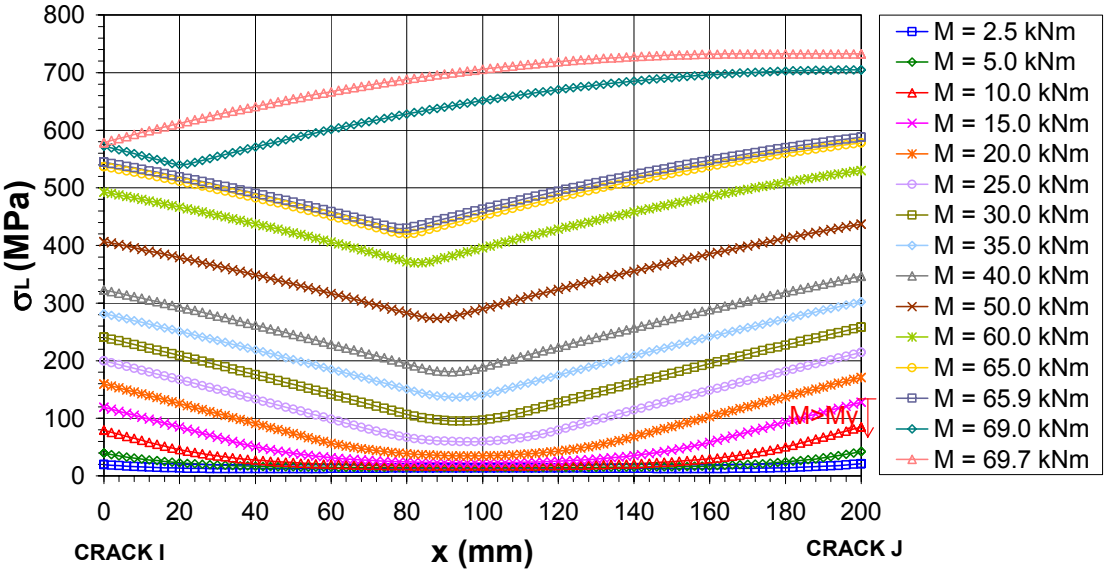

Figure 4.38. Laminate tensile stress distribution between two cracks subjected to shear and bending during Stage 1, 2a.2 and 3a.

Figure 4.38 shows the evolution of the laminate tensile stresses as long as the applied moment on crack J increases during Stages 1, 2a.2 and 3a. Some observations are listed below.

1) The tensile stress is at maximum on the crack tips and decreases from those points to a minimum value which corresponds to the zero shear stress location x_K.
2) In Figure 4.38, it is also possible to observe the evolution of x_K towards crack I with the applied load.
3) As in the previous example, once the internal steel reinforcement yields, the increase in the laminate tensile stresses is more significant.
4) As shown in Figure 4.36, when the maximum relative displacement between concrete and laminate s_{L0} is reached, the shear stresses decrease to zero. As a consequence, according to equation (3.9) of Chapter 3, the laminate tensile stress along the macrocrack length is constant and equal to that at the maximum sliding location. Therefore, there is always a horizontal branch near crack J in Figure 4.38 after the maximum sliding is reached, that is when the applied moment is higher than 69.0 *kNm*.
5) Once the bending moment in crack J has decreased beyond the steel yiending bending moment, the macrocrack length remains constant.

Figure 4.39 shows the tensile stress distribution during Stage 3b, from which some observations can be drawn.

1) For an applied moment on crack J of 69.7 *kNm*, the shear stress location will reach crack I, and Stage 3b will initiate. From this point on, if the applied moment on crack J is increased, the laminate will completely debond and no tensile stresses will be observed. On the contrary, for decreasing values of the applied moment, equation (4.65) will be satisfied and the data in Figure 4.39 will be obtained.

2) During Stage 3b, the tensile stress distribution is monotonically decreasing from crack J to crack I. The slope of the plotted lines turns smoother as the transferred force decreases (see Figure 4.39).
3) In addition, there is no minimum value in between both cracks because the shear stresses are different from zero along the remaining bonded length.
4) As shown in Figure 4.39, and in a similar manner as in Stage 3a, the tensile stress is constant along the macrocrack which propagates during Stage 3b. This is because the laminate is detached from the support and there is no shear transfer along this area.

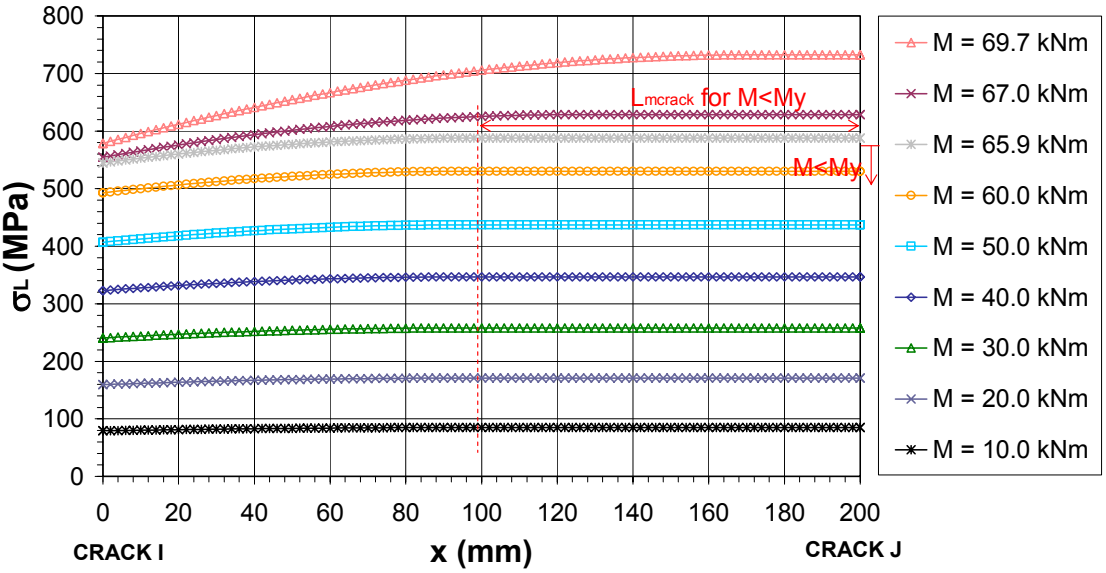

Figure 4.39. Laminate tensile stress distribution between two cracks subjected to shear and bending during Stage 3b.

The transferred force between two points can be calculated as either the difference between the laminate tensile forces under each crack or as the total shear stress area enclosed between both crack tips. As in the previous section, the increment of force between crack I and J and between each of these cracks and the zero shear stress point x_K, ΔP_{scr}, are plotted against the applied moment of crack J (Figure 4.40). Some observations are listed below.

1) The force transferred between crack J (higher moment) and the zero shear stress point is always higher than the force transferred between crack I (lower moment) and the zero shear stress point due to the non-symmetric form of the shear stress distribution.
2) As shown in Figure 4.33, the zero shear stress point is always closer to crack I than crack J. This point moves from its initial position on the left of the midpoint crack distance towards crack I. Therefore, the transferred force between crack I and J will rise with increasing values of the applied moment.
3) In the plotted line associated to crack I, there is a maximum value from which an increase of the moment at the crack location does not imply an increase of the force transferred between the laminate and the support. In this case, the maximum force transferred between crack I and x_K is 20.4 *kN* and it corresponds to a 30.0 *kNm* moment.

4) The maximum force transferred between crack J and x_K is 23.2 *kN* and it corresponds to a 40.0 *kNm* moment. This value is slightly lower than the theoretical maximum transferable force of 24.0 *kN* for a pure shear specimen of 100 *mm* length laminate (equation (3.76) of Chapter 3).
5) Beyond an applied moment of 65.9 *kNm*, there is a slight increase in the transferred force between crack J and x_K, implying a decrease of the force transferred between crack I and x_K. This may be related to the steel yielding in crack J that causes a fast movement of the zero shear stress point, x_K, before failure occurs. This fast movement is caused by the laminate in crack J, assuming alone the tensile increments of the section.
6) As previously mentioned, the force transferred between crack I and J can be obtained by subtracting the force between crack I and x_K from the force between x_K and crack J. This force represents the increment of tensile stresses between both cracks, an increment resulting from the shear force acting on the beam element. Due to the shear force there is an increment of the bending moment which generates a shear stress distribution to achieve equilibrium. The sum of the shear stresses is the transferred force.
7) The transferred force between crack I and J gradually inclines with the applied moment. After the internal steel yields in crack J, the slope increases sharply to the point where the zero shear stress point x_K reaches crack I. At this instant, the maximum transferred force between crack I and crack J of 21.5 *kN* is attained.
8) The maximum transferred force between crack I and J occurs when Stage 3b starts. At this point the maximum shear stress location $x_{LM,right}$ reaches crack I and the shear stresses follow the same direction. Therefore, the transferred force is directly equal to the sum of shear stresses along the remaining bonded crack distance.
9) By performing displacement control instead of load control, and if the applied moment is not increased after the initiation of Stage 3b, the laminate will not debond. The transferred force will follow the same previous pattern of development, diminishing as Stage 3b develops.
10) At the end of Stage 3b failure occurs, the maximum sliding s_{L0} is attained along the crack distance and the laminate will completely debond from the support. Thus, no force transfer will be possible.

Figure 4.41 plots the transferred force between crack I and J together with the maximum theoretical transferred force at the beginning of Stage 3b (as given by equation (4.78) in §4.3.6). The theoretical maximum transferred force plotted for different applied bending moments depends on the crack distance limit associated to the bending moment. As observed, the maximum transferred force, which is reached at the beginning of Stage 3b, is similar to the maximum theoretical value of equation (4.78). After Stage 3b is initiated, the maximum transferred force starts to decrease, and the transferred force becomes lower than the maximum value associated to any applied bending moment.

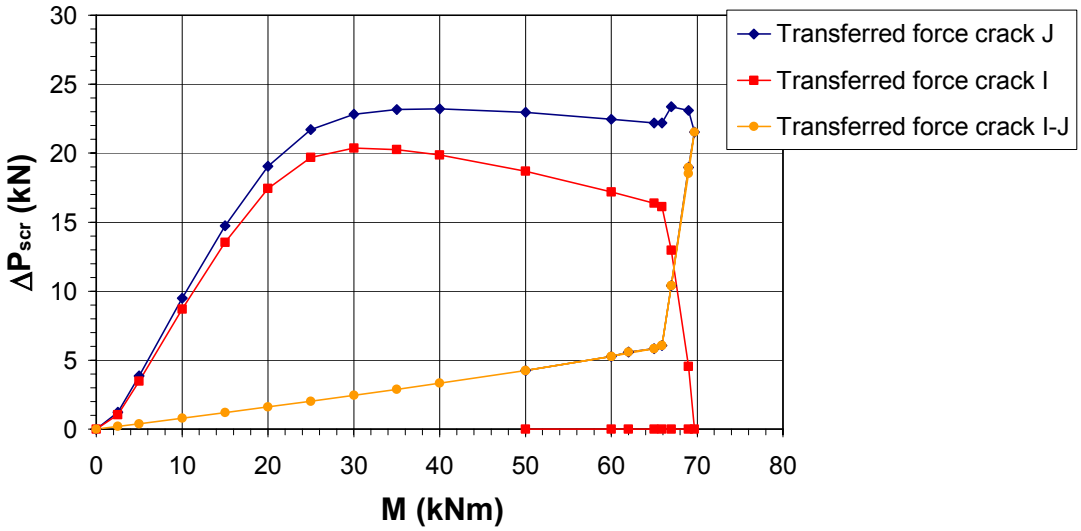

Figure 4.40. Force increment between each crack and the zero shear stress point. Transferred force along the crack distance.

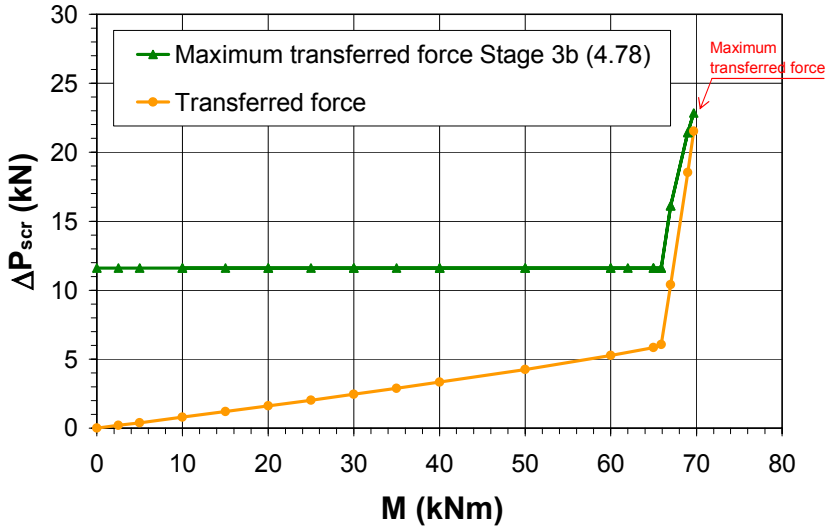

Figure 4.41. Maximum transferred force between cracks I and J.

In Figure 4.42 the relative displacement between concrete and laminate is shown.

1) The sliding is in the same direction as the tensile forces acting under each crack. Therefore, the relative displacement at the zero shear stress location is zero as well.
2) There is a plotted line related to the maximum sliding s_{L0}. If the maximum sliding is reached in crack J, an interfacial macrocrack will be initiated. In this example, once the applied moment on crack J is higher than 69.0 *kNm*, the macrocrack will start its propagation near crack J and will propagate to crack I.
3) The relative displacement between concrete and laminate of the debonded area, where the sliding is above s_{L0}, can be calculated as the maximum sliding plus the elastic elongation of the laminate debonded length.

$$s(x) = s_{L0} + \varepsilon_L(x)(x - x_{L0}) \qquad when \quad x \geq x_{L0} \tag{4.83}$$

4) As previously mentioned, a brittle and sudden debonding of the laminate may occur when Stage 3b initiates, even though the maximum sliding has not been reached in crack I. However, in a theoretical situation, the premature debonding can be avoided when the slip and not the applied force is controlled under both cracks.
5) Once Stage 3b initiates, the sliding continues to increase along the crack distance and the macrocrack propagates towards crack I. The macrocrack tip is located at the point where the shear stress is equal to zero. The sliding along the remaining bonded length increases up to the maximum value s_{L0}.
6) Since the internal steel is yielded in crack J at the beginning of Stage 3b, the macrocrack length increases with the evolution of this stage. Although the tensile force in crack J is diminishing, the slip along the macrocrack length is increasing because of the macrocrack growth.
7) When the applied moment has decreased to the value which causes steel yielding in crack J (65.9 *kNm*), the macrocrack length remains constant. From this point on, the sliding along the remaining bonded length increases to reach the maximum value of Zone II, s_{L0}. Meanwhile, the sliding along the macrocrack length decreases because the tensile force acting in crack J, that causes the laminate elastic elongation, diminishes as well. This trend is similar to that observed in Stage 3b of a pure shear specimen.
8) At the end of Stage 3b, the slip at any location is equal to the maximum value in Zone II, s_{L0}, and the laminate debonds.

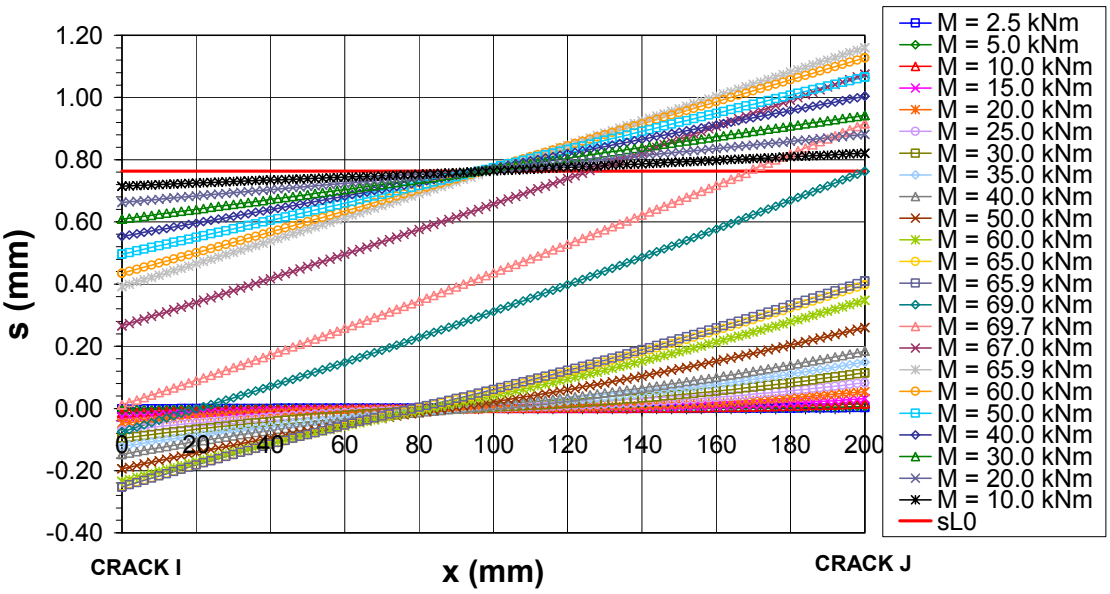

Figure 4.42. Relative displacement between support and laminate.

A study of the influence of the β parameter has been performed. The comparison in terms of shear stress and laminate tensile stress profiles shows the same general trends as in the pure flexure example. In short, the β factor which helps to reduce the laminate tensile stress does not have a significant influence in both stress distributions. Therefore, the simplest solution will be to designate β as equal to 0.0.

4.4. Stress and strain distribution at the laminate end

The following case between the end of the laminate and the crack that appears nearest to it is very similar to that of a beam element between two cracks. The main difference lies in not having an applied force at the end of the external reinforcement, so there is no restriction in the laminate to slide at this point, whenever no external anchorage is applied.

4.4.1. Conceptual analysis

Before giving the expressions for the tensile stress in the laminate, a description of the crack propagation problem is presented. Assuming a bilinear bond-slip relationship between the support and the external reinforcement, different stages can be distinguished depending on the tensile stress acting in crack J.

Stage 1

If the tensile stress in the laminate under the crack causes a sliding lower than the value associated to the maximum shear stress, s_{LM}, the complete interface between the laminate end and the nearest crack (crack J) will be under a linear elastic state (Zone 1). By applying the appropriate contour conditions to the general solution of Zone I, the distribution of tensile stresses can be obtained. From this expression, the shear stresses on the interface and its sliding can be derived. Figure 4.43 shows a shear stress distribution scheme between the laminate end and the nearest crack under Stage 1. The shear stresses decrease in an exponential manner from the crack tip, where the maximum value is reached, to the end of the laminate. In Stage 1, the shear stress under the crack is always lower than the maximum value τ_{LM}. In addition, as will be shown in a later example, there is a concentration of shear stresses at the free laminate end where the stresses are unequal to zero. Note that the shear stresses are opposite to the tensile stress in crack J as long as there is no tensile force acting at the laminate end.

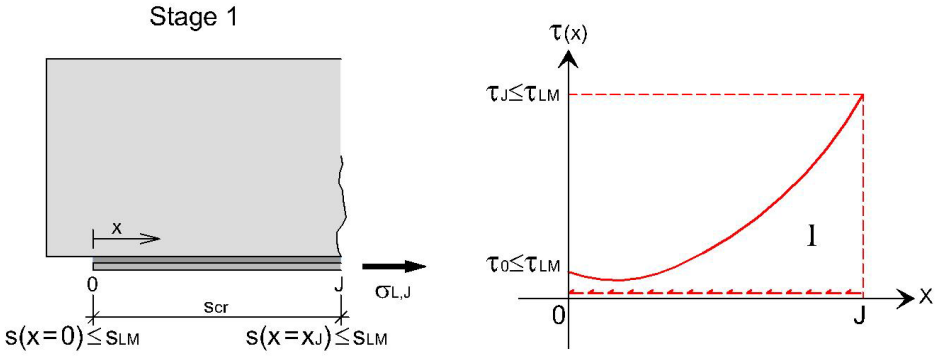

Figure 4.43. Shear stress distribution at the laminate end in Stage 1.

Throughout all the stages, the laminate tensile stress distribution decreases from its maximum value at the crack tip to a zero value at the free laminate end.

Stage 2

Stage 2 is characterized by having part of the bonded connection in Zone II of the bond-slip relationship. Stage 2 can be divided into Stage 2a and Stage 2b. Stage 2a always develops, and initiates at the end of Stage 1. Stage 2b appears only under certain circumstances depending on the distance between the free laminate end and the nearest crack.

Stage 2a

When the maximum shear stress τ_{LM} is reached on the cracked section, the formation of microcracks is initiated. From this point on, the interface behaves under Stage 2a. The bonded length will be divided into two regions (Zones I and II) depending on the slip value of each point. The nearest region to the loaded end of the laminate (Zone II) will behave in a non-linear way. The concrete-reinforcement slip at Zone II will be larger than s_{LM}, so it will be positioned on the descending branch of the bond-slip curve. The rest of the connection (Zone I) will remain in a linear elastic state. As long as the applied load increases, the shear stress peak will move towards the free laminate end. A scheme of the distribution of shear stresses is shown in Figure 4.44.

As mentioned, the tensile stress distribution decreases from the crack location to the laminate end. The slope of the tensile stress profile is steeper along Zone II than in Zone I.

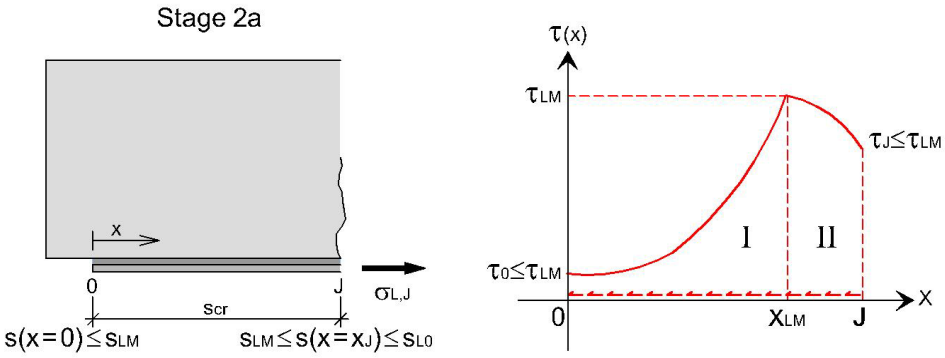

Figure 4.44. Shear stress distribution at the end of the laminate in Stage 2a.

Stage 2b

If the distance between crack J and the laminate end is longer than a certain limit, there will be enough length for the development of the complete shear stress distribution. If the bonded length is not long enough, the maximum shear stress τ_{LM} may reach the laminate end before the complete development of Zone II; in other words, before the maximum sliding is attained on crack J. In this case, Stage 2b will initiate.
During Stage 2b, the complete interface is in the downward branch of the bilinear bond-slip relationship (Zone II). Therefore, the shear stresses decrease monotonically as the sliding along the bonded length increases (see Figure 4.45). Microcracks propagate along the distance between the crack and the laminate end. The development of

Stage 2b is only possible if the shear stress at the laminate end is decreasing from its maximum value. The end of Stage 2b is attained once the maximum sliding is reached in crack J. The maximum sliding is reached simultaneously not only in crack J but along the complete bonded length. Therefore, laminate debonding occurs at the same instant at every location.

As a conclusion, the debonding process for a short distance between the laminate end and the nearest crack finishes at the end of Stage 2b.

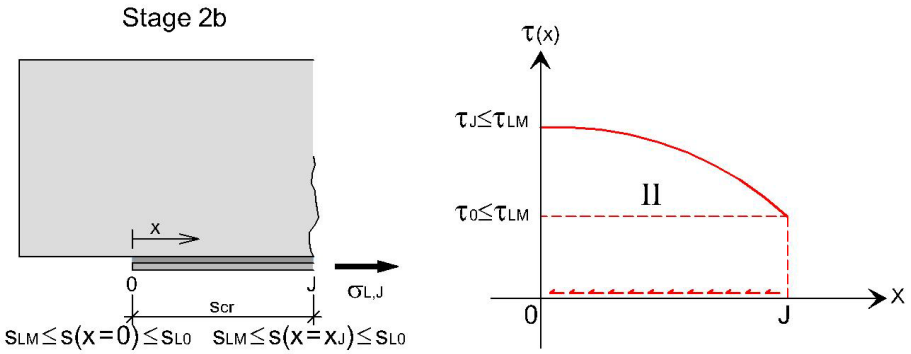

Figure 4.45. Shear stress distribution at the end of the laminate in Stage 2b.

Stage 3

At the beginning of Stage 3, an interfacial macrocrack opens and starts its propagation process. Part of the laminate debonds from the surface. For laminates with long enough lengths, Stage 3a will develop at the end of Stage 2a, and afterwards, Stage 3b will appear. As previously mentioned, when the laminate is not long enough, Stage 3a will never occur and the laminate completely debonds at the end of Stage 2b.

Stage 3a

Once the maximum slip s_{L0} is reached in the cracked section, a horizontal macrocrack will appear and the laminate will start its debonding process. The shear stresses along the macrocrack extension are zero, and as a consequence the tensile stresses are constant along the debonded length. As long as the relative sliding under the flexural or shear crack increases, the macrocrack propagates to the end of the laminate. Figure 4.46 shows the shear stress distribution between the laminate end and the nearest crack when the debonding process has started.

The laminate will be completely detached when the maximum slip location reaches the laminate end.

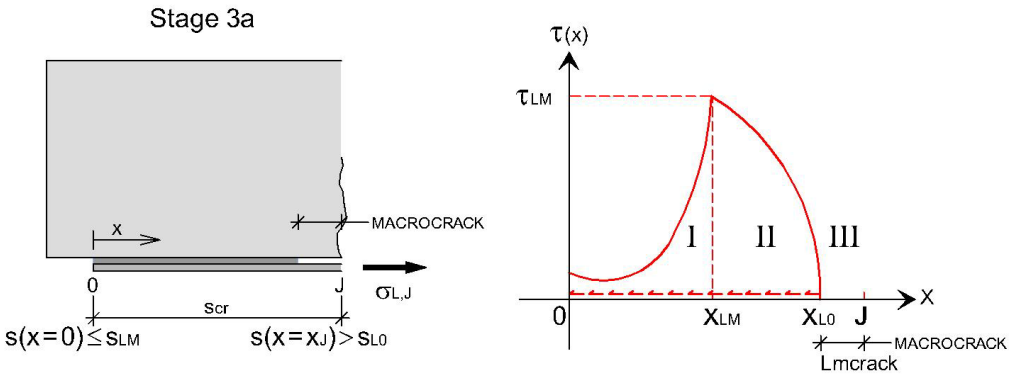

Figure 4.46. Shear stress distribution at the end of the laminate in Stage 3a.

Stage 3b

As Stage 3a develops, the maximum shear stress will eventually reach the laminate end. Then, Stage 3b will initiate.

Since the complete bonded length is in Zone II of the bond-slip curve, microcracks will appear along the remaining bonded length. As shown in Figure 4.47, the shear stress distribution decreases as long as the sliding increases to the maximum value s_{L0}. As will be explained in §4.4.4, the macrocrack does not grow at all during Stage 3b.

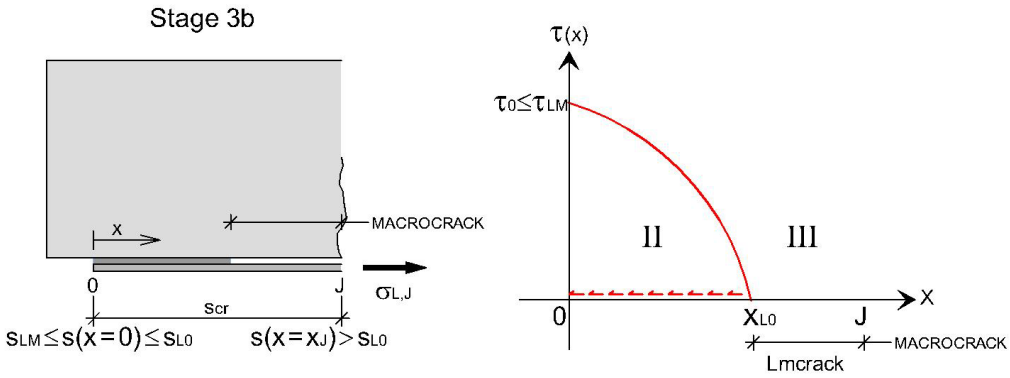

Figure 4.47. Shear stress distribution at the end of the laminate in Stage 3b.

It is observed that the shear stresses profiles of Stages 1, 2 and 3 are very similar to that of a pure shear test given in Chapter 3. If no transverse load is applied between the laminate end and the nearest crack, this element will behave in a similar way than a single/double shear test.

4.4.2. General equations for the stress distribution at the laminate end

The stress distribution can be found by solving the governing differential equations (4.1) and (4.3), derived in §4.2. Again, it is necessary to determine the tensile stress in the concrete bottom fiber.

In the crack tip, the concrete tensile stress is zero. In most cases, at the end of the laminate the concrete section is uncracked. In these cases, the Navier-Bernouilli assumption of plane and normal section remains plane and normal to the deformed axis after loading is accomplished at the laminate end. Between both sections, the concrete stress distribution is approached as a parabolic function with its axis of symmetry at the end of the laminate, as shown in Figure 4.48.

$$\sigma_{c,b}(x) = -\frac{1}{s_{cr}^2}\sigma_{c,b}(x=0)\left(x^2 - s_{cr}^2\right) \tag{4.84}$$

where:

$\sigma_{c,b}(x=0)$ is obtained according to the strength of materials approach:

$$\sigma_{c,b}(x=0) = \frac{M(x=0)}{I_{tr,c}^{*}} y_{G^*} \tag{4.85}$$

To make the stress formulae at the end of the laminate similar to that of the previous section, the concrete tensile stress is defined as a fraction β of the concrete tensile strength.

$$\sigma_{c,b}(x=0) = \frac{M(x=0)}{I_{tr,c}^{*}} y_{G^*} = \beta f_{ctm} \tag{4.86}$$

Therefore, the β parameter for $x = 0$ can be defined as shown in equation (4.87) as the ratio between the linear elastic concrete stress due to the applied moment and the tensile concrete strength. It should be mentioned that the β factor should be lower than 1.0 because the concrete stresses should be lower than the tensile strength as long as no crack has appeared at the laminate end section.

$$\beta = \frac{1}{f_{ctm}}\left(\frac{M(x=0)}{I_{tr,c}^{*}} y_{G^*}\right) \not> 1.0 \tag{4.87}$$

In the following, the parabolic function that approaches the concrete stress distribution is given by equation (4.88) which depends on a β parameter.

$$\sigma_{c,b}(x) = -\frac{1}{s_{cr}^2}\beta f_{ctm}\left(x^2 - s_{cr}^2\right) \tag{4.88}$$

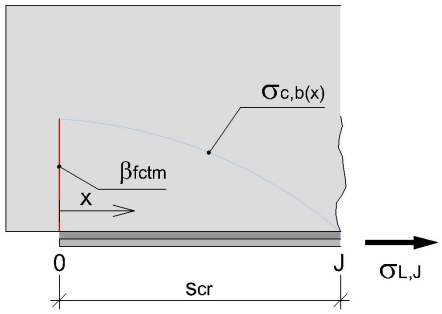

Figure 4.48. Assumed concrete tensile stress distribution.

By incorporating equation (4.88) in the governing differential equations for Zone I and II, the general solutions for both zones are easily derived depending on four integration constants C_1, C_2, C_3 and C_4. Equations (4.89) and (4.90) are very similar to equations (4.25) and (4.26) associated to the case between two cracks.

$$\sigma_L^I(x) = C_1 \cosh(\Omega_1 x) + C_2 \sinh(\Omega_1 x) + \frac{\mu}{2\Omega_1^2} + \frac{\mu}{4}\left(x^2 - s_{cr}^2\right) \tag{4.89}$$

$$\sigma_L^I(x) = C_3 \cos(\Omega_2 x) + C_4 \sin(\Omega_2 x) - \frac{\mu}{2\Omega_2^2} + \frac{\mu}{4}\left(x^2 - s_{cr}^2\right) \tag{4.90}$$

where:

Ω_1: constant given by equation (4.2)
Ω_2: constant given by equation (4.4)
μ: constant given by equation (4.23)

For the different stages previously mentioned, the integration constants are obtained by applying the appropriate contour conditions which are defined in terms of laminate tensile stress and shear stress.

4.4.3. Stress distribution at the laminate end prior to the initiation of the debonding process

In this section, the equations for the tensile stress in the laminate are given for Stages 1 and 2 of the debonding process. As previously mentioned, to obtain the shear stress distribution, the laminate tensile stress expression must be differentiated by x and multiplied by the thickness of the laminate, as shown in equation (3.9) of Chapter 3. The slip between concrete and the laminate is easily found by using the bond-slip relationship (equation (3.12) of Chapter 3).

Stage 1: $s(x = x_J) \le s_{LM}$

For $0 \le x \le x_J$ (Zone I)

$$\sigma_L^I(x) = \frac{1}{\sinh(\Omega_1 s_{cr})}\left\{-\frac{\mu}{4}\left(\frac{2}{\Omega_1^2} - s_{cr}^2\right)\sinh(\Omega_1(s_{cr} - x)) + \left(\sigma_{L,J} - \frac{\mu}{2\Omega_1^2}\right)\sinh(\Omega_1 x)\right\} + \\ + \frac{\mu}{2\Omega_1^2} + \frac{\mu}{4}\left(x^2 - s_{cr}^2\right) \tag{4.91}$$

The derivative of equation (4.91) gives the shear stress distribution which is a decreasing function for the distance from crack J until the laminate end. The shear stress at the laminate end is given by equation (4.92).

$$\tau^I(x = 0) = \frac{\Omega_1 t_L}{\sinh(\Omega_1 s_{cr})}\left\{\frac{\mu}{4}\left(\frac{2}{\Omega_1^2} - s_{cr}^2\right)\cosh(\Omega_1 s_{cr}) + \left(\sigma_{L,J} - \frac{\mu}{2\Omega_1^2}\right)\right\} \tag{4.92}$$

Stage 2

Stage 2a: $s(x = x_J) > s_{LM}$

For $0 \le x \le x_{LM}$ (Zone I)

$$\sigma_L^I(x) = \frac{1}{\cosh(\Omega_1 x_{LM})}\left\{-\frac{\mu}{4}\left(\frac{2}{\Omega_1^2} - s_{cr}^2\right)\cosh(\Omega_1(x_{LM} - x)) + \left(\frac{\tau_{LM}}{\Omega_1 t_L} - \frac{\mu}{2\Omega_1}x_{LM}\right)\right. \\ \left.\sinh(\Omega_1 x)\right\} + \frac{\mu}{2\Omega_1^2} + \frac{\mu}{4}\left(x^2 - s_{cr}^2\right) \tag{4.93}$$

For $x_{LM} \le x \le x_J$ (Zone II)

$$\sigma_L^{II}(x) = \frac{1}{\cos(\Omega_2(s_{cr} - x_{LM}))}\left\{\left(\sigma_{L,J} + \frac{\mu}{2\Omega_2^2}\right)\cos(\Omega_2(x - x_{LM})) - \left(\frac{\tau_{LM}}{\Omega_2 t_L} - \frac{\mu}{2\Omega_2}x_{LM}\right)\right. \\ \left.\sin(\Omega_2(s_{cr} - x))\right\} - \frac{\mu}{2\Omega_2^2} + \frac{\mu}{4}\left(x^2 - s_{cr}^2\right) \tag{4.94}$$

The location of the maximum stress point, x_{LM}, is easily found solving the equation given by (4.95).

$$\frac{1}{\cosh(\Omega_1 x_{LM})}\left\{-\frac{\mu}{4}\left(\frac{2}{\Omega_1^2} - s_{cr}^2\right) + \left(\frac{\tau_{LM}}{\Omega_1 t_L} - \frac{\mu}{2\Omega_1}x_{LM}\right)\sinh(\Omega_1 x_{LM})\right\} + \frac{\mu}{2\Omega_1^2} = \\ \frac{1}{\cos(\Omega_2(x_J - x_{LM}))}\left\{\left(\sigma_{L,J} + \frac{\mu}{2\Omega_2^2}\right) - \left(\frac{\tau_{LM}}{\Omega_2 t_L} - \frac{\mu}{2\Omega_2}x_{LM}\right)\sin(\Omega_2(x_J - x_{LM}))\right\} - \frac{\mu}{2\Omega_2^2} \tag{4.95}$$

The shear stress at the free laminate end can be found using equation (4.96). Note that the shear stress at this location increases as Stage 2a develops. Only when the maximum shear stress, τ_{LM}, reaches the laminate end, will the entire interface be in Zone II.

$$\tau^{I}(x=0)=\frac{\Omega_1 t_L}{\cosh(\Omega_1 x_{LM})}\left\{\frac{\mu}{4}\left[\frac{2}{\Omega_1^2}-s_{cr}^2\right]\sinh(\Omega_1 x_{LM})+\left[\frac{\tau_{LM}}{\Omega_1 t_L}-\frac{\mu}{2\Omega_1}x_{LM}\right]\right\} \tag{4.96}$$

Stage 2b: $s(x = x_J) > s_{LM}$

For short bonded lengths, the maximum shear stress will eventually reach crack I before the complete development of Zone II. In this case, the whole bonded length is in Zone II of the bond-slip curve and the equations of Stage 2a are no longer valid. Thus, the laminate tensile stress can then be expressed as equation (4.97)

For $0 \le x \le x_J$ (Zone II)

$$\sigma_L^{II}(x)=\frac{1}{\sin(\Omega_2 s_{cr})}\left\{\left(\sigma_{L,J}+\frac{\mu}{2\Omega_2^2}\right)\sin(\Omega_2 x)+\frac{\mu}{4}\left(\frac{2}{\Omega_2^2}+s_{cr}^2\right)\sin(\Omega_2(x_J-x))\right\} -\frac{\mu}{2\Omega_2^2}+\frac{\mu}{4}\left(x^2-s_{cr}^2\right) \tag{4.97}$$

For the development of Stage 2b, the shear stress at the laminate end should be lower than the maximum value τ_{LM}. Therefore, after incorporating equation (4.45) into the derivative of equation (4.97), the following condition is obtained for the laminate tensile stress in crack J.

$$\sigma_{L,J} \le \frac{P_{\max,L=scr}}{A_L}-\frac{\mu}{2\Omega_2^2}(1-\cos(\Omega_2 s_{cr}))+\frac{\mu}{4}s_{cr}^2\cos(\Omega_2 s_{cr}) \tag{4.98}$$

If the concrete's contribution in tension is not considered, equation (4.98) is simplified as equation (4.99).

$$\sigma_{L,J} \le \frac{P_{\max,L=scr}}{A_L} \tag{4.99}$$

Equation (4.99) is a particular case of equation (4.47) between two cracks when assuming a zero tensile stress in crack I ($\upsilon = 0$). In addition, equation (4.99) shows that the tensile force during Stage 2b has an upper limit which is the maximum transferred force for a pure shear specimen. Hence, the maximum transferred force of Stage 2b between the laminate end and the nearest crack is obtained when Stage 2b initiates and is equal to the upper limit given by equation (4.99).

For short bonded lengths, the shear stress distribution decreases as Stage 2b evolves. Meanwhile, the relative sliding increases until the maximum value s_{L0} is attained along the complete bonded length. This occurs at the same instant at any laminate location.

Therefore, under these circumstances, the laminate completely debonds at the end of Stage 2b.

Limit length between a short and long distance in an element between the laminate end and the nearest crack

As previously mentioned, depending on the laminate length between the laminate end and the nearest crack, during Stage 2a, the maximum shear stress may reach the laminate end. The limit length for the non-development of Stage 2b is obtained in this section.

In a limit situation, the maximum shear stress reaches the laminate end when the shear stress simultaneously decreases to a zero value at the crack location. By imposing both conditions into equation (4.97) and by solving equation (4.100), the length that gives the transition between a short and long distance at the laminate end is obtained. Equation (4.101) gives the value of the laminate tensile stress in crack J in this limit situation.

$$\sigma_{L,J}\cos\left(\Omega_2 s_{cr,\lim end}\right)-\frac{\mu}{2\Omega_2}\left[\frac{1-\cos\left(\Omega_2 s_{cr.\lim end}\right)}{\Omega_2}-\frac{\Omega_2 s_{cr,\lim end}^2}{2}+\right. \\ \left.+s_{cr,\lim end}\sin\left(\Omega_2 s_{cr,\lim end}\right)\right]=0 \tag{4.100}$$

$$\sigma_{L,J}=\frac{P_{\max,L=scr}}{A_L\left(1+\cos\left(\Omega_2 s_{cr,\lim end}\right)\right)}-\frac{\mu}{2\Omega_2}\left(\frac{\Omega_2 s_{cr,\lim end}^2}{2}+s_{cr,\lim end}\frac{\sin\left(\Omega_2 s_{cr,\lim end}\right)}{\left(1+\cos\left(\Omega_2 s_{cr,\lim end}\right)\right)}\right) \tag{4.101}$$

After incorporating equation (4.101) into equation (4.100), the resulting equation will be fulfilled if one of the following conditions is verified:

a) $$\cos\left(\Omega_2 s_{cr,\lim end}\right)=0 \tag{4.102}$$

b) $$\frac{P_{\max,L=scr}}{A_L}+\frac{\mu}{4}\left(s_{cr,\lim end}^2+\frac{2}{\Omega_2^2}\right)\sin^2\left(\Omega_2 s_{cr,\lim end}\right)-\frac{\mu}{2\Omega_2}\sin\left(\Omega_2 s_{cr,\lim end}\right)=0 \tag{4.103}$$

Since equation (4.103) is always different from zero, especially for μ = 0, equation (4.102) will give the limit length for the distance at the laminate end, which is expressed as (4.104). This limit length is in fact the limit between a short and long laminate in a pure shear specimen (see equation (3.34) of Chapter 3).

$$s_{cr,\lim end}=\frac{\pi}{2\Omega_2} \tag{4.104}$$

From now on, the short laminate end distance denominations will comprise those distances between the laminate end and the nearest crack to it whose lengths are shorter than the limit $s_{cr,\lim end}$. On the contrary, long laminate end distances are longer than this limit.

$$s_{cr}\le s_{cr,\lim end} \qquad \text{Short laminate end distance} \tag{4.105}$$

$s_{cr} \geq s_{cr,\lim end}$ Long laminate end distance (4.106)

4.4.4. Stress distribution at the laminate end during the debonding process

Once the slip at the loaded end of the laminate ($x = 0$) reaches the maximum sliding s_{L0}, the microcracks become a macrocrack, and the debonding process initiates. This section compiles the laminate tensile stress equations during Stages 3a and 3b for a long distance between the laminate end and the nearest crack. As explained in §4.4.1, for short bonded lengths, the laminate debonds at the end of Stage 2b.

Long laminate end distance

Stage 3a: $s(x = x_J) > s_{L0}$

Stage 3a initiates when the tensile stress in crack J reaches the value given by equation (4.107). At this point, a macrocrack opens near crack J and starts to grow towards the laminate end.

$$\sigma_{L,J} = \frac{1}{\sin\left(\Omega_2\left(x_J - x_{LM,right}\right)\right)}\left[\frac{\tau_{LM}}{t_L\Omega_2} - \frac{\mu}{2\Omega_2}x_{LM,right}\right] + \frac{\mu s_{cr}}{2\Omega_2\tan\left(\Omega_2\left(x_J - x_{LM,right}\right)\right)} - \frac{\mu}{2\Omega_2^2} \quad (4.107)$$

In case the concrete's contribution in tension is neglected, equation (4.107) will be simplified to equation (4.57), which agrees with the condition for the development of Stage 3a in an element between two cracks.

When an interfacial macrocrack appears near crack J, the laminate bonded length is reduced to s_{cr} - L_{mcrack}. The formulae of Stage 3a are similar to Stage 2a when the origin of coordinates moves from crack J to the interfacial crack tip. For simplicity, to continue with the same reference system, the formulae of Stage 3a will be equal to equations (4.93) to (4.95) but referring all distances to the maximum sliding location x_{L0}. For example, the crack distance s_{cr} is substituted by s_{cr} - L_{mcrack}.

In addition, note that if the concrete stress contribution is neglected in equations (4.93) to (4.95), that is if $\mu = 0$, the equations for the tensile stress at the laminate end will be the same as the equations derived for a single or double shear case.

The macrocrack length can be obtained at any load level by assuming a zero shear stress value at the macrocrack tip location.

$$\frac{t_L\Omega_2}{\cos\left(\Omega_2\left(s_{cr}-L_{mcrack}-x_{LM}\right)\right)}\left\{-\left(\sigma_{L,J}+\frac{\mu}{2\Omega_2^2}\right)\sin\left(\Omega_2\left(s_{cr}-L_{mcrack}-x_{LM}\right)\right)+\frac{\tau_{LM}}{t_L\Omega_2}-\right.$$
$$\left.-\frac{\mu}{\Omega_2}x_{LM}\right\}+\frac{\mu t_L}{2}\left(s_{cr}-L_{mcrack}\right)=0 \tag{4.108}$$

If the concrete's contribution in tension is neglected, the macrocrack length, L_{mcrack}, can explicitly be written as (4.109).

$$L_{mcrack}=s_{cr}-\left(x_{LM}+\frac{1}{\Omega_2}\arcsin\left(\frac{\tau_{LM}}{t_L\Omega_2\sigma_{L,J}}\right)\right) \tag{4.109}$$

As shown by equation (4.109), the macrocrack length increases during Stage 3a since both x_{LM} and the arc sine decreases as this stage evolves.

Stage 3b: $s(x = x_J) > s_{L0}$ and $s(x = 0) > s_{LM}$

While the macrocrack propagates along Stage 3a, the maximum shear stress τ_{LM} will eventually reach the laminate end. The remaining bonded length between the laminate end and the macrocrack tip will be then in Zone II of the bond-slip relationship.

This situation will occur once the remaining bonded length reaches the limit between a short and long distance at the laminate end, which is expressed as (4.110) in the case when the concrete tensile stresses are neglected.

$$\left(s_{cr}-L_{mcrack}\right)_{\lim end}=\frac{\pi}{2\Omega_2} \tag{4.110}$$

The formulae of the previous stages are no longer valid since the remaining bonded interface is in the descending branch of the bond-slip curve. Thus, the laminate tensile stresses are given by equation (4.111) which is similar to Stage 2b but the crack distance is replaced by the remaining bonded length.

For $0 \le x \le x_J$ (Zone II)

$$\sigma_L^{II}(x)=\frac{1}{\sin\left(\Omega_2\left(s_{cr}-L_{mcrack}\right)\right)}\left\{\left(\sigma_{L,J}+\frac{\mu}{2\Omega_2^2}\right)\sin\left(\Omega_2 x\right)+\frac{\mu}{4}\left(\frac{2}{\Omega_2^2}+\left(s_{cr}-L_{mcrack}\right)\right)\right.$$
$$\left.\sin\left(\Omega_2\left(s_{cr}-L_{mcrack}-x\right)\right)\right\}-\frac{\mu}{2\Omega_2^2}+\frac{\mu}{4}\left(x^2-\left(s_{cr}-L_{mcrack}\right)^2\right) \tag{4.111}$$

The macrocrack length, or alternatively the macrocrack tip location, can be obtained by solving equation (4.112) which is derived by imposing a zero shear stress value at this location.

$$\frac{1}{\sin(\Omega_2(s_{cr}-L_{mcrack}))}\left\{\left(\sigma_{L,J}+\frac{\mu}{2\Omega_2^2}\right)\cos(\Omega_2(s_{cr}-L_{mcrack}))-\right.$$
$$\left.-\frac{\mu}{4}\left(\frac{2}{\Omega_2^2}+(s_{cr}-L_{mcrack})^2\right)\right\}+\frac{\mu}{2\Omega_2}(s_{cr}-L_{mcrack})=0 \quad (4.112)$$

If the concrete's contribution in tension is neglected, the macrocrack length stays constant and equal to the limit between a short and long end laminate distance distance, as shown in (4.113).

$$s_{cr}-L_{mcrack}=\frac{\pi}{2\Omega_2} \quad (4.113)$$

The macrocrack length grows during Stage 3a until the maximum shear stress reaches at the laminate end and Stage 3b initiates. During the development of Stage 3b, the sliding in the remaining bonded length increases, but no macrocrack growth exists when neglecting the concrete's contribution in tension. Once the shear stress diminishes to a zero value, the laminate completely debonds from the support. At this point, the macrocrack grows from the value given by equation (4.110) to the value given by the distance between the laminate end and the nearest crack. Such a behavior is similar to that observed in a pure shear specimen as described in Chapter 3. Contrary to the case between two cracks, the macrocrack growth does not depend on the steel yielding.

For the development of Stage 3b, the shear stress at the laminate end should be lower than the maximum value τ_{LM}. Therefore, equation (4.120) should be accomplished.

$$\sigma_{L,J}\le\frac{P_{\max,\,L=scr-Lmcrack}}{A_L}-\frac{\mu}{2\Omega_2^2}(1-\cos(\Omega_2(s_{cr}-L_{mcrack})))+$$
$$+\frac{\mu}{4}(s_{cr}-L_{mcrack})^2\cos(\Omega_2(s_{cr}-L_{mcrack})) \quad (4.114)$$

From this later equation, it can be inferred that the tensile force in crack J should be lower than the maximum transferred force of a pure shear specimen whose length is the remaining bonded length between the laminate end and the macrocrack tip. For $\mu = 0$, this condition is exactly the same as for a pure shear specimen (Chapter 3).

Since the remaining bonded length is lower than the limit between a short and long distance, the transferred force during Stage 3b as derived from equation (4.114) is always lower than the transferred force in Stage 2a. The decreasing trend of the transferred force implies a decreasing elastic elongation and then a decreasing sliding along the debonded length.

4.4.5. Summary

This section presents a brief summary of the sequence of stages that arise during the debonding process. Table 4.2 summarizes them, distinguishing between short and long distances between the laminate end and the nearest crack in proximity.

Table 4.2. Stages that arise at the laminate end for short and long laminates.

At the laminate end				
LONG END DISTANCES				
Flexure and shear	Stage 1	Stage 2a	Stage 3a (*)	Stage 3b (*)
SHORT END DISTANCES				
Flexure and shear	Stage 1	Stage 2a	Stage 2b (*)	

(*) This stage will arise if displacement control is performed

4.4.6. Transferred force in an element between the laminate end and the nearest crack

Since the tensile force at the laminate end is zero when no external force or external anchorage device has been applied at this location, the transferred force in an element between the laminate end and the nearest crack is equal to the tensile force in crack J to reach equilibrium.

When the concrete's contribution is not considered, the transferred force is equal to that of a pure shear specimen. Therefore, the same trends described in §3.3.4 in relation to the maximum transferred force are valid in this case.

A brief summary is presented here for the sake of completeness. For long laminates, the maximum transferred force is obtained during Stage 2a before the zero shear stress appears in crack J. For short laminates, the maximum transferred force is obtained at the beginning of Stage 2b when the maximum shear stress reaches the laminate end. Equation (3.76) of Chapter 3 gives the maximum transferred force for both short and long bonded lengths as a function of fracture energy.

In a general case where the concrete's contribution is considered, the maximum transferred force for long distances between the laminate end and the nearest crack to it is reached during Stage 2a. From equation (4.95), the transferred force along Stage 2a can be written as a function of the length of Zone II, x_{LM}, as shown in equation (4.115).

$$\begin{aligned}\Delta P_{scr,end} = &\left(\frac{\tau_{LM} b_L}{\Omega_2} - \frac{\mu A_L x_{LM}}{2\Omega_2}\right)\left[\frac{\Omega_2}{\Omega_1}\tanh(\Omega_1 x_{LM})\cos(\Omega_2(x_J - x_{LM}))+\right.\\ &\left.+\sin(\Omega_2(x_J - x_{LM}))\right]+\frac{\mu A_L}{2\Omega_1^2}\cos(\Omega_2(x_J - x_{LM}))\left(1-\frac{1}{\cosh(\Omega_1 x_{LM})}\right)-\\ &-\frac{\mu A_L}{2\Omega_2^2}(1-\cos(\Omega_2(x_J - x_{LM})))+\frac{\mu A_L}{4}s_{cr}^2\frac{\cos(\Omega_2(x_J - x_{LM}))}{\cosh(\Omega_1 x_{LM})}\end{aligned} \quad (4.115)$$

The maximum transferred force for long distances between the laminate end and the nearest crack to it is associated to the length of Zone II, $x_{LM,P}$, which equals to zero the derivative of the transferred force given by equation (4.116).

$$\left(\tau_{LM} b_L - \frac{\mu A_L x_{LM,P}}{2}\right)\tanh\left(\Omega_1 x_{LM,P}\right)\left[\tanh\left(\Omega_1 x_{LM,P}\right)\cos\left(\Omega_2\left(x_J - x_{LM,P}\right)\right) + \right.$$
$$\left. + \frac{\Omega_2}{\Omega_1}\sin\left(\Omega_2\left(x_J - x_{LM,P}\right)\right)\right] - \frac{\mu A_L}{2}\frac{\Omega_2}{\Omega_1}\sin\left(\Omega_2\left(x_J - x_{LM,P}\right)\right)\left[\frac{\Omega_2}{\Omega_1} + \left(\frac{s_{cr}^2}{2}\Omega_1 - 1\right)\right. \quad (4.116)$$
$$\left.\frac{1}{\cosh\left(\Omega_1 x_{LM,P}\right)} - \frac{\Omega_1^2}{\Omega_2}\frac{s_{cr}^2}{2}\tanh\left(\Omega_1 x_{LM,P}\right)\tan\left(\Omega_2\left(x_J - x_{LM,P}\right)\right)\right] = 0$$

Therefore, by incorporating the value of $x_{LM,P}$ that solves equation (4.116) into equation (4.115), the maximum transferred force is obtained.

For short distances between the laminate end and the nearest crack to it, the maximum transferred force is reached just when Stage 2b starts. At this point the maximum transferred force, as given by equation (4.117), coincides with the limit condition for the development of Stage 2b (see equation (4.98)). $P_{\max,L=scr}$ is the maximum transferred force for a pure shear specimen whose length is equal to the laminate end distance.

$$\Delta P_{\max scr,end} = P_{\max,\,L=scr} - \frac{\mu A_L}{2\Omega_2^2}\left(1 - \cos\left(\Omega_2 s_{cr}\right)\right) + \frac{\mu A_L}{4} s_{cr}^2 \cos\left(\Omega_2 s_{cr}\right) \quad (4.117)$$

In terms of transferred force, the difference between the laminate end element and the element between two cracks is the non-direct dependence of the first case on the steel yielding. The maximum transferred force will have the same expression regardless of the steel stress in either crack J or at the laminate end.

4.4.7. Example of a beam element between the laminate end and the closest crack in proximity

An example of applying the formulae at the end of the laminate is presented. The beam segment is analyzed while it is subjected to different bending moments applied on the crack tip section. As in the previous cases, a required data when calculating the stress profiles on the laminate and the interface is the value of the laminate tensile stress in the crack. This value is calculated by means of a moment-curvature analysis.

The distance between the laminate end and the nearest crack is 200 *mm*. This is shorter than the limit between a short and long laminate end distance, 401 *mm*, as given by equation (4.104). Therefore, as this example is of a short laminate end distance, the following stages will be observed: Stage 1, 2a and 2b. The section and material properties are the same as Beam 2 of the Experimental Program described in Chapter 2. The model parameters in this example are: τ_{LM} = 2.46 *MPa*, s_{LM} = 0.008 *mm*, and s_{L0} = 0.764 *mm*.

In this example, the concrete's contribution in tension is considered. As mentioned in §4.4.2, the β parameter is given by equation (4.87) after assuming Navier-Bernouilli assumption. Note that β should always be lower than or equal to 1.0.

Figure 4.49 show the shear stress distribution between the laminate end and the nearest crack along Stages 1 and 2a. The shape is very similar to that of the pure shear example presented in Chapter 3. The only difference in this case is that the concrete's contribution in tension is taken into account. A set of comments to Figure 4.49 is presented below.

1) Unlike the case between two cracks, the shear stresses along the complete bonded length at the laminate end are acting in the opposite direction to the tensile stress in the laminate under the crack. There is no zero shear stress point. Therefore, the displacement between concrete and laminate is in the same direction as the tensile force as shown in Figure 4.49.
2) Stage 1 finishes when the applied moment is slightly higher than 5.0 *kNm*. At this point, the maximum shear force τ_{LM} acts in the cracked section and Stage 2a starts.
3) As long as the applied moment increases, the maximum shear stress location x_{LM} moves towards the laminate end.
4) Since the distance between the laminate end and crack J is classified as a short distance, the maximum shear stress reaches the laminate end during Stage 2a. In this example, this situation occurs for an applied moment of 37.5 *kNm*. At this point, Stage 2a finishes and Stage 2b starts.
5) In some experimental programs of externally reinforced beams tested under a three or four-point bending configuration, a shear stress concentration at the end of the laminate was observed. This phenomenon can be appreciated also in Figure 4.49. As long as the applied moment increases, the shear stress at the end of the laminate increases as well.
6) By looking at Table 4.3, the following comparisons can be made. First the shear stress at the laminate end calculated according to §4.4.3 can be compared to the values derived from the formulae associated to a pure shear case derived in Chapter 3. Then, the laminate end shear stress can be compared to the values obtained by performing a linear elastic analysis described in Chapter 2. Neglecting the concrete's contribution in tension on the stress transmission, which is equivalent to apply the formulae derived for a pure shear case, can be unconservative because the shear stresses obtained at the laminate end are much lower compared to those calculated by using a certain concrete contribution. The values derived from the linear elastic analysis are not realistic. Even for low load levels the shear stress at the end is higher than the concrete tensile strength which means that a crack has appear at the interface which may be unreal.

Table 4.3. Comparison of the shear stress values at the laminate end $x = 0$ *mm*.

	$\tau(x = 0)$ (*MPa*)		
M (*kNm*)	At the laminate end Chapter 4 β (plain section) $\not>$ 1	Pure shear Chapter 3 or Chapter 4 with $\beta = 0$	Linear elastic analysis Chapter 2
2.5	0.24	0.00	0.52
5.0	0.49	0.00	1.04
10.0	0.75	0.01	2.08
15.0	0.76	0.02	3.12
20.0	0.78	0.04	4.16
25.0	0.84	0.11	5.20
30.0	1.01	0.34	6.24
35.0	1.62	1.22	7.28

7) Neglecting the concrete's tensile stresses in deriving shear stresses not only influences the shear stress at the end of the laminate but also the complete shear stress distribution. As shown in Figure 4.50, the shear stress profile for $\beta = 0$ is similar to that given in the example of a short laminate in §3.8.2 of Chapter 3, because in this case, both formulations are very similar. When comparing both Figure 4.49 and Figure 4.50, the progress of Zone II is more accelerated for $\beta = 0$. As a consequence, the maximum shear stress location x_{LM} is much closer to the end of the laminate for $\beta = 0$ than when considering the concrete's contribution in tension.

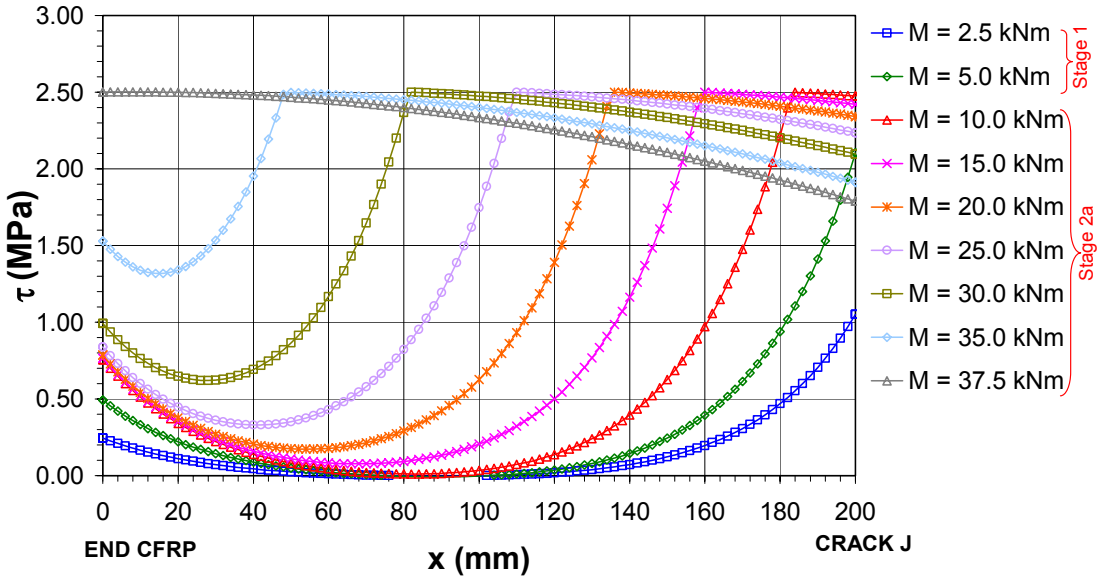

Figure 4.49. Shear stress distribution at the interface between the end of the laminate and the nearest crack during Stages 1 and 2a.

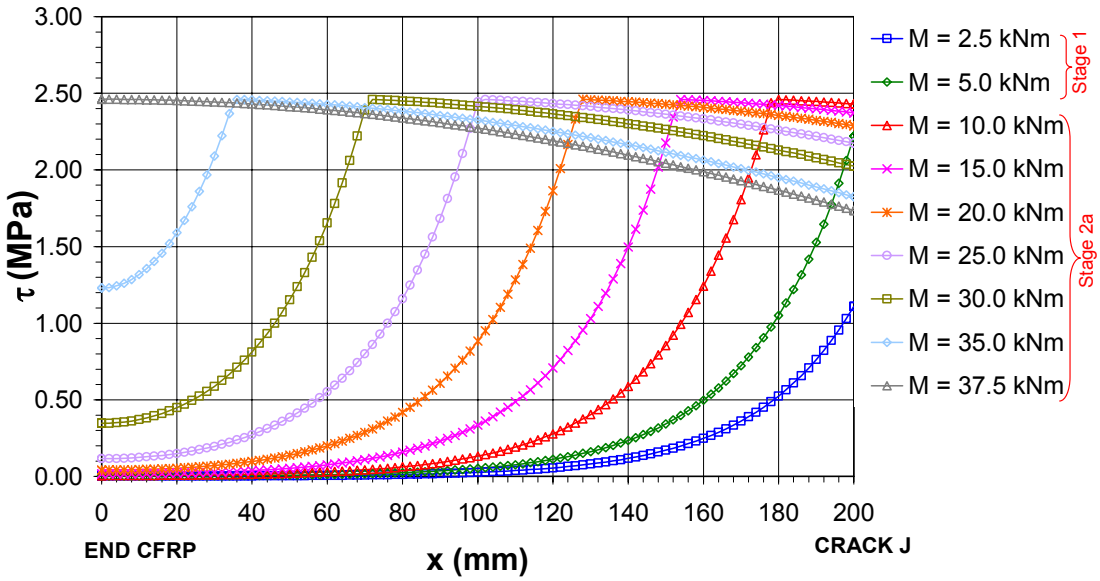

Figure 4.50. Shear stress distribution at the interface between the end of the laminate and the nearest crack during Stages 1 and 2a when the concrete's contribution in tension is not considered.

Figure 4.51 illustrates the shear stress distribution along Stage 2b between the end of the laminate and the nearest crack to it. Some observations regarding Figure 4.51 follow:

1) Stage 2b is only possible for decreasing values of the tensile stress in crack J, or in other words, for decreasing values of the applied moment at this location.
2) During this stage, the shear stress distribution is in Zone II of the bond-slip relationship. Therefore, as Stage 2b evolves, the shear stress distribution decreases along the complete bonded length while the relative sliding increases up to the maximum value, s_{L0}.
3) The slope of the shear stress profiles decreases with the evolution of Stage 2b. This decreasing tendency is more accentuated near the laminate end than in the vicinity of crack J.
4) Failure due to the appearance of an interfacial macrocrack will start when the shear stress has already decreased to zero along the complete bonded length. The laminate will then debond in a sudden and brittle manner. This laminate debonding occurs simultaneously at any location between the laminate end and crack J.
5) If only the interfacial shear stresses are considered, the laminate debonding will occur as explained above. However, special care should be taken at the laminate end because the shear stresses combined with the interfacial normal stress concentration (described in Chapter 2) can lead to a premature failure. If the principal stresses at the laminate end exceed either the concrete tensile strength or the values given by the different failure criteria described in Chapter 2, a crack will appear, and then the laminate will start its debonding process, starting from the laminate end towards the nearest crack.

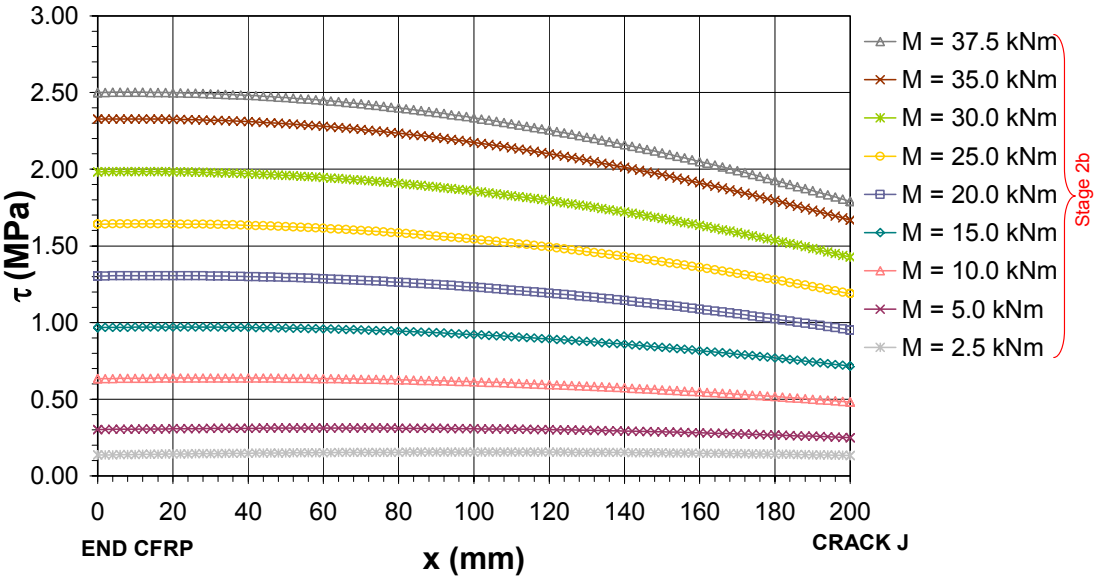

Figure 4.51. Shear stress distribution at the interface between the end of the laminate and the nearest crack during Stage 2b

In Figure 4.52, the laminate tensile stress distribution during Stages 1 and 2a is shown. The following observations can be drawn:

1) The tensile stress profiles increases with increasing values of the applied moment on crack J.
2) During Stage 1, the tensile stress distribution is a decreasing function, with a smooth slope, from crack J to the laminate end.
3) Once the maximum shear stress reaches crack J, part of the interface will be in Zone II of the bond-slip relationship. The stress decreases gradually with a pronounced slope from crack J to the laminate end. Along Zone I, the slope of the tensile stress distribution becomes smoother.
4) The maximum tensile stress is always located on the crack tip. In addition, the tensile stress at the laminate end is zero because no force is applied at this location.

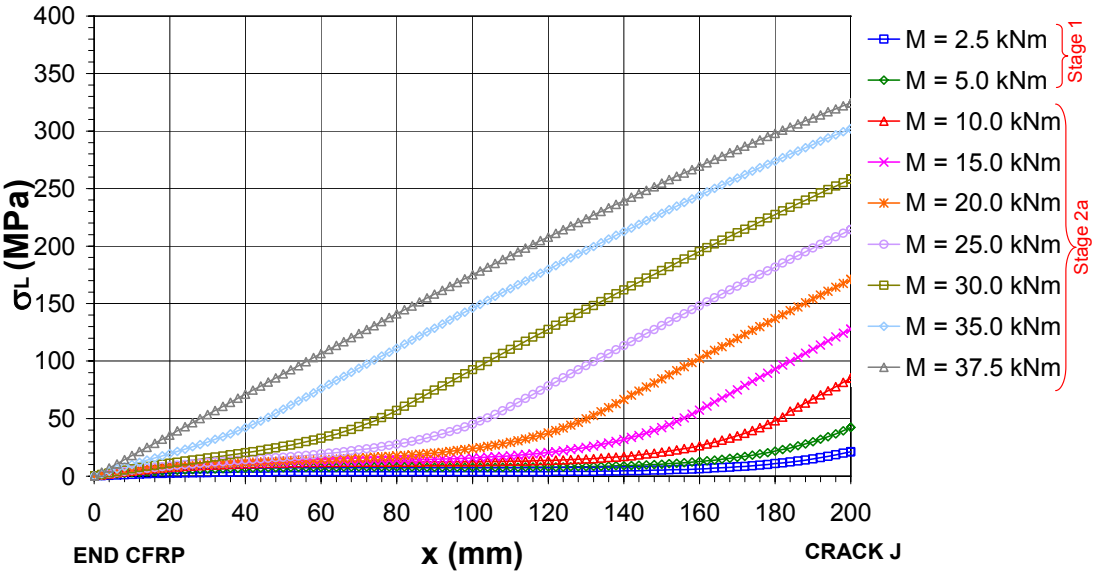

Figure 4.52. Laminate tensile stress distribution at the end of the laminate during Stage 1 and 2a.

Figure 4.53 shows the laminate tensile stress distribution during Stage 2b. The tensile stress profiles decrease to zero as long as the applied moment on crack J decreases. The maximum value of the tensile stress reached in crack J during the previous stages is not exceeded during Stage 2b. In addition, the laminate tensile profiles are concave for Stages 1 and 2a, and convex for Stage 2b.

Both Figure 4.52 and Figure 4.53 are similar to those obtained for a pure shear specimen in the example of a short bonded length given in §3.8.2 of Chapter 3.

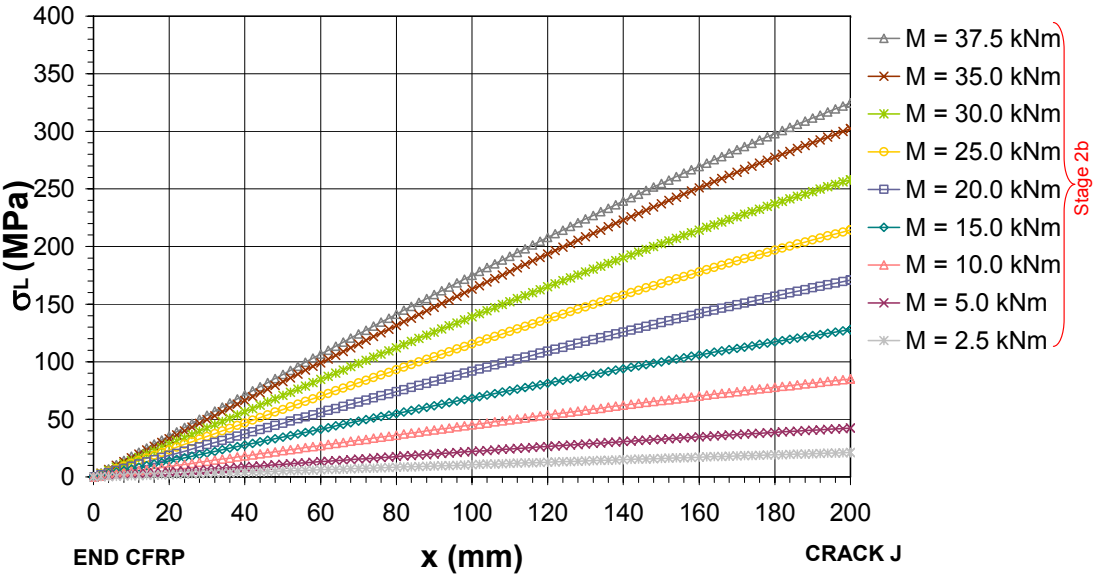

Figure 4.53. Laminate tensile stress distribution at the end of the laminate during Stage 2b.

The maximum transferred force between the last crack and the laminate end is equal to the tensile force of crack J because no tensile stress is acting at the laminate end. The maximum transferred force, 44.80 *kN*, is reached at the end of Stage 2a, that is, when the maximum shear stress reaches the laminate end (at 37.5 *kNm*). At this point, the steel has steel not yielded either in crack J or at the laminate end (M_y = 65.9 *kNm*). Afterwards, during Stage 2b, the tensile stress in crack J decreases as observed in Figure 4.53, so the transferred force decreases as well. If the concrete's contribution in tension is not considered, the maximum transferred force will be equal to the theoretical maximum transferred force of a pure shear specimen given by equation (3.76) of Chapter 3, which in this case is 44.20 *kN*. When both maximum values are compared regardless of whether the concrete's contribution in tension is considered, it can be inferred that the influence of the concrete is almost negligible in terms of transferred force.

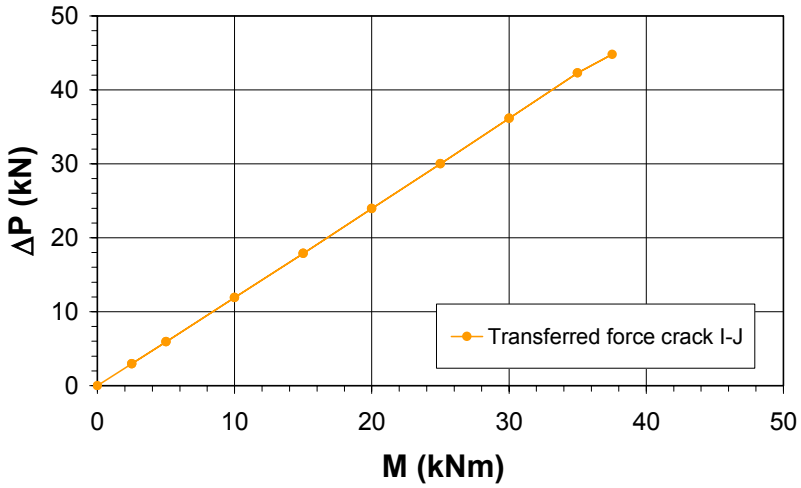

Figure 4.54. Transferred force along the interface at the end of the laminate.

In relation to the relative displacement between concrete and laminate as shown in Figure 4.55, the profile is very similar to a pure shear state. The values of sliding along the bonded length during Stages 1 and 2a ($M < 37.5$ *kNm*) are much lower than the maximum sliding s_{L0}. For example, when the applied moment is 37.5 *kNm*, the relative displacement in crack J is 0.223 *mm*, which represents 29.1 percent of the maximum value s_{L0}. During Stage 2b, the relative sliding increases up to s_{L0}. A significant increase in the relative sliding at the laminate end is observed during this stage. Since the sliding increments are higher at this location compared to the increments in crack J, the slope of the plotted lines decrease as Stage 2b develops.

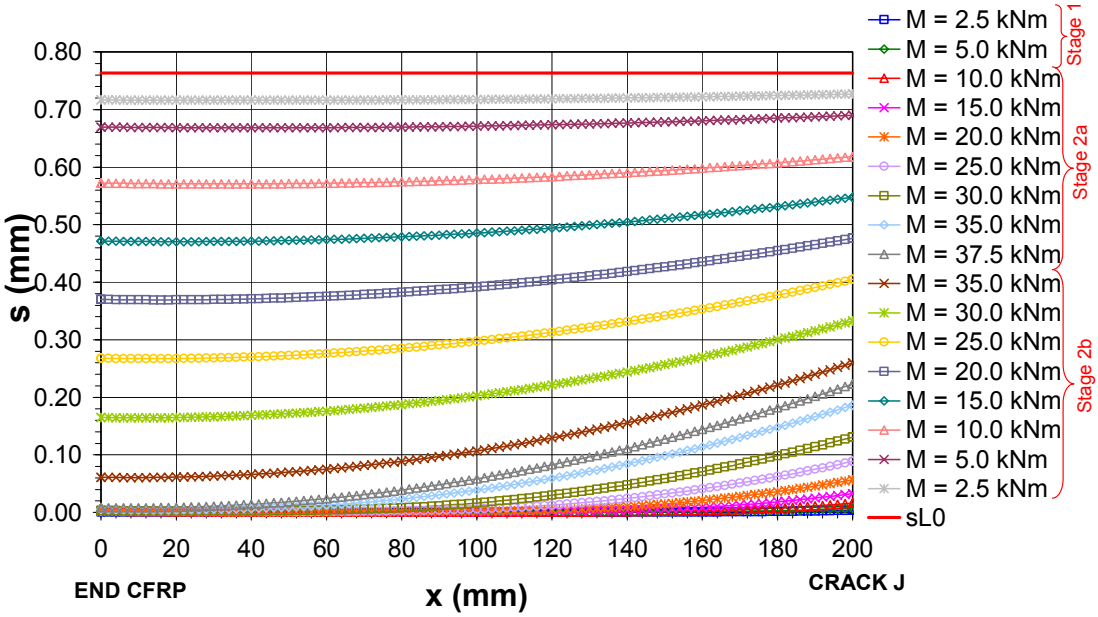

Figure 4.55. Relative displacement between concrete and laminate at the laminate end.

From this example, it can be concluded that all the stress profiles at the laminate end are similar to that of a pure shear specimen (see Chapter 3) when the concrete's contribution in tension is not considered. In addition, the influence of the concrete's contribution is especially significant in the shear profiles at the laminate end.

4.5. Stress and strain profiles on a cracked beam

In the previous sections §4.3 and §4.4, the formulae for an element between two cracks and for an element at the laminate end were developed. In this section, these formulae will be applied to the particular case of a beam under transverse loads. For this purpose, Beam 2/C was chosen from the experimental program described in Chapter 2 where its geometry and materials properties were fully described.

The beam was precracked before applying the external reinforcement. The crack pattern under service load of the unstrengthened beam is shown in Figure 4.56.

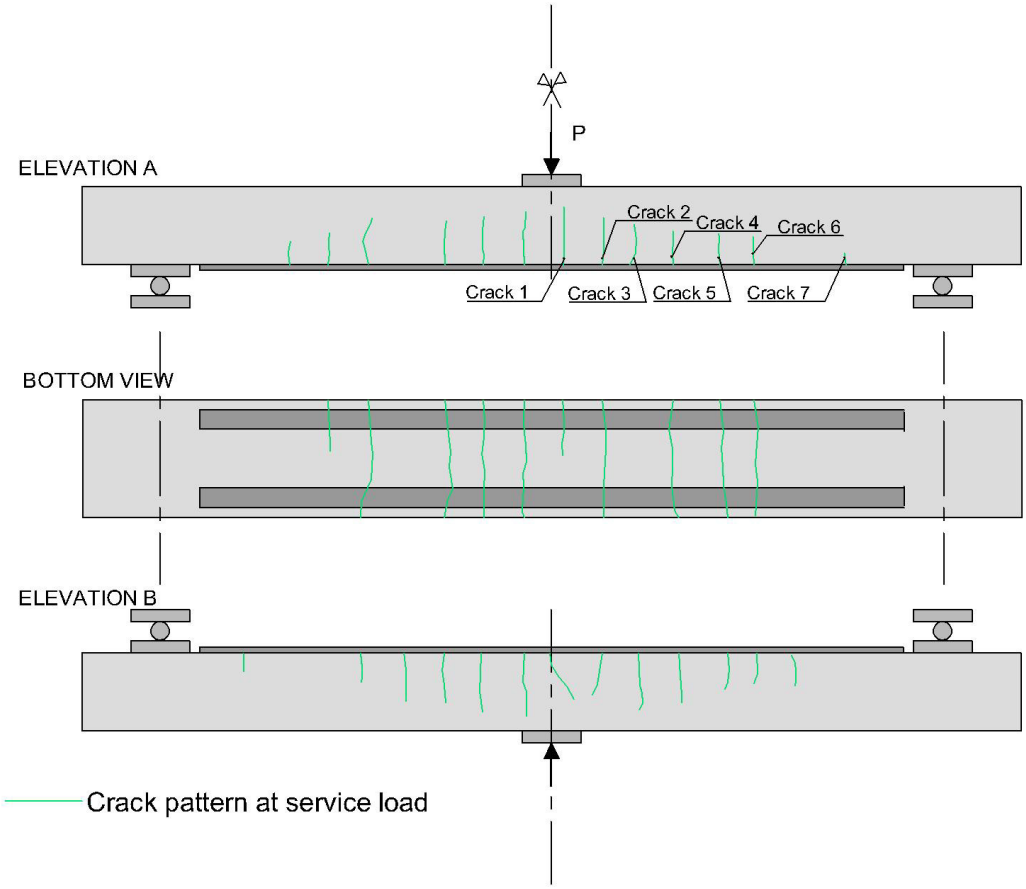

Figure 4.56. Crack pattern of Beam 2/C before strengthening.

The position of the cracks on the right side of the beam, with the origin of coordinates at the end of the laminate, x, and the distance between cracks, Δx, are shown in Table 4.4. The observed average crack spacing was 125 *mm*.

Table 4.4. Crack position and distance between cracks in Beam 2/C.

	Crack 1	Crack 2	Crack 3	Crack 4	Crack 5	Crack 6	Crack 7
x (*mm*)	872	770	700	590	470	382	147
	Crack1-2	Crack2-3	Crack3-4	Crack4-5	Crack 5-6	Crack 6-7	Crack 7-End
Δx(*mm*)	102	70	110	120	88	235	147

Once the CFRP laminates were applied, the beam was tested up to load failure using a three-point bending load configuration. As described in Chapter 2, when the applied load reached F_u = 142.8 *kN*, one of the laminates suddenly debonded and a sharp decrease on the applied load was observed. Later on, the applied load recovered and increased again up to the point when the remaining bonded laminate peeled-off.

As shown in Figure 4.56, two laminates of 50 *mm* x 1.40 *mm* with a 190 *mm* distance between their edges were applied to strengthen the section. To simplify the problem, the effect of using separate laminates has not been considered, though the external reinforcement has been assumed to be acting as one whole laminate.

The model parameters obtained for Beam 2/C are τ_{LM} = 2.46 *MPa*, s_{LM} = 0.008 *mm*, and s_{L0} = 0.764 *mm*. The laminate tensile stresses in each crack have been obtained by means of a moment-curvature analysis of the strengthened section. Using the data obtained, the equations of the previous sections (§4.3 and §4.4) have then been applied, and have provided the shear stress distribution at the interface, the laminate tensile stress, the laminate strain, and the relative displacement between the support and the external reinforcement profiles (Figure 4.58, Figure 4.59, Figure 4.60, Figure 4.61, respectively).

Only the right hand side of the laminate bonded length has been studied. The load increments up to 90% F_u, have been ten percent of the failure load, ΔF = 10% F_u. Just before reaching load failure, some more cases have been studied: 92.5% F_u, 95% F_u and 97.5% F_u.

As previously discussed, the internal steel yielding helps to interpret the debonding process. During the test, no strain gauges were affixed to the internal steel reinforcement. Therefore, the experimental value of the yielding load is an interpretation of the laminate strain profiles obtained from the strain gauges bonded to the laminate. According to the moment-curvature analysis, the internal steel reinforcement yielded when the applied force at midspan was 131.7 *kN*, which represents 92 percent of the failure load. The rebars in crack 1 yielded at an applied load of 135.5 *kN*. In addition, the internal steel was supposed to yield in crack 2 for an applied load at midspan of 151.4 *kN*. So long as the failure load is lower than the last value, when the laminate peels-off, the internal steel has yielded from a certain point between crack 1 and 2 (x = 781 *mm*) to midspan.

According to the conclusions of the examples given in the previous sections, the β value which defines the concrete's contribution in tension does not have a significant influence at failure loads. It seems reasonable to assume β = 0 between cracks, since it leads to a conservative and simple solution. However, as shown in §4.4.7, the concrete's contribution in tension especially affects the shear stresses at the laminate end. Therefore, the β parameter, which was defined in §4.4.2, has been considered between the laminate end and the nearest crack to it.

According to §4.3.3, the limit length between a short and long crack distance depends on the internal steel state, in other words, it depends on the bending moment acting on crack J. As shown in Figure 4.57, the crack distance limit ranges between 93 to 189 *mm*. According to this range, the concrete teeth between crack 2 and 3, and between crack 5 and 6 are short crack distances regardless of the internal steel state. On the contrary, the distance between crack 6 and 7 has been considered long because it is always above the crack distance limit range. The remaining concrete teeth will be short or long depending on the bending moment acting on the most loaded crack.

The limit length for a short and long distance between the laminate end and the nearest crack is 398 *mm*. Since the actual distance at the laminate end is 147 *mm*, it has been assumed as a short laminate end length.

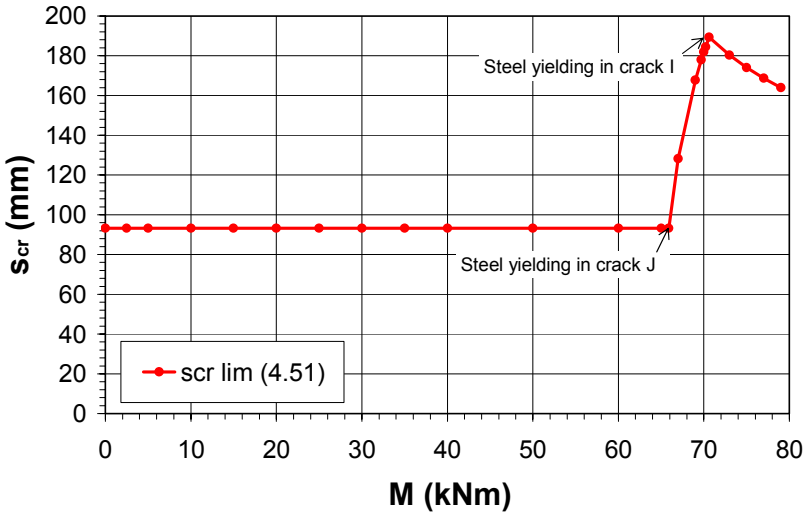

Figure 4.57. Limit between a short and long crack distance for Beam 2/C.

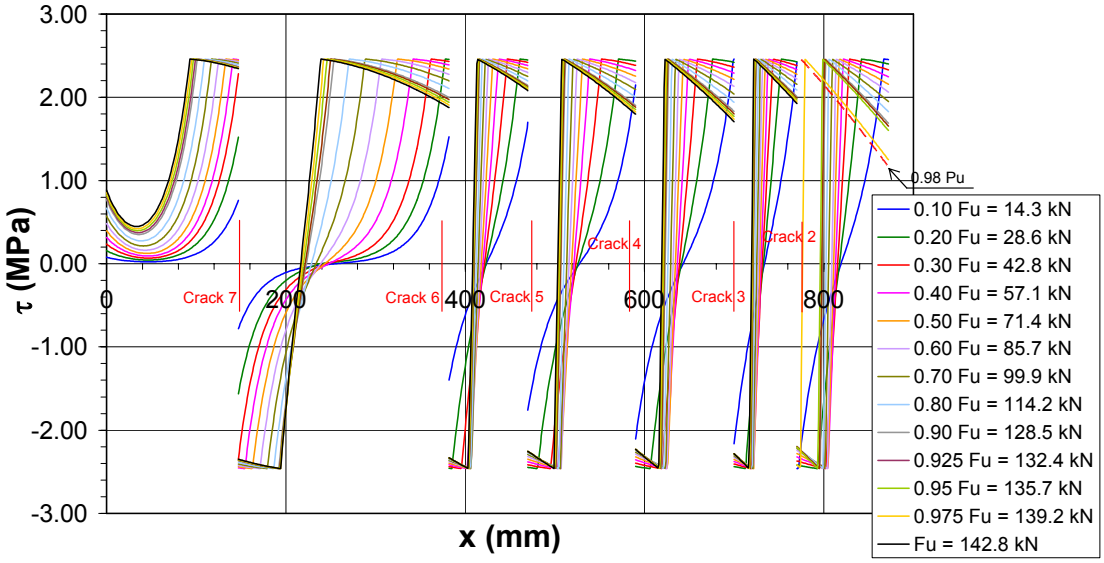

Figure 4.58. Shear stress distribution along the interface.

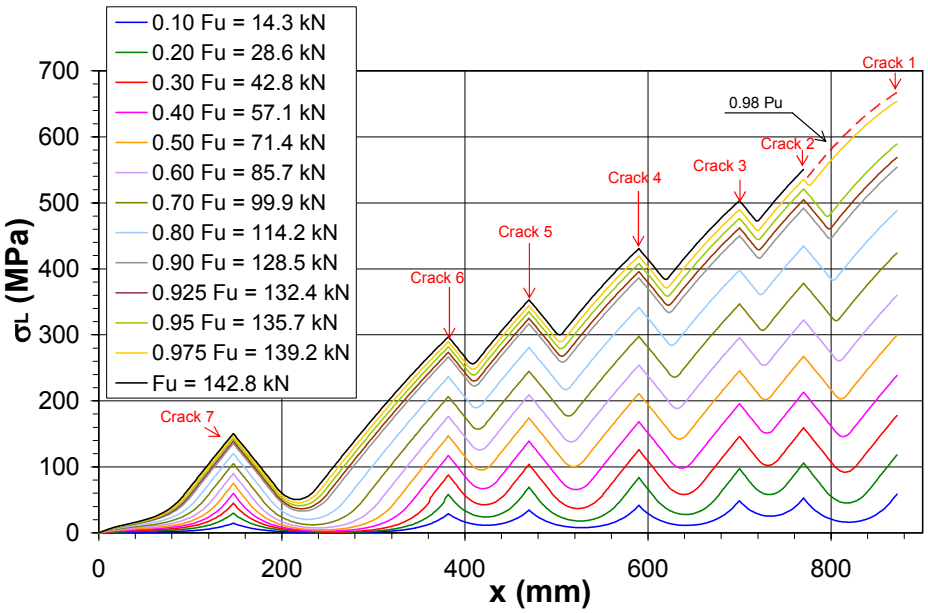

Figure 4.59. Laminate tensile stress distribution.

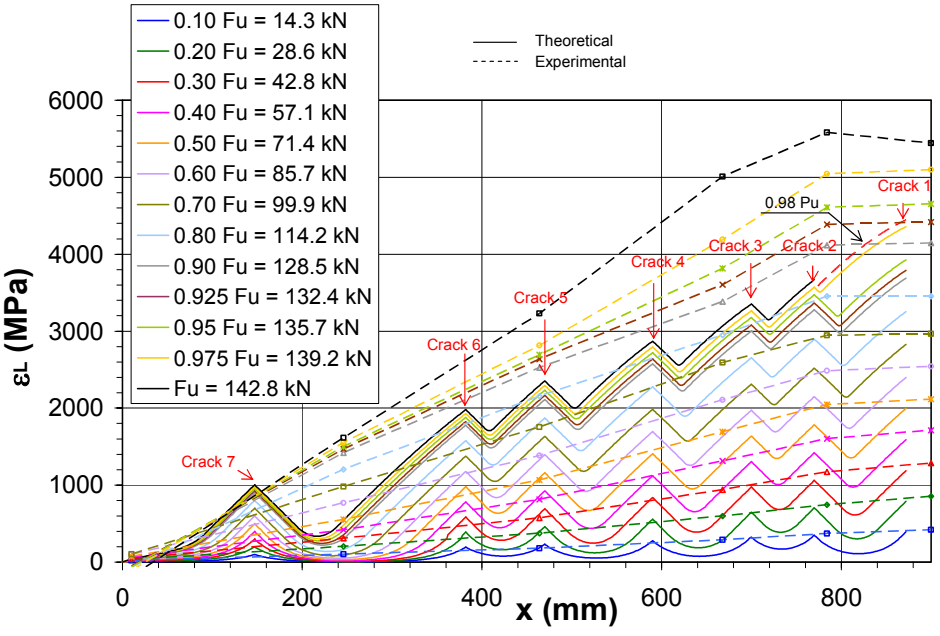

Figure 4.60. Analyitical and experimental strain distribution along the laminate.

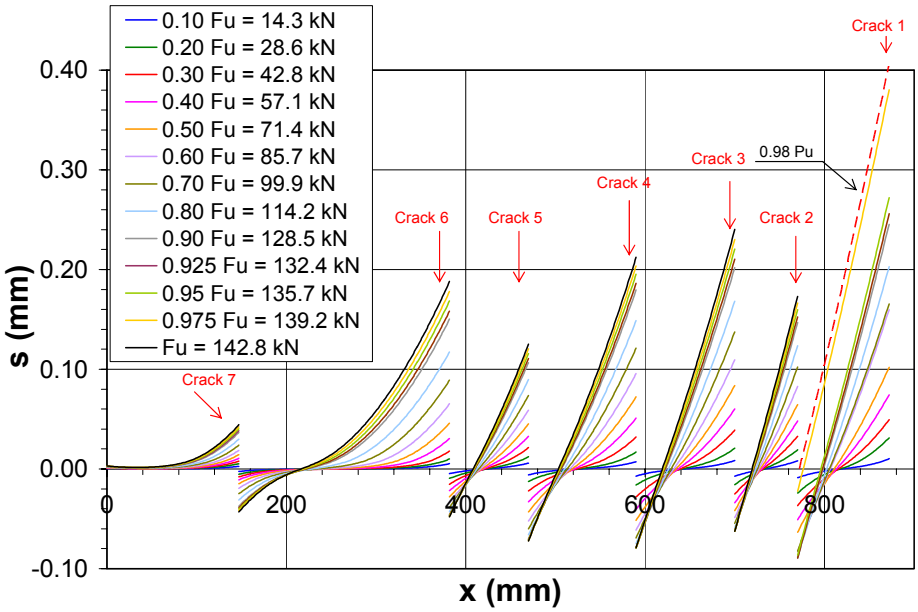

Figure 4.61. Slip between concrete and the CFRP laminate.

In the following lines a set of comments regarding the stress profiles of Figure 4.58 to Figure 4.61 are presented.

1) The general observations from the example of a beam element between two cracks subjected to bending moments and shear forces (see §4.3.8) and from the example of a beam element at the laminate end (see §4.4.7) can be applied here.

2) From the shear stress distribution, in Figure 4.58, it can be observed that only at the beginning of the test, when the applied load is 14.3 *kN* (10% F_u), is the interface linear elastic from the end of the laminate up to a distance of 865 *mm* to the beam midspan. At the vicinity of crack 1 (872 *mm*), the downward branch of the bilinear bond-slip relationship has already started. Therefore, at 10% F_u, Stage 1 is observed between cracks 2 to 7. When the load increases an additional ten percent, up to 28.6 *kN* (20% F_u), the descending branch of the bond-slip relationship starts near cracks 1 to 6. At this load level, Stage 2a.2 has already started between cracks 1 to 6. In addition, Stage 2a.1 is observed between cracks 6 and 7. By using the actual load increments, the exact transition between stages cannot be appreciated. The interface near crack 7 remains linear elastic up to an applied load of 40% F_u. From 57.1 *kN* (40% F_u) up to load failure, the complete interface between cracks behaves in Stage 2a.2 and the laminate end element behaves in Stage 2a.

3) The shear stress profile in Figure 4.58 shows that the debonding process of the laminate will initiate near crack 1 immediately before the applied load reaches 140.0 *kN* (98% F_u). At this moment the shear stress in crack 2 will reach its maximum value, τ_{LM}, and Stage 2a.2 will end. Since the slip between laminate and concrete was not controlled during the test, Stage 2b will not develop. From this point on, a slight load increase will cause the laminate to debond between crack 1 and 2. Then, a horizontal macrocrack will appear between those cracks and propagates towards the laminate end. Therefore, according to this analysis,

the peeling failure is initiated when the applied load was 98% F_u. Afterwards, the laminate debonding propagated up to load failure, when the laminate was completely detached.

4) To predict the initiation of the debonding process in a beam under transverse loads, it is essential to know when the internal steel yields. Once the steel yields, the internal reinforcement is not able to increase its tensile stress. As a consequence, when the internal steel reinforcement yields along part or the whole crack distance, the laminate should by itself assume the bending moment increase along the yielded length. This implies a significant increase in the tensile stress values and a fast propagation of the debonding process. In Beam 2C, and according to the moment-curvature analysis, when the applied load is 135.5 *kN*, the internal steel yields in crack 1. Therefore, as shown in Figure 4.58, once the internal steel yields in crack 1 (95% F_u), the propagation of Zone II between cracks 1 and 2 accelerates.

5) At the end of the laminate where the tensile stress is zero, a shear stress concentration is observed. The shear stress at the laminate end combined with the transverse normal peeling stress can result in a local laminate debonding. The maximum value for the shear stress at the end of the laminate in Beam 2/C is 0.85 *MPa* which corresponds to load failure. As shown in Figure 4.58, the laminate end remains linear elastic up to failure (Zone I). The linear elastic analysis described in Chapter 2 gives a higher value for the shear stresses at the end of the laminate 2.33 *MPa*. Figure 4.58 shows that the shear stress at the end of the laminate is always lower than both the maximum shear stress τ_{LM} and the shear stress at the nearest crack, (crack 7 in this case). For example, at failure the shear stress is 0.85 *MPa* at the laminate end, 2.32 *MPa* on crack 7, and the maximum value is 2.46 *MPa*.

6) In Figure 4.59, the tensile stress distribution is presented. The tensile stresses achieve its maximum at each crack location. Due to the tension stiffening effect, the profile decreases from the crack tips to a minimum value which corresponds to the zero shear stress location. In addition to the previous comment, it can be observed that the distance between 95% F_u bar and 97.5% F_u plotted line is higher between crack 1 and 2 than in the rest of the laminate. This fact can be explained due to the steel yielding in crack 1.

7) Figure 4.60 shows the analytical strain distribution in the laminate applying the formulae of the previous section together with the experimental distribution derived by linear interpolation of the values recorded by instrumentation during the test. The theoretical value of the FRP strain in crack 1 under failure load derived from the moment-curvature analysis is 6111 $\mu\varepsilon$. The experimental value derived by interpolation of the registered values through the use of the strain gauges near this crack is 5446 $\mu\varepsilon$. The actual error made in estimating the maximum strain is 9.2%. At the theoretical initiation of debonding under a load of 140.0 kN (98.0% F_u), the theoretical strain value on crack 1 is 4445 $\mu\varepsilon$, lower than the observed during the test. The estimation error made was 18.3%. However, the error when predicting the strain before debonding occurs is lower. For example, when observing the strain in a point located between two cracks, for example x = 668 *mm*, when the applied load is 114.2 *kN* (80% *Fu*) the

theoretical strain is 2802 $\mu\varepsilon$ and the experimental value is 2947 $\mu\varepsilon$. To obtain a similar profile during the test as what can be analytically derived, a huge number of strain gauges should have been used.

8) Figure 4.61 shows the relative displacement between the support and the laminate. As can be observed between cracks 1 and 2, when the maximum shear stress is attained in the less loaded crack, the complete interface slides in one direction.

9) To protect the internal steel from corrosion, crack widths should be limited. For design purposes, under the service limit state, the calculated crack width should be compared to the maximum crack width allowed for an exposure class that is related to the environmental conditions. The FIB Task Group 9.3 FRP (2001) calculates the characteristic value of the crack width according to Eurocode 2, but modifies the crack spacing and the reinforcement strain in the fully cracked state to take into account the external reinforcement. In a specific case, where the existing cracks are known, the crack width can be estimated as the sum of the relative sliding values between concrete and laminate on both sides of the crack. For safety reasons, the crack width was only measured for a few load levels during the test. When the acting load was 75.5 *kN*, the measured width of crack 2 was 0.100 *mm*. This value is similar to the 0.128 *mm* obtained analytically.

10) In this particular case, the service load was estimated to be 70.1 *kN* (49.1% F_u). The maximum calculated crack width was 0.158 *mm* which is lower than the limit value allowed for exposure class II, 0.300 *mm*, according to the Spanish Concrete Code EHE (1999).

11) In beam design under service limit state, the FIB Task Group 9.3 FRP (2001) recommends avoiding the local debonding to guarantee the long-term integrity of the bond interface. For long crack distances, the local debonding occurs if the slip is larger than the maximum value s_{L0}.The maximum crack width before debonding occurs can be calculated as twice the maximum sliding s_{L0}, ($w_k = 2s_{L0}$). In this case, this value is 1.528 *mm*, much higher than the limit value allowed by the Spanish Concrete Code. By using the range of s_{L0} values given in Chapter 3, the maximum crack width is in the range between 0.48 *mm* and 3.49 *mm*. Those values will always be higher than the maximum limit value associated to any exposure class. Therefore, for long bonded crack distances and according to the FIB Task Group 9.3 FRP, if the characteristic value of the crack width under service load is limited either to a maximum value of 0.30 *mm* (FIB Task Group 9.3 FRP) or to the values given in Table 49.2.4 of the Spanish Concrete Code, no local debonding will occur in the Service Limit State.

12) The transferred force between each pair of cracks associated to different load levels (see Figure 4.62), is easily obtained by subtracting the tensile force under each crack tip derived from the moment curvature analysis of the strengthened section. This value can also be obtained as the area enclosed by the shear stress distribution between the pair of cracks under consideration. Since the internal steel has not yielded from crack 2 to the laminate end, the transferred force between adjacent pairs of cracks increases in a linear way with the external load.

The transferred force between cracks 1 and 2 changes its slope once the internal steel yields in crack 1. In addition, the theoretical maximum transferred force between these locations, according to §4.3.6, is shown in Figure 4.62. This maximum value is attained before failure load, when the external applied load is 140.0 *kN*. At this point in time, Stage 2a.2 finishes and the maximum shear stress reaches crack 2.

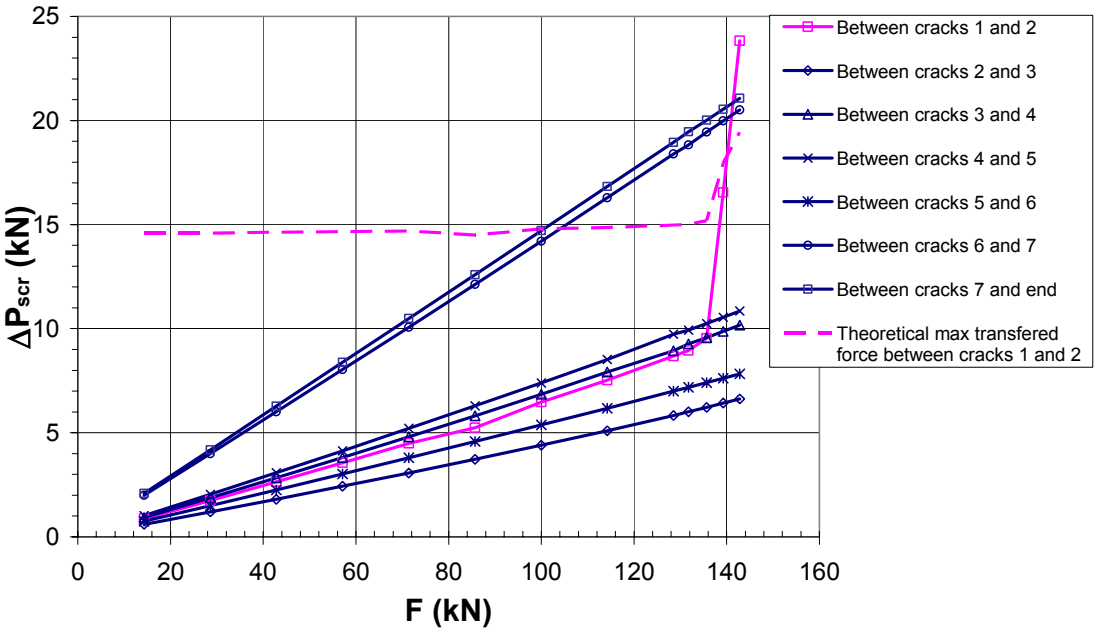

Figure 4.62. Transferred force to maximum transferred force ratio between crack 1 and 2.

13) During the Beam 2/C test, the formation of some intermediate cracks between the flexural cracks mentioned above, as observed in Figure 4.63. In any case, they appeared once the applied load surpassed the service load. These intermediate cracks reduce the crack distance to half. This fact will be considered in the design proposal that will be presented in Chapter 5, by studying the influence of different crack distances, for instance both the whole and half of the value given by the FIB Task Group 9.3 FRP (2001).

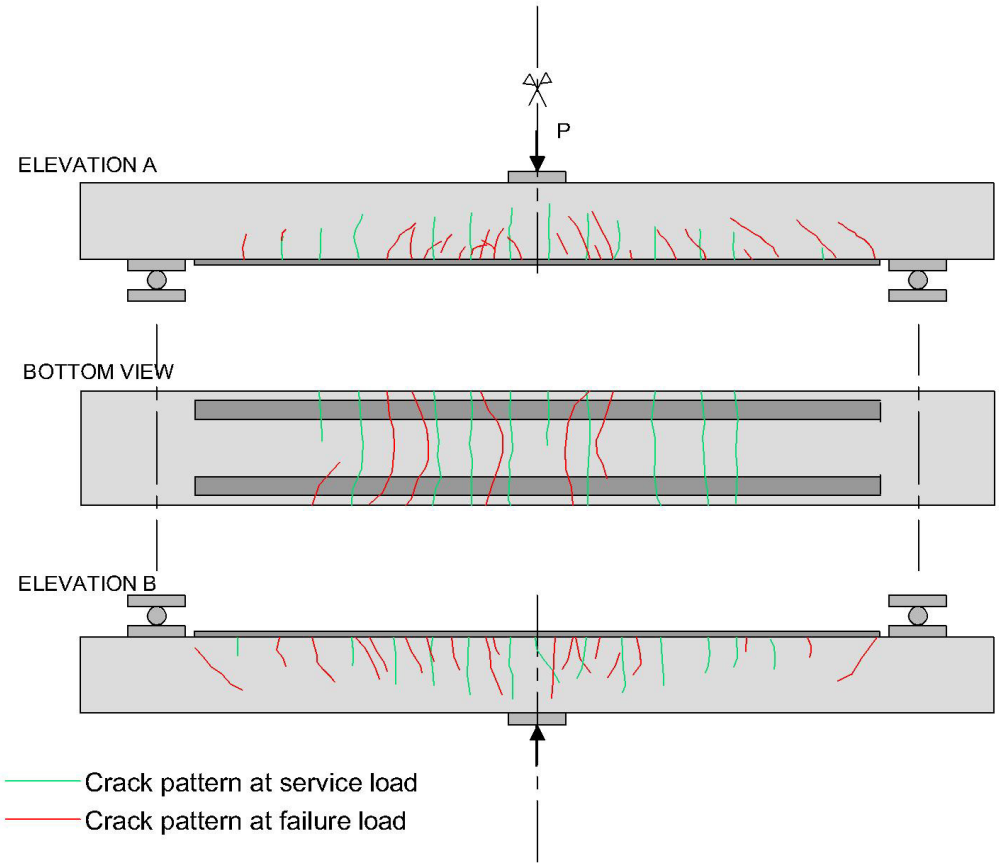

Figure 4.63. Crack pattern of Beam 2/C at failure load.